Characterizing thyroid hormone mediated action on gene expression in mice: mechanistic insight into thyroid hormone response elements, thyroid hormone receptor-binding sites, and microRNAs

by
Martin A. Paquette

A thesis submitted to the Faculty of Graduate and Postdoctoral Affairs
in partial fulfillment of the requirements for the degree of

Doctor of Philosophy
in
Biology

Carleton University
Ottawa, Ontario

ABSTRACT

Thyroid hormone (TH) exerts its effects by binding to the TH receptor (TR), which binds to TH response elements (TREs) to regulate target gene expression. Disruption of TH action can have detrimental health effects. The precise molecular mechanisms involved in TH mediated gene expression remain unclear. The overall objectives of this thesis were to: i) characterize global gene and microRNA (miRNA) expression in early response to TH perturbation in mouse liver; ii) identify TREs and TR-binding sites found throughout the mouse genome; and iii) compare TRE half-site organizations and their ability to drive gene expression. Transcriptional profiling of mRNA liver samples from TH disrupted mice enabled the identification of genes that were under direct TH-regulation. TREs in the promoter region of *Tor1a*, *Hectd3*, *Slc25a45* and *2310003H01Rik* were validated *in vitro*, adding four genes to the battery of only 13 known TRE-containing mouse genes. Hepatic miRNAs were also found to be significantly altered following perturbations in TH levels. *In vitro* analyses confirmed TH regulation of miR-206. Moreover, *Mup1* and *Gpd2* were confirmed to be targeted by miR-206 in response to TH, demonstrating that miRNAs can act as master regulators of the TH response pathway. ChIP-chip analysis identified TR-DNA interactions in juvenile mouse liver revealing only a few TR-binding sites consistent between all analyzed samples, suggesting that relatively few genes are under direct TH/TR control. Reporter assays confirmed the presence of TREs in the promoter regions of *Ddx54* and *Thrsp*, thus validating two additional functional mouse TREs. Finally, we investigated the relative ability of liganded homodimers of TR and retinoid X receptor (RXR), and the heterodimer TR/RXR, to regulate gene expression for three TRE half-site organizations. We found that there were fundamental differences between TRE configurations that affect nuclear receptor interactions with the response element and the ability to specifically bind their

ligands. These studies provide mechanistic insight into TREs, TR-binding sites and TH action. Collectively this thesis increases our understanding of how TH operates to control genome function and provides a basis to develop appropriate testing strategies for environmental chemicals that may disrupt TH-associated genes expression by interaction with TR.

ACKNOWLEDGEMENTS

I would like to express my deep and sincere gratitude to my advisor Dr. Carole Yauk – thank you for your guidance and support throughout this project. Thank you to the committee members; Dr. Iain Lambert, Dr. Mike Wade, Dr. Vance Trudeau and Dr. Michel Dumontier for helpful discussions and input. Special thanks to Dr. Ella Atlas for guidance with the cell culture work, Dr. Hongyan Dong for performing the animal work, Rémi Gagné for performing bioinformatics analyses and to Andrew Williams for helping with statistical analyses. Thank you to the many wonderful people that I have met at Health Canada's Environmental Health Center that have supported and helped me in different ways, notably, Alexandra Long, Jaime Nead, Meghan Murphy, Julie Cox, Sarah Labib, Julie Bourdon, Amal Malik, Julie Buick and Andrea Rowan-Carroll. Finally, a big thank you to my family, friends and loved ones for the support and motivation provided throughout the past five years.

TABLE OF CONTENTS

LIST OF TABLES

LIST OF FIGURES

LIST OF ABBREVIATIONS

9cRA	9-cis-retinoic acid
Actb	Actin beta
Apoa1	apolipoprotein A1
Arl4d	ADP-ribosylation factor-like 4D
Bdnf	Brain-derived neurotrophic factor
CAT	Chloramphenicol acetyltransferase
CH	Congenital hypothyroidism
ChAP	Chromatin affinity purification
ChIP	Chromatin immunoprecipitation
ChIP-seq	Chromatin immunoprecipitation-sequencing
CHX	Cycloheximide
Cyp17a1	Cytochrome P450, family 17, subfamily A, polypeptide 1
DAVID	Database for Annotation, Visualization and Integrated Discovery
Ddx54	DEAD (Asp-Glu-Ala-Asp) box polypeptide 54
Dio1	Deiodinase, iodothyronine, type I
Dio2	Deiodinase, iodothyronine, type II
DIO3	Deiodinase, iodothyronine, type III
DIT	Diiodo-tyrosine
DR4	Direct repeat 4
Duoxa2	Dual oxidase maturation factor 2
EMSA	Electrophoretic mobility shift assays
ER6	Everted repeat 6
ERE	Estrogen response element
Esr1	Estrogen receptor 1
FA	Fanconi anemia
FDR	False discovery rate
FOS	FBJ murine osteosarcoma viral oncogene homolog
FXR	Farnesoid X receptor
GD	Gestational day
Gh1	Growth hormone 1
GO	Gene ontology
Gpd2	Glycerol-3-phosphate dehydrogenase 2 (mitochondrial)
Hectd3	HECT domain containing E3 ubiquitin protein ligase 3
Hmbs	Hydroxymethylbilane synthase
Hprt	Hypoxanthine phosphoribosyltransferase 1
HPT	Hypothalamic-pituitary-thyroid
Hyper	Hyperthyroid
Hypo	Hypothyroid
Hypo+	Hypothyroid/replacement
I.p.	Intraperitoneal
Ihh	Indian hedgehog
IP	Immunoprecipitated
IR0	Inverted repeat 0
JUN	Jun proto-oncogene
Klf9	Kruppel-like factor 9
LBD	Ligand binding domain
LDL	Low-density lipoprotein
MAPK	Mitogen-activated protein kinase

Mbp	Myelin basic protein
Me1	Malic enzyme 1, NADP (+)-dependent, cytosolic
MeDIP-seq	Methylated DNA immunoprecipitation-sequencing
MiRNA	MicroRNAs
MIT	Monoiodo-tyrosine
Mlxipl	MLX interacting protein-like
MMI	Methimazole
Mup1	Mitochondrial uncoupling protein 1
NCOA1	Muclear receptor coactivator 1
NCOR2	Muclear receptor corepressor 2
NIS	Na+/I- symporter
Nr3c1	Muclear receptor subfamily 3, group C, member 1 (glucocorticoid receptor)
Nrgn	Neurogranin
Nrp1	Neuropilin 1
OECD	Organization for Economic Co-operation and Development
PBS	Phosphate buffered saline
PCA	Principal component analysis
Pde8a	Phosphodiesterase 8A
Phlda1	Pleckstrin homology-like domain, family A, member 1
PND	Postnatal day
PPAR	Proliferator-activated receptor
Ppara	Peroxisome proliferator-activated receptor alpha
Pre-miRNA	Precursor microRNA
Pri-miRNA	Primary microRNA
Prl	Prolactin
PTU	6-propyl thiouracil
PWN	Position weight matric
PXR	Pregnane X receptor
RAR	Retinoic acid receptor
Reln	Reelin
RIA	Radioimmunoassay
RT-qPCR	Real time-quantitative PCR
RXR	Retinoid X receptor
RXRE	RXR response element
Slc16a2	Solute carrier family 16, member 2 (thyroid hormone transporter)
Slc25a45	Solute carrier family 25, member 45
Ston2	Stonin 2
T3	Triiodothyronine
T4	Thyroxine
TaqMan	Low density array TLDA
TDC	TH disrupting chemical
Tg	Thyroglobulin
TH	Thyroid hormone
Thra	Thyroid hormone receptor alpha
Thrb	Thyroid hormone receptor beta
Thrsp	Thyroid hormone responsive Spot14
TI	Total input
Tor1a	Torsin family 1, member A
TPO	Thyroid peroxidase
TR	Thyroid hormone receptor
TRE	Thyroid hormone response elements

TRH	Thyrotropin releasing hormone
Trim24	Tripartite motif containing 24
TSS	Transcription start site
Tuba1b	Tubulin, alpha 1b
Upp2	Uridine phosphorylase 2
UTR	Untranslated region
VDR	Vitamin D receptor
Vldlr	Very low density lipoprotein receptor

STATEMENT OF CONTRIBUTION

Chapter 2

Experimental design	*Martin Paquette* *Hongyan Dong* *Mike Wade* *Carole Yauk*
Animal Exposure and tissue collection	*Hongyan Dong*
Radioimmunoassays for T4 levels	*Hongyan Dong*
RNA extractions and DNA microarray hybridizations	*Martin Paquette*
Microarray analysis and MAANOVA	*Morie Malowany* *Andrew Williams*
Pathway analysis and PCA	*Martin Paquette*
RT-qPCR experiments and analysis	*Martin Paquette*
Bioinformatics for TRE search	*Remi Gagné*
ChIP-PCR and agarose gels	*Martin Paquette*
EMSAs	*Martin Paquette*
Drafted the manuscript	*Martin Paquette*
Revised manuscript	*Martin Paquette* *Hongyan Dong* *Carole Yauk* *Mike Wade* *Remi Gagné* *Andrew Williams*

Chapter 3

Experimental design	*Martin Paquette* *Hongyan Dong* *R. Thomas Zoeller* *Mike Wade* *Carole Yauk*
Animal Exposure and tissue collection	*Hongyan Dong*

RNA extractions and DNA microarray hybridizations ..... *Martin Paquette*

Microarray analysis and MAANOVA ..... *Andrew Williams*

TaqMan low density array hybridizations ..... *Hongyan Dong*

Cell culture and RT-qPCR experiments ..... *Hongyan Dong*

Drafted manuscript ..... *Hongyan Dong*

Revised the manuscript ..... *Martin Paquette*
Carole Yauk
Mike Wade
R. Thomas Zoeller

Chapter 4

Experimental design ..... *Martin Paquette*
Hongyan Dong
Ella Atlas
Mike Wade
Carole Yauk

Animal Exposure and tissue collection ..... *Hongyan Dong*

ChIP and microarray hybridization ..... *Martin Paquette*

ChIP-chip data analysis ..... *Martin Paquette*
Remi Gagné

ChIP-PCR experiments and analysis ..... *Martin Paquette*

RT-qPCR experiments and analysis ..... *Martin Paquette*

Plasmid construction ..... *Martin Paquette*

Cell culture, transfection and luciferase reporter assays ..... *Martin Paquette*

Bioinformatics for TRE search ..... *Remi Gagné*

Bioinformatics for Thrsp promoter region alignment ..... *Martin Paquette*

Drafted the manuscript ..... *Martin Paquette*

Revised the manuscript ..... *Martin Paquette*

Remi Gagné
Hongyan Dong
Ella Atlas
Mike Wade
Carole Yauk

Chapter 5

Experimental design..... *Martin Paquette*
Ella Atlas
Mike Wade
Carole Yauk

Plasmid construction..... *Martin Paquette*

Cell culture, transfection and luciferase reporter assays..... *Martin Paquette*

Drafted the manuscript..... *Martin Paquette*

Revised the manuscript..... *Martin Paquette*
Ella Atlas
Mike Wade
Carole Yauk

CHAPTER 1: INTRODUCTION

1.1 Thyroid Function and Regulation

1.1.1 Thyroid Hormones

Thyroid hormones (THs) are produced by the thyroid gland, a small organ with two elongated oval lobes, one on each side of the trachea. The thyroid gland is part of the endocrine system, which consists of a series of organs that releases signalling molecules (hormones) to regulate basic physiological processes. The thyroid participates in the regulation of these processes by producing THs, which include tetraiodothyronine or thyroxine (T4) and triiodothyronine (T3). These tyrosine-based hormones contain multiple iodine molecules. Iodide is actively pumped and concentrated into the thyroid via a Na^+/I^- symporter (NIS) (Dai et al., 1996). Thyroid peroxidase (TPO) then oxidizes the iodide and incorporates it into tyrosine residues of a thyroglobulin (Tg) molecule forming monoiodo-tyrosine (MIT) and diiodo-tyrosine (DIT). Enzymatic coupling of these residues enables the formation of T4 and T3.

The thyroid releases more T4 than T3, although T3 is a much more powerful and effective hormone. T4 is generally considered to be the precursor hormone and T3 to be the biologically active form, as it has a greater efficacy and affinity for nuclear receptors (i.e. the TH receptors (TRs)) than T4 (Hassi et al., 2001). Most of the circulating T3 is produced from the deiodination of T4 by enzymes known as deiodinases (Kohrle, 2000). This conversion takes places in various peripheral tissues such as the liver, kidney, brain, brown fat and skin.

THs have been shown to exert their effects on the growth, development, and metabolism of practically every cell and organ (Yen, 2001). THs play an important role in early development and throughout adulthood having profound effects on metabolism.

1.1.2 Thyroid Hormone Regulation

The production of THs is tightly regulated by a negative-feedback mechanism (Figure 1.1), which involves the hypothalamic-pituitary-thyroid (HPT) axis (Shupnik et al., 1989). The hypothalamus produces and releases thyrotropin releasing hormone (TRH) that is transported to the pituitary, and binds TRH receptors. This, in turn, stimulates the production and release of thyrotropin (also known as thyroid stimulating hormone (TSH)) that acts on the thyroid, and binds the TSH receptor. Thyrotropin binding stimulates numerous thyroid responsive genes (including the genes responsible for the production of NIS, Tg and TPO) and promotes the production of THs; however, only a small percentage of THs are unbound. The majority of THs are bound to carrier proteins such as thyroxine binding globulin, albumin, and thyroid binding prealbumin. THs that are released into the bloodstream have the ability to negatively regulate the production of TRH and TSH.

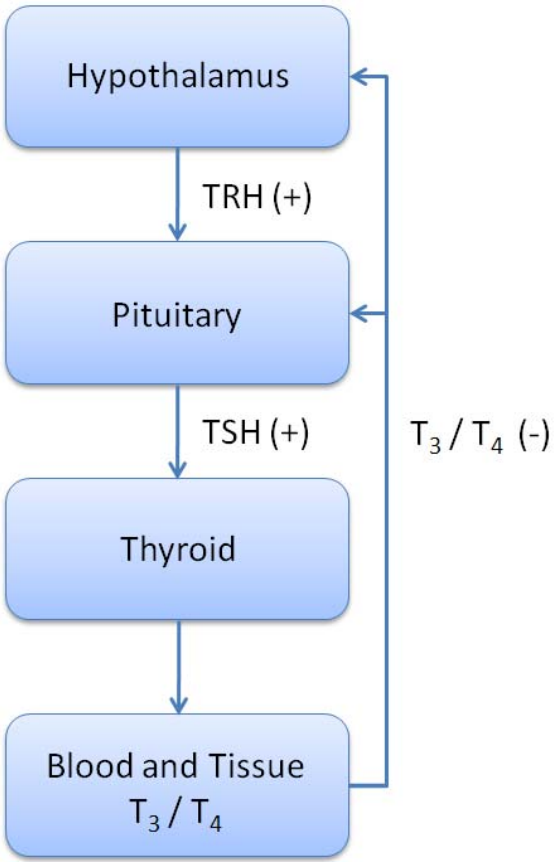

Figure 1.1. Feedback system regulating the production of THs.

1.1.3 Thyroid Hormone Receptors and Thyroid Hormone Response Elements

The primary effect of THs is on the transcriptional regulation of targeted genes. THs are lipophilic and diffuse passively through the plasma membrane. They bind to specific nuclear receptors known as TRs. TRs are part of a large superfamily of hormone receptors. Similar to other nuclear receptors, TRs contain: i) a transactivation domain that interacts with other transcription factors to form complexes, which in turn may activate or repress transcription; ii) a DNA-binding domain that is capable of interacting with specific DNA sequences known as TH response elements (TREs); and iii) a ligand-binding and dimerization domain.

TRα and TRβ are encoded by separate genes: thyroid hormone receptor alpha (*Thra*) and thyroid hormone receptor beta (*Thrb*) (Lazar, 1993). The main isoforms of these genes are TRα-1, TRα-2, TRβ-1 and TRβ-2 (Wagner et al., 1995). The two TRα isoforms are generated from alternate splicing and therefore have fairly similar amino acid sequences. However, TRα-2 does not contain a functional TH-binding site and therefore, cannot bind T3. The TRβ isoforms are generated by alternative promoters (Hodin et al., 1989); both TRβ isoforms and the TRα-1 isoform have very high identity. TRα-1 and TRβ-1 are expressed in virtually every tissue, although studies in rodents have shown that TRα-1 expression is highest in skeletal muscle and brown fat, whereas TRβ-1 expression is highest in the brain, liver and kidney (Hodin et al., 1990; Yen et al., 2003). TRα-2 expression is highest in the testis and brain, whereas TRβ-2 expression is restricted to the anterior pituitary gland and hypothalamus, as well as the developing brain and inner ear (Cook et al., 1992; Yen et al., 1992).

TRs regulate gene expression through TREs. Typically, TREs are composed of two or more hexamer half-site sequences arranged in tandem array (Brent et al., 1992). TRs have the ability to bind to various imperfect TRE half sites. The number of half sites, the spacing between

half sites, as well as their orientation are all features that vary between TREs (Glass, 1994). TRs can bind to TREs as monomers or homodimers, although the majority of the time TRs will bind to the TREs as a heterodimer with the retinoid X receptor (RXR) (Bugge et al., 1992; Lazar et al., 1991). TRs also have the ability to bind to TREs in the presence or absence of the ligand (T3). The numerous arrangements of features (spacing, orientation, half-site sequence, and dimerizations) have made the identification and characterization of TREs particularly difficult.

The mechanism by which positive gene regulation by TH (up-regulation in the presence of TH) occurs is more understood than that of negative gene regulation. Typically, the TR-RXR heterodimer binds to a TRE located in the regulatory region of the target gene. If liganded, the TR recruits a coactivator complex (such as nuclear receptor coactivator 1 – NCOA1 (Jeyakumar et al., 1997)) that in turn leads to promoter DNA demethylation and histone acytelation, and subsequent opening of the chromatin region of the target gene. If unliganded, the TR releases the co-activator complex and recruits a corepressor complex (such as nuclear receptor corepressor 2 – NCOR2 (Horlein et al., 1995)), which in turn leads to DNA methylation, histone deacetylation and subsequent condensing of the chromatin region of the target gene (Brent, 2012) (Figure 1.2).

Negatively TH-regulated target genes have been documented, but the exact mechanism by which this occurs is not completely understood. Microarray studies have identified negative gene regulation in response to TH in various tissues (Dong et al., 2007; Flores-Morales et al., 2002). Several models have been suggested, although no uniform model appears to take into account all aspects of negative gene regulation (Weitzel, 2008). One of the proposed models suggests that the TR-RXR heterodimer sits on a “negative” TRE. This heterodimer interacts with a co-activator to drive expression of the target gene. In the presence of T3 or T4, the co-repressor replaces the co-activator leading to down-regulation of the target gene(Weitzel, 2008).

1.1.4 Alternate Regulatory Mechanisms Mediated by Thyroid Hormones

It is generally accepted that most of the effects of TH are mediated through the TRs, although it is clear that THs can also exert effects though non-genomic mechanisms (Davis and Davis, 1996, 2002; Davis et al., 2011; Davis et al., 2002). Integrin αvβ3, a cell surface receptor, has been shown to bind T4 (Davis et al., 2011). Binding of TH leads to the activation of the mitogen-activated protein kinase (MAPK) signal transduction cascade, which regulates multiple cellular responses such as gene expression, proliferation and apoptosis (Davis et al., 2005; Horn and Heuer, 2010).

An additional non-genomic mechanism by which TH may affect gene expression is through microRNAs (miRNAs). MiRNAs are small non-coding RNAs that target the 5' untranslated region (UTR) of mRNA to destabilize and cause degradation ultimately reducing protein output (Guo et al., 2010). MiRNAs arise from primary miRNAs (pri-miRNA)s that are processed into hairpin-shaped precursor miRNAs (pre-miRNAs), which are ultimately processed into ca. 22 nucleotide long mature miRNA (Alvarez-Garcia and Miska, 2005). Two studies have shown the involvement of TH in regulating miRNA activity. The first study found that pre-miR-208 expression was decreased in the heart tissue of mice rendered hypothyroid by treatment with 6-propyl thiouracil (PTU) (van Rooij et al., 2007). The second study found that pri-miR-206 and pri-miR133b were strongly down-regulated in the presence of TH in human skeletal muscle (Visser et al., 2009). Neither of these studies confirmed alteration of mature miRNA in response to TH, although they provide evidence to suggest the possibility that THs play an important role in the regulation of miRNA expression.

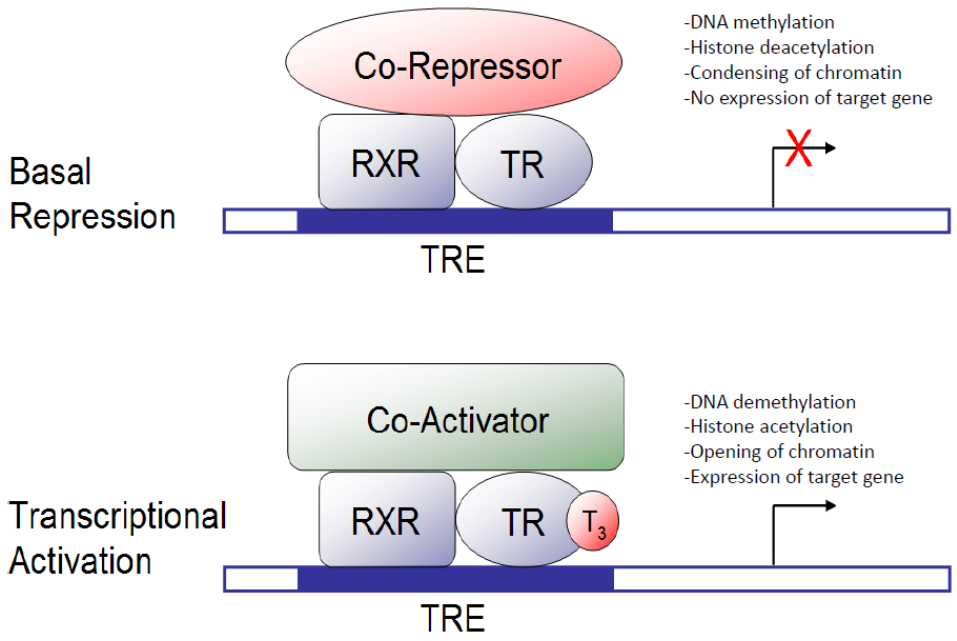

Figure 1.2. Binding of heterodimer TR/RXR to a TRE in the absence (upper panel) and presence (lower panel) of T3 binding, leading to gene expression.

1.2 Characterizing Thyroid Hormone Action in the Liver

THs are essential for normal organ growth, development and function . They regulate the basal metabolic rate of all cells, including hepatocytes. The liver expresses deiodinase 1, which participates in the production of T3 (Sanders et al., 1997); however, the liver also expresses deiodinase 3, which is a major inactivator of THs (Tu et al., 1999). These characteristics give the liver the ability to metabolize THs, and in turn regulate their systemic endocrine effects. In addition to activating and inactivating THs, the liver plays an important role in the transportation and metabolism of THs by filtering out bound T4 from the circulating plasma (Mendel et al., 1988). The liver is also involved in the production of plasma proteins that bind THs (Bianco et al., 2002).

THs play an important role in hepatic lipid homeostasis by regulating low-density lipoprotein (LDL) receptors (Ness et al., 1998), lipid lowering liver enzyme, cholesterol 7α-hydroxylase (Ness and Lopez, 1995), and apolipoprotein A1 (*Apoa1*: a major component of high-density lipoprotein) (Taylor et al., 1997). THs in the liver have also been shown to regulate malic enzyme (*Me1*) (Goodridge, 1978), which plays a role in fatty acid biosynthesis, and thyroid hormone responsive Spot14 (*Thrsp*), which regulates lipogenesis and biosynthesis of triglycerides (Wu et al., 2013). Thus, maintaining hepatic TH levels is critical for proper lipid homeostasis. Ultimately, perturbation of hepatic TH levels can lead to changes in overall metabolic rates that can have detrimental health effects and lead to long-term consequences (Rosenbaum et al., 2000).

In the following subsections several key studies are presented to provide a brief overview of important findings pertaining to the identification and characterization of TH-mediated gene

expression, TR-binding sites and TREs. The overview focuses mainly on studies conducted on mouse liver.

1.2.1 Characterizing Thyroid Hormone-mediated Gene Expression

Several studies have investigated the effects of TH disruption on global hepatic gene expression. There are many variables to take into consideration when interpreting the results of these studies including: i) the animal model and the age of the animals; ii) the chemical used to induce TH-disruption, the dose, duration and route of exposure; and iii) the technology used to assess changes in gene expression. Below, studies that characterize TH-mediated gene expression in the liver are reviewed.

Studies characterizing TH-mediated global gene expression generally demonstrate that a large portion of genes are positively regulated by TH (Bungay et al., 2008; Ventura-Holman et al., 2007; Yen et al., 2003). The duration of the exposure and sampling time reveals a distinction between the expression changes measured at early and late time points, demonstrating that there is an immediate direct TH-action effect as well as a down-stream indirect TH-action, and that some effects are only manifested after longer-term sub-chronic or chronic exposures. For example, a study in the liver of hypo- and hyperthyroid mice showed that genes involved in metabolism are rapidly altered (within hours), whereas mitochondrial functions only seem to be affected with sustained TH disruptions (Flores-Morales et al., 2002).

In another study, hepatic gene expression profiling of adult mice under various TH conditions revealed distinct positive and negative expression patterns (Yen et al., 2003). The TH statuses of the mice analyzed were: euthyroid, T3 treated - hyperthyroid, PTU treated - hypothyroid and T3+PTU treated. Positively regulated genes showed three main expression

patterns: i) down-regulation during TH deprivation and up-regulation during TH treatment; ii) no response to TH deprivation and up-regulation to TH treatment; and iii) down-regulation during TH deprivation and no response to TH treatment. Negatively regulated genes showed two expression patterns: i) up-regulation in response to TH deprivation and down-regulation in response to TH treatment; and ii) no response to TH deprivation and down-regulation in the response to TH treatment. These finding show the complexity and variety of mechanisms regulating TH-mediated gene expression.

Considering the importance of TH, it has been suggested that some tissues may be capable of managing minor TH fluctuations by adjusting cellular transporters or deiodinases (i.e., compensatory mechanisms). Deiodinase, iodothyronine, type III (DIO3) protein expression in rats was downregulated in response to xenobiotic-induced toxicity resulting from TH disruption in the liver and plasma (Dudek et al., 2013). DIO3 is considered a major inactivator of TH (Bianco et al., 2002), therefore, it is hypothesized that in the early stages of hepatotoxicity, the liver would decrease the expression of *DIO3* to rapidly maintain TH levels (Dudek et al., 2013). This would suggest a possible mechanism capable of compensating for low TH. However, compensatory responses to low TH have not been directly shown. To investigate this concept, a study was conducted using rats exposed to decreasing doses of PTU (up to 200-fold lower than traditionally used) to induce hypothyroidism (Sharlin et al., 2010). TSH, Deiodinase, iodothyronine, type II (*Dio2*) (activator of TH) and solute carrier family 16, member 2 (thyroid hormone transporter) (*Slc16a2*) were all analyzed and did not support the hypothesis of a compensatory mechanism for low TH.

Congenital hypothyroidism (CH) has been associated with neurological and motor development impairment that can persist through to adulthood (Kempers et al., 2006; Oerbeck et

al., 2003). A recent study investigating the specific influence of CH in rat liver discovered that CH can influence hepatic transcriptional response to TH disruption in adulthood (Santana-Farre et al., 2012). For example, perturbation in the expression of peroxisome proliferator-activated receptor alpha (*Ppara*), which is involved in lipid metabolism, was found to persist in adult rats following CH. In addition, circulating levels of cholesterol and triglycerides were significantly reduced in CH adult rats when compared to controls. This suggests that maintaining thyroid TH levels during development is crucial for normal liver function later in life

Studies have also investigated TR knock-outs to characterize the function and resulting phenotypes of different TR isoforms. Gene expression profiles of *Thra* and *Thrb* knock-out mice are highly similar following TH-disruption compared to wild-type mice, suggesting that the two isoforms are able to co-regulate most hepatic TH-mediated target genes (Yen et al., 2003). *Thra/Thrb* double knock-out mice are viable, demonstrating that TRs are not essential for viability (Gauthier et al., 1999; Gothe et al., 1999), although these mice show extreme TH resistance (Flamant et al., 2002). Indeed, hepatic gene expression patterns of *Thra/Thrb* double-knockout mice and TH-deprived wild-type mice are remarkably different (Yen et al., 2003). This is most likely because of differences in basal repression or expression caused by the presence or absence of the TR.

1.2.2 Characterizing Thyroid Receptor Binding Sites

Directly investigating TR-binding sites is another way to determine which genes are under the control of TH. TR-binding sites can be identified at the genome-scale using chromatin immunoprecipitation (ChIP) followed by microarray analysis (ChIP-chip) or sequencing (ChIP-seq), although this technique requires a high quality antibody. Alternatively, tagged TRs can be

produced that can be isolated using an antibody against the tag (chromatin affinity purification (ChAP)), followed by microarray analysis (ChAP-chip) or sequencing (ChAP-seq).

No studies to date have applied the techniques described above to broadly characterize TR-binding sites in the liver genome. However, two studies have attempted to do so in the cerebellum and in neuronal cells. Using a TRβ antibody, ChIP-chip on mouse cerebellum DNA revealed numerous genes bound by TR that were involved in apoptosis, neurodevelopment, metabolism and signal transduction (Dong et al., 2009). Surprisingly, bioinformatics analyses were unable to identify classic TRE binding sites, suggesting that: i) most TR binding sites are not highly similar to the classic TRE motif; and/or ii) other regulatory elements may be involved. In a different study, ChAP-seq was employed to investigate binding sites for the two main TR isoforms, TRα1 and TRβ1, in the neural cell line C17.2 (Chatonnet et al., 2013). The two isoforms were found to share many TR-binding sites, although some sites were isoform specific. A search for consensus binding sites for TRα1 and TRβ1 identified a DR4 element very similar to that of the classic DR4 TRE. The newly identified DR4 consensus element was used to search for similar elements. Half of all newly identified TR-binding sites contained a DR4-like element. A search for other half-site organizations was conducted, including IR and ER organizations. Surprisingly, DR4 was the only half-site organization found to be overly represented in the TR-binding sites (Chatonnet et al., 2013), which may suggest that the DR4 TRE is the main binding site for TR/RXR heterodimer mediated gene expression.

1.2.3 Characterizing Thyroid Hormone Response Elements

Very few studies to date have attempted to use global genomics approaches to identify TREs. This may be due to the lack of a strong antibody to TR in combination with the

bioinformatics complexity associated with the identification of degenerated response elements. Some success has been achieved in characterizing TREs in *Xenopus laevis* tadpoles (Das et al., 2009). Frogs tadpoles are an effective model for the study of TH action because metamorphosis is completely dependent on TH levels. Transcriptional profiling of tadpoles treated with T3 and/or or cycloheximide (CHX – a protein synthesis inhibitor) was used to identify genes directly targeted by TH. Genes were hypothesized to be directly regulated when they were identified as being up- or down- regulated in the CHX + T3 treated group when compared to controls. RT-qPCR and electrophoretic mobility shift assays (EMSAs) were used to validate the findings. A few genes known to be directly regulated by TH/TR were identified in their study, including Kruppel-like factor 9 (*Klf9*), *Dio3* and *Thrb*. A search for TREs in the promoter regions of the genes thought to be directly TH-regulated led to identification of TREs in 67 out of the 68 promoter regions. The TRE pattern that was used for the search was (A/G)(A/G)GT(C/T)ANNNN(A/G)(A/G)GT(C/T)A and allowed for up to two mismatches when searching through the promoter regions. This study is an excellent example of experimental models/designs to identifying genes directly regulated with TH and their associated TREs. However, it is unclear if the experimental design used could be applied to mammalian models to identify genes directly regulated by TR. In addition, it is clear that a more flexible/liberal TRE search approach could be beneficial to identify TREs that are more degenerated.

In a recent study, a position weight matric (PWM) was built that was based on all known TREs motifs in mice in order to mine a ChIP-chip experiment performed on mouse cerebellum (Gagne et al., 2013). Application of the PWM search algorithm identified 85 putative TREs in the 211 ChIP-chip peaks. Although none of the putative TREs were wet-lab validated, the search

algorithm developed in this study appeared to be quite robust and could be adapted to search for various TRE half-site organizations.

1.3 Disrupting Thyroid Hormone Levels

Hypothyroidism is classically defined as a decrease in circulating T4 accompanied by an increase in TSH. It is often assumed that a significant decrease in T4 is followed by an increase in TSH levels. The technical terms for changes in T4 are hypo- and hyper- thyroxinemia, although the terms hypo and hyper-thyroidism is often used in this thesis to described changes in T4 levels alone.

Numerous adverse health effects are associated with TH imbalances. These effects are mediated by the timing, the severity and the duration of the perturbation. TH imbalances can be caused by: i) autoimmune disorders (e.g., Graves' disease, Hashimoto's disease); ii) iodine deficient diets; and iii) environmental exposures to contaminants such as polychlorinated biphenyls, bisphenol A, phthalates and polybrominated diphenyl ethers (see (Boas et al., 2006; Boas et al., 2009; Brucker-Davis, 1998; Jugan et al., 2010; Zoeller, 2010) for review).

Graves' disease (an autoimmune disease) is one of the most common causes of hyperthyroidism (Lazarus and Obuobie, 2000). Hyperthyroidism in patients diagnosed with Graves' disease is brought on by the production of an antibody that causes an increase in TSH and leads to an increase in T3 production (Brent, 2008). Hashimoto's thyroiditis, also an auto immune disease, is one of the most common causes of hypothyroidism (Lazarus and Obuobie, 2000). Hypothyroidism in patients diagnosed with Hashimoto's thyroiditis is brought on by the production of immune cells that target the thyroid gland leading to a decrease in TH production (Dayan and Daniels, 1996).

Another way that TH levels can be altered is through diet. Iodine deficiency is the most common cause of hypothyroidism and affects almost one-third of the world's population (Zimmermann, 2009). It is also the world's most prevalent yet preventable cause of brain damage (World Health Organization, 2007). A recent study on marginal iodine deficiency during development in rats found that adult offspring from dams fed iodine deficient diet showed no changes neurobehavioral assessments, although biological testing revealed that excitatory synaptic transmission was impaired (Gilbert et al., 2013). They concluded that as little as a 15% reduction of cortical T4 during fetal brain development was sufficient to cause permanent alterations to excitatory synaptic functions in adult offspring. These findings are particularly important for the regulation of chemicals that target TH-signalling since sensitive stages of development can be affected by minimal changes to TH levels.

TH disrupting chemicals (TDCs) are defined as xenobiotics that can interfere with TH action. TDCs can act through a variety of mechanisms including: i) altering the structure or function of the thyroid gland; ii) interfering with the binding of THs to TRs; iii) disrupting regulatory enzymes responsible for the production of THs; iv) altering TH transport proteins; v) modifying hepatic clearance; and vi) inhibiting deiodinases (Crofton et al., 2005). Exposure to TDCs ultimately leads to alterations in TH-mediated gene expression.

Epidemiological studies have identified a significant relationship between TH levels and exposures to various environmental chemicals (Blount et al., 2006; Boas et al., 2006). Since THs are evolutionarily conserved molecules (Heyland and Moroz, 2005), and the mechanisms by which THs exert their effect are conserved between vertebrate species (Bertrand et al., 2004; Buchholz et al., 2005), environmental chemicals that affect one species would most likely have an effect on countless others. Indeed, the effects of TDCs have been documented across a broad

array of species including fish (Crane et al., 2005; Yu et al., 2013), rodents (Crofton et al., 2005; Richardson et al., 2008), birds (Ishihara et al., 2003; Verreault et al., 2004) and crustacean (Flint et al., 2012; Iguchi et al., 2006). Thus, the potential ramifications of exposure to TDCs extend to both human and ecological health. Studies in rodents and humans have shown that severe TH deficiencies lead to somatic and brain growth retardation, although the most alarming findings suggest that even moderate or transient TH insufficiencies may result in developmental defects (Auso et al., 2004; Goodman and Gilbert, 2007; Oerbeck et al., 2007; Pop and Vulsma, 2005).

Many environmental chemicals have been proposed to act as TDCs. For example, polychlorinated biphenyls (PCBs) have structural resemblances to T4 and some act as TDCs. Many studies have documented the effects of PCB exposure on peripheral TH levels and have found that PCB exposures lead to a decrease in TH levels (Hallgren and Darnerud, 2002; van der Plas et al., 2001). Studies conducted in rats have also shown that perinatal PCB exposures cause a decrease in TH levels (Morse et al., 1996). Furthermore, PCBs can act directly on the fetus itself, rather than via induced maternal hypothyroidism alone (Gauger et al., 2004). Other chemicals that have been characterized as TDCs include dioxins, flame retardants (tetrabromobisphenol A, polybrominated diphenyl ethers and polybrominated biphenyls), nonylphenol, pentachlorophenol, bisphenol A, as well as phthalates (Boas et al., 2006; Zoeller, 2010).

Perchlorates are a class of relatively well-characterized TDCs that can be found in drinking water. Perchlorate contamination is most often associated with the release of ammonium perchlorate by military operations and aerospace programs (Urbansky, 2002). Perchlorates competitively inhibit and block the NIS in the thyroid gland (Wolff, 1998), which leads to a decrease in TH synthesis, and ultimately a decrease in circulating THs. Anti-thyroid

drugs have also been developed, such as 6-propyl thiouracil (PTU) and mercapto-methylimidazole or methimazole (MMI). Both MMI and PTU decrease TH synthesis by inhibiting TPO activity, which is required for the oxidation and incorporation of iodide molecules into tyrosine residues of Tg molecules (Crofton, 2008); PTU also decreases deiodinase activity.

The incidence of human neurological disorders (i.e. autism) has increased within the past two decades (Roman, 2007; Sadamatsu et al., 2006). Some studies suggest that this increase may be related to persistent environmental exposures to anti-thyroid agents that interfere during crucial TH-mediated developmental stages (Roman, 2007; Sadamatsu et al., 2006). Given the increase in reports of environmental chemicals targeting TH-action, it is clear that there is a need to develop an effective assay to screen for chemicals that perturb TH levels and function.

1.4 Screening Methods for Thyroid Hormone Disruptors

The current Organization for Economic Co-operation and Development (OECD) Guidance Document on Standardized Test Guidelines for Evaluating Chemicals for Endocrine Disruption does not contain an *in vitro* screen geared specifically at detecting TDC, although there are a number of *in vitro* screens to assess the ability of chemicals to disrupt estrogen and androgen action. There are a number of *in vivo* screens to detect disruption of TH action such as: i) the amphibian metamorphosis assay that looks at specific endpoints such as daily mortality and hind limb length to determine if a chemical may be interfering with the normal function of the HTP axis; and ii) the male and female rat peripubertal assays, which determines the effects of a substance on pubertal development and thyroid function (OECD Guidance Document No. 150) . The endpoints measured in the peripubertal assays to assess TH disruption are: i) thyroid

histology; ii) serum T4 level; and iii) serum TSH level. Thus, the default approach for identifying TDCs has been mostly based on assessing TH levels and thyroid histology (DeVito et al., 1999). However, chemicals that act directly on the TR may not be altering hormonal levels and could therefore remain undetected by these conventional testing methods.

There is a clear need for the development of *in vitro* screening tools that detect alterations in TR ligand binding. The general need for *in vitro* screening tools has been highlighted by the United States National Research Council in their document entitled Toxicity Testing in the 21st Century (National Academies of Sciences, 2007), which recommends a decrease in current expensive/lengthy *in vivo* toxicity testing and the incorporation of higher-throughput *in vitro* screening tools. However, carefully designed experiments are first required to examine differences between TR homodimer and the TR/RXR heterodimer and how TH interacts with the ligand binding domain (LBD) to modulate gene expression. It is currently unclear whether TREs that are composed of different half-site orientation and spacing exhibit differences in LBD interaction. Since environmental chemicals may directly interact with the LBD, investigations in this area are critical to enable an understanding of the complex transcriptional responses that occur following TDC exposure. In addition to providing data and approaches for the development of new assays to be included in the existing battery of assays for identifying TDC, such experiments would provide important information pertaining to existing knowledge gaps in this field that could lead to decreased uncertainties in regulatory decisions making.

Knowledge gaps that exist in the field include the lack of understanding: i) the key molecular mechanisms surrounding TH mediated transcription, ii) the effect of TRE half-site organization on binding partners and ligand activation, and iii) the functional role of TREs in the promoter regions.

1.5 Thesis Overview

1.5.1 Rationale

Disruption of TH is associated with adverse health outcomes (Meeker, 2012; Miller et al., 2009). Environmental contaminants that interfere with TH signaling are increasingly being reported (Boas et al., 2012). However, little is known about the TH-TR network and the underlying drivers of TH-TR gene regulation. Previous studies have typically worked with adult rodents that were often rendered hypo- or hyperthyroid for prolonged periods. In addition to missing critical developmental windows during which TH perturbations may permanently or more severely impair health, those approaches may fail to identify genes that are directly regulated by THs by focusing on chronic time points alone. Therefore, studies employing more powerful and well-validated methods are required. The use of younger rodents at developmental stages that are susceptible to TH imbalances in combination with sampling at very early time points, will enable the identification of genes directly regulated by THs and TRs.

The overall objectives of this Ph.D. thesis are:

i) To characterize global gene and microRNA expression in mouse liver at an early time point of TH perturbation in order to identify candidate genes that may be directly controlled by TH;

ii) To identify and characterize TREs found in the promoter regions of directly regulated TH-mediated genes;

iii) To identify TR binding sites found throughout the mouse genome by using ChIP-chip;

iv) To compare TRE half-site organization and its ability to drive gene expression in the presence and absence of TH and/or its dimerization partner retinoic acid; and

v) To investigate the effects of TR-antagonists on gene expression for different TRE half-site organization.

Thus, overall the work will provide important insight into TH action, TR-binding sites and TRE half-site organization.

1.5.2 Specific Objectives and Hypotheses

Chapter 2:

Hypotheses: Short-term TH perturbation causes alteration to transcripts directly regulated by TH. Genes directly regulated by TH contain TREs in their promoter regions.

Objectives: To investigate hepatic transcriptional response to transient hyper- and hypothyroidism. To identify key genes that are directly controlled by THs. To identify TREs within the promoter regions of genes found to be directly regulated by TH.

Chapter 3:

Hypotheses: TH regulates specific miRNAs that in turn alter the abundance of specific mRNAs.

Objectives: To examine hepatic perturbations of miRNAs in response to TH changes. To identify genes regulated by these TH-mediated miRNAs in order to provide a comprehensive overview of genomic TH responsiveness.

Chapter 4:

Hypotheses: (This chapter is discovery-based rather than hypothesis driven.)

Objectives: To identify TR-binding sites using ChIP-chip in combination with region-specific targeted validation. To search for TREs within these binding sites and to assess transcriptional response to TH in genes associated with the novel TR-binding sites.

Chapter 5:

Hypotheses: TRE half-site organization dictates binding partners and ability to drive gene expression. TR-antagonist binding to the TR is affected by TRE half-site organization and the dimerization partner.

Objectives: To investigate the relative ability of liganded homo- or heterodimers TR, retinoid X receptor (RXR) and TR/RXR to drive gene expression in respect to TRE half-site organization. To investigate the efficacy of a TR-antagonist in relation to TRE organization in the presence TR homodimers and TR/RXR heterodimers.

CHAPTER 2: THYROID HORMONE-REGULATED GENE EXPRESSION IN JUVENILE MOUSE LIVER: IDENTIFICATION OF THYROID RESPONSE ELEMENTS USING MICROARRAY PROFILING AND *IN SILICO* ANALYSES

Modified from: Martin A. Paquette, Hongyan Dong, Rémi Gagné, Andrew Williams, Morie Malowany, Mike G. Wade and Carole L. Yauk. (2011), *BMC Genomics*, 12:634.

2.1 Abstract

Disruption of thyroid hormone (TH) signalling can alter growth, development and energy metabolism. TH exert their effects through interactions with TH receptors (TRs) that directly bind TH response elements (TREs) and can alter transcriptional activity of target genes. The effects of short-term TH perturbation on hepatic mRNA transcription in juvenile mice were evaluated, with the goal of identifying genes containing active TREs. TH disruption was induced from postnatal day 12 to 15 by adding goitrogens to dams' drinking water (hypothyroid). A subgroup of TH-disrupted pups received intraperitoneal injections of replacement THs four hours prior to sacrifice (replacement). An additional group received only THs four hours prior to sacrifice (hyperthyroid). Hepatic mRNA was extracted and hybridized to Agilent mouse microarrays. Transcriptional profiling enabled the identification of 28 genes that appeared to be under direct TH-regulation. The regulatory regions of the genome adjacent to these genes were examined for half-site sequences that resemble known TREs. A bioinformatics search identified 33 TREs in the promoter regions of 13 different genes thought to be directly regulated by THs. TREs found in the promoter regions of torsin family 1, member A (*Tor1a*), *2310003H01Rik,* HECT domain containing E3 ubiquitin protein ligase 3 (*Hectd3*) and solute carrier family 25, member 45 (*Slc25a45*) were further validated by confirming that the TR is associated with these

sequences *in vivo* and that it can bind directly to these sequences *in vitro*. Three different arrangements of TREs were identified. Some of these TREs were located far up-stream (> 7 kb) of the transcription start site of the regulated gene. Transcriptional profiling of TH disrupted animals coupled with a novel bioinformatics search revealed new TREs associated with genes previously unknown to be responsive to TH. The work provides insight into TRE sequence motif characteristics.

2.2 Background

The thyroid participates in the regulation of basic physiological processes by producing thyroid hormones (THs), which include thyroxine (T4) and triiodothyronine (T3). THs exert their effects on growth, development and metabolism of practically every cell and organ (Yen, 2001). Their primary effect is the transcriptional regulation of target genes. This occurs when THs interact with TH receptors (TRs). Similar to other nuclear receptors, TR contains a DNA-binding domain that is capable of interacting with specific DNA sequences known as TH response elements (TREs). Typically, TREs are composed of two or more hexamer half-site sequences arranged in tandem array. TRs have the ability to bind to various imperfect TRE half-sites. The number of half-sites, the spacing between half-sites and their orientation are all features that can vary between TREs (Glass, 1994). TRs can bind to TREs as monomers or homodimers, although it is thought that TRs interact as heterodimers with the retinoid X receptor (RXR) the majority of the time (Bugge et al., 1992; Lazar et al., 1991).

Disruption of TH physiology during critically sensitive periods in development can lead to adverse outcomes. Studies have shown that severe TH insufficiencies lead to somatic and brain growth retardation (Oerbeck et al., 2007). Less severe and/or transient hypothyroidism has

also been shown to cause adverse structural and functional effects (Auso et al., 2004; Goodman and Gilbert, 2007). In humans, subclinical hypothyroidism during fetal development has been shown to result in reduced cognitive function (Haddow et al., 1999).

Exposures to a broad array of substances, including both natural and synthetic chemicals, have been shown to alter TH physiology. Environmental contaminants such as perchlorates, polychlorinated biphenyls, bisphenol A, and polybrominated diphenyl ethers have all been shown to have a negative effect on TH function, ranging from reducing circulating THs to altering TH-signalling (see (Boas et al., 2006; Boas et al., 2009; Brucker-Davis, 1998; Jugan et al., 2010; Zoeller, 2010) for review).

Much effort has been expended to identify direct transcriptional targets of TH (Das et al., 2009; Dong et al., 2009; Dong et al., 2007). Identification of the thyroid regulated transcriptome will provide insights into the molecular impact of THs in directing tissue function/development. We have previously characterized TH-regulated global gene expression in the livers of juvenile mice (Dong et al., 2007). This study evaluated transcriptional effects in animals in which TH production had been severely depressed through a relatively long-term treatment with a high concentration of an antithyroid drug (6-propyl thiouracil (PTU)). This model proved inefficient for the identification of genes directly regulated by TH as the lengthy period of treatment with antithyroid substance prevented a clear interpretation of the mode of action for altered genes. It was unclear if altered gene expression was caused by direct TH action, or due to downstream effects in the liver resulting from an altered developmental trajectory.

There is overwhelming evidence that environmental contaminants can act as endocrine disrupters with possible negative consequences for human health. However, major needs in the field include the identification of key initiating events leading to impaired development and

tissue function. In the current study, we apply a well-validated animal model and robust microarray analysis to investigate hepatic transcriptional response to transient hyper- and hypothyroidism. The transient treatment time in combination with conditions of both hyper- and hypothyroidism provide a more efficient approach to identify direct hepatic targets of THs during liver development. In addition to identifying key genes that are directly controlled by THs, the work sheds light on the TRE sequences that direct TR binding. To identify TH targets, livers were collected from juvenile mice (postnatal day (PND) 15) rendered transiently hypo- or hyperthyroid. This developmental period corresponds to a dramatic increase in circulating THs. In PND 15 mice, circulating T4 is higher than at any other age (Ahmed et al., 2008) suggesting that chemically-induced disruption of TH levels should cause a marked response in transcription. Using DNA microarrays, we identify genes that are differentially expressed between control and TH-modulated animals, and provide supporting evidence for the presence of TREs in the regulatory regions of several of these genes. Collectively, the results provide an important addition to general knowledge of the genes that are directly regulated by THs and are useful for defining an improved TRE consensus sequence.

2.3 Methods

2.3.1 Animals and Exposures

All animal care and handling was in accordance with Canadian Council for Animal Care Guidelines and was reviewed by the Health Canada Animal Care Committee prior to commencement of the study.

C57BL/6 mice were purchased from Charles River (St. Constant, QC, Canada) and were housed in hanging polycarbonate cages under a 12:12 hr light-dark cycle at 23ºC. Animals were

provided with shelters, nesting material, food *ad libitum* (Purina rodent chow 5010; Ralston-Purina, St. Louis, MO, USA) and drinking water containing 1 % (wt/vol) sucrose (*ad libitum)*. Mice were acclimated for 10 days. Breeding was accomplished by transferring two sexually mature female mice (eight weeks post natal) into the home cage of a sexually mature (10 weeks post natal) male. After four nights of co-housing, each female was transferred to a separate cage. Dams were allowed to litter naturally and pup numbers were not adjusted. To produce hypothyroid (hypo) pups, dams were provided with drinking water that contained methimizole (MMI, 0.05 % wt/vol) and perchlorate (1 % wt/vol) for three days (PND 12 to 15). To produce hyperthyroid (hyper) pups, intraperitoneal injections (i.p.) of THs (50 μg of T4 + 5 μg of T3 per 100 g body weight) were administered to pups on PND 15, four hours before decapitation and tissue collection. For the hypothyroid/replacement group (hypo+); dams were provided with drinking water that contained MMI (0.05 % wt/vol) and perchlorate (1 % wt/vol) for three days (PND 12 to 15). Pups then received *i.p.* injections of THs (20 μg of T4 + 2 μg of T3 per 100 g body weight) on PND 15, four hours before decapitation and tissue collection. The control and hypo groups received saline *i.p.* injections four hours before decapitation and tissue collection.

2.3.2 Tissue Collection, RNA Extraction and Purification

On PND 15, pups were sacrificed by decapitation. Serum prepared from trunk blood using serum separator tubes (BD Biosciences, Mississauga, ON, Canada) was used for T4 analyses by radioimmunoassay (RIA) kits (MP Biomedicals, Medicorp, Montreal, QC, Canada) as per the manufacturer's instructions. The hypo + group was subdivided into two sub groups – hereafter called hypo+ and hypo++ - based on measured serum T4 levels. Animals allotted to the hypo++ group had serum T4 levels that approximated those seen in the hyperthyroid group while

those that remained as hypo+ had T4 levels near or slightly in excess of control levels. Statistical significance was determined by one way ANOVA followed by Tukey's HSD test. The detection limit or sensitivity of the RIA is 0.76 μg/dL, as determined by the manufacturer (MP Biomedicals, Medicorp).

Pup livers were rapidly dissected and flash frozen in liquid nitrogen. Total RNA was extracted from liver samples with TRIzol reagent (Invitrogen, Burlington, ON, Canada) followed by RNeasy Mini Kit (Qiagen, Missisauga, ON, Canada) clean-up according to the manufacturer's instructions. RNA quality assessment was determined by Nanodrop (Thermo Scientific, Billerica, MA, USA) and Agilent 2100 Bioanalyzer and RNA 6000 NanoLab Chip Kit (Agilent Technologies, Mississauga, ON, Canada). All samples had 260/280 ratios over 2.1, and RNA integrity numbers over 9.0.

2.3.3 Microarray Hybridization

Hepatic gene expression was assessed by hybridizing samples to Agilent 4x44k Whole Genome Microarrays (G4122F) using a reference design (details below). Briefly, 200 ng of total RNA from the liver was used to synthesize double-stranded cDNA and cyanine labelled cRNA. Experimental samples were labelled with Cyanine 5-CTP and reference RNA (universal mouse RNA; Agilent Technologies) with Cyanine 3-CTP (Perkin-Elmer Life Sciences, Woodbridge, ON, Canada) according to the manufacturer's instructions (Agilent Linear Amplification, Agilent Technologies). Cyanine labelled cRNA targets were *in vitro* transcribed using T7 RNA polymerase and purified using RNeasy Mini Kit (Qiagen). Experimental and reference samples (825 ng each) were hybridized to arrays at 60ºC for 17 hours. Slides were washed and scanned on an Agilent Microarray Scanner (G2565CA). The data were acquired using Agilent Feature

Extraction software version 10.1.1.1. Prior to statistical analysis, the scans were inspected using the Agilent Quality Control report as well as an internal quality control metric including spike-in RNA controls.

2.3.4 Experimental Design and Statistical Analysis of Microarray Data

The Agilent 4x44k Whole Genome Microarray features four sub-arrays per slide. A reference design (Kerr, 2003; Kerr and Churchill, 2001) with sub-arrays as blocks of size two (each block containing the corresponding reference: Cy3=green, and sample: Cy5=red channels) was used to analyze the median signal intensities of the two-color microarray data. The experiment included the main effects of treatment groups (four conditions: hyper, hypo, hypo+, and one control) plus the sub-array as a block term. Five biological replicates per condition were used for three of the four groups, while four replicates were used for the remaining hypo+ condition (due to a shortage of animals with suitable serum T4 levels in that group), yielding a total of 19 microarrays. An identical experimental structure was followed for each gender. Separate statistical analyses were carried out for the male and female samples, respectively, to eliminate any correlation effect due to the dam as samples within genders were independent.

All pre-processing of the data was conducted using R. The data were normalized using loess normalization (Yang et al., 2002) in the R library "MAANOVA". Background fluorescence was measured using the (-)3xSLv1 negative control probes; probes with median signal intensities less than the trimmed mean (trim = 5 %) plus three trimmed standard deviations of the (-)3xSLv1 probes were flagged as absent (within the background signal). Ratio intensity plots (also known as MA plots) were constructed for the raw and normalized data for each array. Boxplots and hierarchical clustering using average linkage were generated to identify outlier arrays (Shieh and

Hung, 2009). Two outlier microarrays were removed from each data set (two microarrays from male samples and two from female samples) based on separate hierarchical clustering of each dataset into sample=Cy5 and reference=Cy3 groups. As a result, the final analysis was based on 17 microarrays for females, and 17 for males.

Genes that were up- and down-regulated in any of the three treatment groups (hyper, hypo, and hypo+) relative to control were identified using the R library "MAANOVA" (Wu et al., 2003). The required ANOVA model was fitted to include the main effects of dose plus the sub-array as a block term. The Fs statistic (Cui et al., 2005), a shrinkage estimator, was used for the gene-specific variance components, and the associated p-values for all the statistical tests were estimated using the permutation method (30,000 permutations with residual shuffling). These p-values were then adjusted for multiple comparisons using the false discovery rate (FDR) approach (Benjamini et al., 2001). All data are available through the Gene Expression Omnibus (GEO) website, accession number: GSE21307.

The least squares mean (Goodnight and Harvey, 1978; Searle et al., 1980), a function of the model parameters, was used to estimate the fold-change for each pairwise comparison of interest (control versus each of the three treatment groups: hyper, hypo, and hypo+.)

2.3.5 Bioinformatics

Promoter regions (-8 kb to +2 kb relative to the transcription start site (TSS)) of genes whose expression profile suggested direct regulation by THs were downloaded from the UCSC Genome Browser (mm9 assembly). Using a list of validated mouse TREs gathered from the literature, a position weight matrix (PWM) was developed to score the information content (bits) for position one to six of TRE half-sites. In this way, each TRE half-site was assigned a ‘score’

against the PWM. The score for each TRE half-site was obtained iteratively by leaving the subject out of the PWM construction. Previous bootstrapping analysis of the validated TREs in mice revealed a difference ($p < 0.001$) between the distribution of scores for the two half-site scores. Cross-validation of the TREs from the literature was carried out with each half-site analyzed separately. This analysis revealed that a low threshold score (i.e., ≥ 3.76 bits) for one half-site and a high threshold score (i.e., ≥ 6 bits) for the second half-site (regardless of half-site order) allowed minimization of type I and type II errors (manuscript in preparation). We therefore used the cut-off scores identified in this cross-validation exercise and scanned the promoter regions for putative TREs. The scan searched for three different types of TREs: direct repeats with a four nucleotide spacer (DR4); inverted repeats with no spacer (IR0); and everted repeats with a spacer of six nucleotides (ER6).

Orthologs in humans and in rats were matched using BioMart (www.biomart.org) for the genes that were identified as having potential TREs in mice. Promoter regions (defined as -8 to +2 kb of the TSS) for these orthologous genes were obtained. A local alignment using a sliding window principle was used to align the TREs identified in mice to the promoter regions of the corresponding orthologous genes in rats and humans. A modified substitution matrix favouring conservation of the guanine in position two and three of the TRE hexamer half-sites was used, since these two sites appear to be highly retained. Three additional features were used to filter identified TREs: i) a maximum mismatch of two when comparing mouse to rat, and mouse to human, ii) a maximum distance of 2 kb between TREs when comparing mouse to rat and mouse to human, and iii) a minimum score determined by the PWM scan.

2.3.6 Gene Ontology Analysis and Principal Component Analysis

Genes with FDR corrected p-values smaller than 0.05 in at least one experimental condition were used for principal component analysis (PCA) and pathway/ontology analysis. PCA was carried out using mean centering and scaling on data from genes that were significant in at least one treatment group using Genespring GX 7.3.1 (Agilent Technologies). Mean fold-change, averaged across all replicates per sex per treatment, was subjected to functional enrichment and Gene Ontology (GO) analysis using Ingenuity Pathway Analysis (Ingenuity Systems Inc., Redwood, CA, USA).

2.3.7 Real-Time Quantitative PCR Analysis

Total RNA was reverse transcribed into cDNA using SuperScriptIII (Invitrogen) as per the manufacturer's instructions. iQ SYBR Green Supermix (BioRad Laboratories, Mississauga, ON, Canada) was used with a reaction volume of 50 μL. All primers were designed using Beacon Designer 7 (Premier BioSoft International, Palo Alto, CA, USA). Hypoxanthine phosphoribosyltransferase 1 (*Hprt*) was used as the reference gene. Microarray analysis and RT-qPCR analysis confirmed that *Hprt* expression was stable across all groups. Reactions were carried out in 96-well plates. PCR were done in duplicate and each plate contained all samples for the gene of interest and reference gene for one sex. Analysis was carried out using a CFX96 Real-Time PCR Detection Systems (BioRad Laboratories). Melting curves were performed for each reaction to ensure primer specificity. Raw data were up-loaded into Relative Expression Software Tool 2009 (REST 2009; Qiagen). where fold-changes and p-values were calculated.

2.3.8 ChIP-PCR

Livers from the male euthyroid control group were used for the ChIP using the EZ ChIP kit (Millipore Corporation, Toronto, ON, Canada), according to the manufacturer's instructions. Briefly, a small piece of liver was homogenized with a hand-held homogenizer in 250 µL PBS containing broad-spectrum protease inhibitors, and was then cross-linked with 1 % formaldehyde. Cross-linking was stopped with glycine and nuclei were collected by adding lysis buffer. To ensure that DNA fragments ranged from 200 to 600 bp, the nuclear solution was sonicated in an ice bath with 30 second bursts at 28 % amplitude. Fifteen bursts were completed, each separated by a 60 second period. DNA fragment size was verified by agarose gel electrophoresis. Six percent (about 100 µL) of the sonicated solution was stored at -20 ^{o}C as total input (TI), while the remainder was incubated with anti-TRβ polyclonal antibody (PA1-213, clone TRβ-62, Affinity BioReagents, Golden, CO, USA) overnight with agitation at 4 ^{o}C. Antibody-bound chromatin was precipitated with Protein G conjugated agarose beads, washed with gradient stringent buffers, and eluted with elution buffer as per the manufacturer's instructions. Both the eluted solution and the stored TI were incubated at 65 ^{o}C overnight to reverse cross-links. Immunoprecipitated (IP) DNA and TI DNA were purified by treatment with RNase, proteinase K and multiple phenol:chloroform:isoamyl alcohol (25:24:1) extractions. Equivalent amounts of IP DNA and TI DNA were amplified in parallel, using a random primer method with GenomePlex Complete Whole Genome Amplification Kit (Sigma-Aldrich, Oakville, ON, Canada). Amplified DNA was then purified using GenElute PCR Clean-Up kit (Sigma-Aldrich).

Primers targeting the TRE identified by bioinformatics analysis were designed using Beacon Designer 7. PCRs were performed using Expand High Fidelity PCR System (Roche,

Laval, QC, Canada). Actin beta (*Actb*) (NM_007393.3) was used as a negative control and MLX interacting protein-like (*Mlxipl*) (NM_021455.3) was used as a positive control (Hashimoto et al., 2009). Gel analyses and band quantifications were carried out using GeneTools (Syngene, Frederick, MD, USA). Binding ratios were calculated by dividing the ratio of IP/TI from the gene of interest by the ratio of IP/TI from the reference gene *Actb*. Mean enrichment, standard deviations, and p-values were calculated using log ratios and were then back-transformed.

2.3.9 Electrophoretic Mobility Shift Assays

Probes were designed against the specific genomic regions of the newly identified TREs. Probe size ranged between 26 and 30 bp. The probe contained the putative TRE sequence plus six to seven nucleotides on each side. Oligonucleotides were labelled using Biotin 3' End DNA Labeling Kit (Thermo Scientific) as per the manufacturer's instructions and were then annealed. Binding reaction and detection of complexed biotin-labeled DNA-protein was accomplished using the LightShift Chemiluminescent electrophoretic mobility shift assays (EMSA) Kit (Thermo Scientific) as per the manufacturer's instructions. Binding reactions were carried out in 20 µL volumes and had final concentrations of 2.5 % glycerol, 5 mN $MgCl_2$, 50 ng/µL Poly (dI•dC) and 0.05 % NP-40. One µg of chicken TRα (Santa Cruz Biotechnology Inc., Santa Cruz, CA, USA) was used per reaction. An amino acid alignment of the TRα DNA-binding domains from *Mus musculus* and *Gallus gallus* showed an approximate 98 % sequence similarity. Amino acids involved in direct base contacts (Rastinejad et al., 1995) were specifically examined and were not found to be substituted between species. We have previously found that TRα and TRβ interact with TREs in a very similar manner (Dong et al., 2007). Amino acid alignment of DNA-binding domains showed an approximate 86 % sequence similarity between the TR isoforms.

Amino acids involved in direct base contacts (Rastinejad et al., 1995) were specifically examined and showed 100% conservation between the two isoforms.

Biotin end-labelled target DNA was diluted 1:4 and 2 µL were used per reaction. Unlabeled probes were used at a 200-fold molar excess compared to labelled probe. For the supershift, 2 µg of antibody TRα/β (Santa Cruz Biotechnology Inc.) or normal mouse IgG (Santa Cruz Biotechnology Inc.) were used per reaction. Samples were run on a 5 % polyacrylamide gel, transferred onto Biodyne Precut A Nylon Membranes (Thermo Scientific) by electrophoretic transfer and UV-cross-linked. Membranes were scanned using ChemiDoc XRS+ (BioRad Laboratories) and images analyzed using Image Lab version 2.0.1 (BioRad Laboratories)

2.4 Results

2.4.1 Validation of the MMI/sodium Perchlorate Mouse Model

Serum T4 levels in all PND 15 pups were measured (Figure 2.1). A significant increase was observed in the hyper pup group compared to control levels, whereas a significant decrease was observed in the hypo pup group compared to control levels. The hypo+ and hypo++ pup groups also showed a significant increase in serum T4 compared to control. The hypo++ pup group received the same doses of THs in the *i.p.* injection as the hypo+, but registered higher levels of circulating T4 (levels similar to the hyperthyroid pup group). Levels of T4 in hyperthyroid and hypo++ groups were not significantly different. Part of this data has already been reported (Dong et al., 2010).

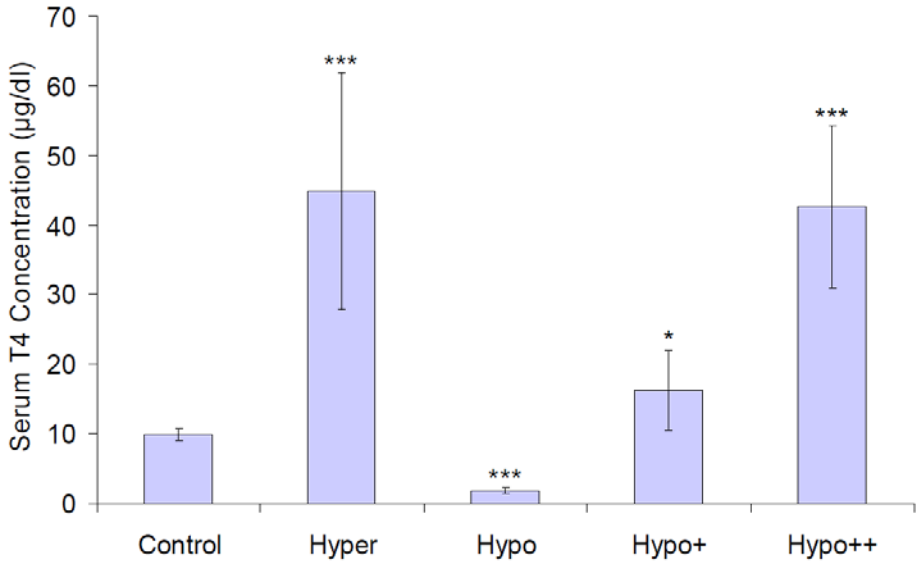

Figure 2.1. PND 15 pup serum T4 levels after short-term TH perturbation. Means are presented as well as ± standard deviations. n=10, 5 from each sex, for control, hyper and hypo; n=8, 4 from each sex for hypo+; n=5, males only for hypo++. All treatment groups were compared to controls. Statistical significance was determined by one way ANOVA followed by Tukey's HSD test; * $p \leq 0.05$, *** $p \leq 0.001$.

2.4.2 Genes Significantly Altered by TH Perturbations

MAANOVA analysis identified approximately 400 significantly altered genes in male and/or female pups, with a FDR-adjusted $p < 0.05$ in at least one of the treatment conditions (see Supplementary Table 2.1 for male data and Supplementary Table 2.2 for female data). Fold-changes ranged from 1.1 to 13.8, and averaged approximately 1.6. In hypo mice, 215 genes were significantly altered relative to euthyroid controls. Of these, transcription levels of 118 genes were reduced and 97 were increased in hypo livers relative to controls. In the hyperthyroid group, 204 genes were significantly altered. Of these, transcript levels of 45 genes were reduced and 159 were increased relative to controls. In the hypo+ group, 68 genes were significantly altered with 14 reduced and 54 increased. Females exhibited more significantly altered genes than males. Females had 300 significantly altered genes whereas males had 185. A comparison of these two lists revealed that there were 100 genes that were differentially expressed by at least one treatment condition in both females and males (i.e., 100 genes in common between the sexes).

Using the full set of significant genes (FDR-adjusted $p < 0.05$) for all groups (control, hyper, hypo and hypo+), a principal component analysis (PCA) was conducted (Figure 2.2). This analysis revealed that expression patterns were highly correlated within sexes and treatment groups. The PCA revealed distinct male and female clusters (Figure 2.2A) and four clusters were also found to separate control, hyper, hypo and hypo+ groups. Thus, the expression profiles reveal both an overall treatment as well as sex effect, with both sexes showing similarities in their response within treatment groups.

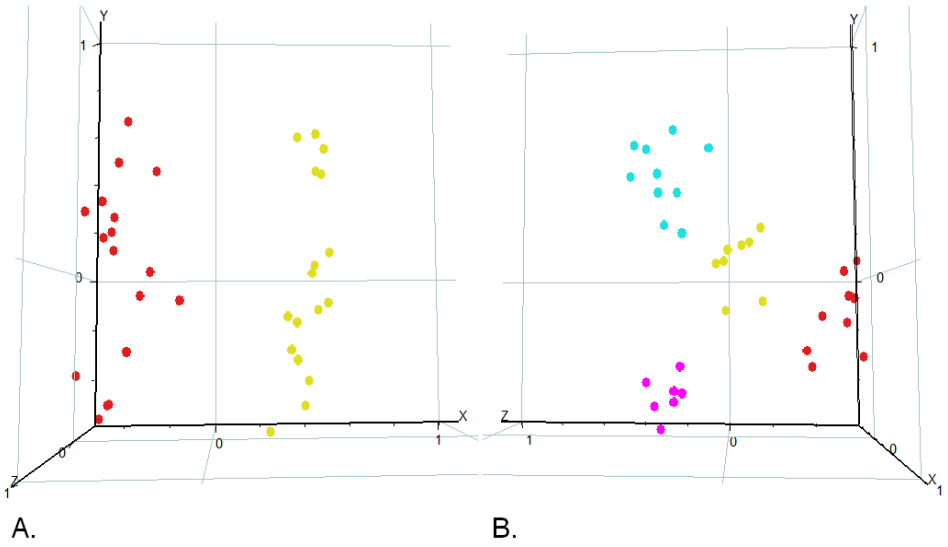

Figure 2.2. Principal component analysis of microarray data carried out with the full set of significant genes (FDR-adjusted $p \leq 0.05$) for all groups (control, hyper, hypo and hypo+). Data are coloured by sex (A) and by treatment group (B). In panel (A) male data points are in red and female data points are in yellow, and in panel (B) control data points are in yellow, hypothyroid data points are in red, hyperthyroid data points are in cyan and hypothyroid/replacement (hypo+) data points are in fuchsia.

The list of all significant genes was subjected to GO and pathway analysis. The analysis revealed several pathways that were significantly altered by the treatment. The five most affected pathways are presented in Supplementary Table 2.3, along with the names of the genes that were affected by TH treatment within the pathway. Many genes were found to be involved in oxidative stress response and xenobiotic metabolism/signalling. A group of genes involved in TR/RXR activation was also identified.

By comparing the response profile of genes that were significantly altered in the hyper, hypo and hypo+ groups, we identified a subset of genes that are most likely to be directly regulated by TH rather than by downstream effects. For example, a directly regulated gene would be expected to show similar responses in the hyper and hypo+ groups, and should be in the opposite direction to the hypo group. The hypo+ group is particularly informative, as these animals were sacrificed four hours after a single injection of TH, but following a more prolonged state of hypothyroidism. In addition, genes showing similar responses in hypo and hypo+ groups would be less likely to be directly regulated by TH. Genes showing a pattern suggesting direct regulation by TH are listed in Table 2.1.

Table 2.1. Genes identified as being directly regulated by THs.

		Hypo		Hyper		Hypo+	
Accession	**Gene**	♂	♀	♂	♀	♂	♀
NM_027980	*2310003H01*			1.4	1.4	1.3	
AK014609	*4633401B06*				1.4	1.6	1.7
AK044145	*AK044145*			2.6	2.7	2.1	1.9
NM_025404	*Arl4d*			2.0		2.0	
NM_177047	*Auts2* *			3.1	3.0	2.5	2.5
NM_145603	*Ces2*			1.5	1.4		1.5
NM_134141	*Ciapin1*			1.4	1.4	1.3	
NM_026424.3	*Coq10b*				1.5	2.0	
NM_00102538	*DXBay18*		-1.7	2.2	1.7	2.6	2.3
NM_175266	*Epm2aip1*			1.3	1.3	1.3	
NM_008058	*Fzd8*			1.8	1.5	1.6	
NM_153528	*Gramd1c*			1.6	1.7		1.4
NM_175244	*Hectd3*				1.3		1.4
NM_010544	*Ihh* *				-1.2		-1.2
NM_008358	*Il15ra*				1.2		1.3
NM_178701	*Lrrc8d*			1.6	1.4	1.6	
NM_172821	*Map3k13*			1.6		1.7	
NM_027418	*Mapk6*			1.3	1.4		1.3
NM_027997	*Serpina9* *				-1.7		-1.9
NM_008018.4	*Sh3pxd2a*			1.7	1.7	1.5	1.5
NM_134154	*Slc25a45* *	-1.7	-1.6	1.7	1.9	1.5	1.6
NM_172463	*Sned1* *	-1.6	-1.6	1.5	1.5	1.5	1.4
NM_00108110	*Stim2*			1.9	2.0	1.5	
NM_173038.2	*Tbcel*			1.3	1.3	1.3	1.4
NM_144884	*Tor1a*				1.2	1.3	
NM_145076	*Trim24* *	-1.4	-1.6	1.6	1.4	1.5	
NM_153162	*Txnrd3*				1.2	1.3	
XM_00148128	*Wipf3*	-1.4		1.4		1.3	

Fold-changes for males and females are presented in comparison to control animals. All fold-changes have an adjusted $p \leq 0.05$. Asterisks (*) denote genes that were analyzed by RT-qPCR. See Supplementary Table 2.1 and File 2.2 for p-value data.

2.4.3 Microarray Data Validation and Hypothyroid Replacement Analysis

Microarray data were validated using real time RT-qPCR for subsets of significantly altered genes (FDR $p < 0.05$). First, we investigated the responses of three genes that have previously been shown to be directly regulated by TH (thyroid hormone responsive SPOT14 (*Thrsp*), deiodinase, iodothyronine, type I (*Dio1*) and malic enzyme 1, NADP(+)-dependent, cytosolic (*Me1*); Table 2.2). Some of these genes were only significant with RT-qPCR (e.g. *Dio1* in hyper males and females was not identified as differentially expressed on the microarray; Table 2.2). Thus, the data produced by the microarray analysis are likely to be conservative, and include some false-negatives.

Second, we validated several genes suspected of being directly regulated by TH using RT-qPCR. For this analysis, we compared gene expression changes in the four treatment groups, as well as in a group of animals subjected to the hypo+ treatment but whose circulating T4 levels were substantially higher than those in the hypo+ animals used for microarray analysis (i.e., the hypo++ group). Here we present the results from the hypo+ and hypo++ groups when compared to control data (Table 2.3). The direction of fold-change was consistent with the microarray data for each of the nine genes selected for RT-qPCR validation. A significant fold-change in the hypo++ group was observed in all genes evaluated except for torsin family 1, member A (*Tor1a*) and tripartite motif containing 24 (*Trim24*).

Table 2.2. Microarray and RT-qPCR results for known TH-regulated genes.

		Microarray		RT-qPCR	
Gene	**Group**	**FC**	**p-value**	**FC**	**p-value**
Male Pups					
Thrsp	Hypo	**-2.8**	**0.036**	**-5.0**	**0.032**
	Hyper	1.6	0.999	2.4	0.170
Dio1	Hypo	**-2.6**	**0.000**	**-4.9**	**0.015**
	Hyper	1.3	0.999	**1.5**	**0.029**
Me1	Hypo	-1.4	0.379	-1.4	0.099
	Hyper	1.3	0.632	**1.5**	**0.017**
Female Pups					
Thrsp	Hypo	**-2.7**	**0.000**	**-5.0**	**0.033**
	Hyper	**2.4**	**0.019**	**4.6**	**0.010**
Dio1	Hypo	**-3.2**	**0.000**	**-7.8**	**0.001**
	Hyper	1.2	0.983	**1.5**	**0.008**
Me1	Hypo	**-1.4**	**0.045**	-1.3	0.143

Fold-changes are presented for treated animals relative to control animals; n=4 for all groups except for hyper, where n=5. Fold-changes (FC) and p-values are in bold when $p \leq 0.05$.

Table 2.3. Microarray and RT-qPCR results for the male hypo+ and male hypo++ treatment groups.

		Microarray		RT-qPCR	
Gene	**Group**	**FC**	**p-value**	**FC**	**p-value**
Slc25a4	Hypo+	**1.5**	**0.000**	1.6	0.314
	Hypo++			**2.4**	**0.000**
Hectd3	Hypo+	***1.4**	**0.000**	***2.4**	**0.026**
	Hypo++			**1.7**	**0.005**
H01Rik	Hypo+	**1.3**	**0.026**	**2.8**	**0.011**
	Hypo++			**1.4**	**0.008**
Tor1a	Hypo+	**1.3**	**0.026**	1.6	0.117
	Hypo++			1.1	0.501
Auts2	Hypo+	**2.5**	**0.000**	**5.3**	**0.006**
	Hypo++			**5.6**	**0.002**
Serpina	Hypo+	***-1.9**	**0.000**		
	Hypo++			**-5.0**	**0.000**
Sned1	Hypo+	**1.5**	**0.000**	**2.4**	**0.027**
	Hypo++			**2.4**	**0.041**
Trim24	Hypo+	**1.5**	**0.000**	2.9	0.398
	Hypo++			1.5	0.352
Ihh	Hypo+	***-1.2**	**0.047**		
	Hypo++			**-2.0**	**0.041**

The hypo++ group was not included in the microarray analysis. The fold-changes represent treated relative to control animals; for RT-qPCR data n=5 for each group. Fold-changes (FC) and p-values are in bold when $p \leq 0.05$. Asterisks (*) denote that the data were taken from female pups due to the absence of significant data from male pups. H01Rik corresponds to *2310003H01Rik*. Absence of data for RT-qPCR values were because of undetectable signal due to low expression level.

2.4.4 Bioinformatics Analysis of Direct TH-Regulated Genes

A search for TREs in the 28 regulatory regions of genes suspected to be under direct TH-regulation (Table 2.1) identified 196 TREs in 24 different genes. When locally aligned with the rat promoter region of the corresponding orthologs, the list was reduced to 68 TREs in 20 different genes. Once this was accomplished, the remaining TREs were locally aligned with the human promoter region of the corresponding orthologs to produce the final list of 33 TREs found in 13 different genes (Table 2.4). The candidate TRE sequences in rats or humans were within 2 kb of the relative distance of the putative TRE identified in mice, and had two or less mismatches when compared to the mouse TRE. Thus, this final list of 33 TREs provides the most likely candidate TRE-containing promoters that may be conserved between mice, rats and humans.

Table 2.4. TREs identified using bioinformatics searches of promoter regions of genes characterized as being directly regulated by THs.

		Mouse		Rat			Human		
Gene	**Type**	**Pos.**	**TRE**	**Pos.**	**TRE**	**MM**	**Pos.**	**TRE**	**MM**
H01Rik ‡	DR4	1597	**GGGTCA**CCAG**GGGCTA**	1513	**GGGTCA**CCAG**GGGCTA**	0	1709	**GGGTCA**CCAG**GGGCTG**	1
H01Rik ‡	DR4	-5778	**AGGGCA**GCAG**AGCTGA**	-5806	**AGGGCA**GCAG**GGCTGA**	1	-7091	**AGGGGC**AGGC**AGCTGA**	1
							-4046	**AGGGAA**AGAC**AGCTCA**	2
H01Rik ‡	DR4	281	**AGGTCA**GGCG**AGGGCA**	243	**AGGTCA**GGCG**AGGGCA**	0	1176	**TGGTCA**GGCC**TGGGCA**	2
H01Rik ‡	IR0	-2311	**AGGTGAAGCCCT** *	-2421	**AGGTGAAGCCCT**	0	-3415	**CGGTGAAACCCT**	2
Arl4d	DR4	-2529	**AGGCCA**GCCA**GGGCTA**	-1594	**AGGCTA**GCCT**GGGCTA**	1	-1286	**AGGCCT**CAAA**GGGCTT**	2
							-922	**AGGCCG**ATGT**GGGCGA**	2
Ces2	DR4	-5950	**AGGCAA**AGCA**AGGTCT**	-7139	**AGGCAA**CTGC**AGGTTT**	1	-7548	**AGGCAA**AAGC**TGGGCT**	2
							-7219	**TGGCAA**TCTG**AGCTCT**	2
							-4185	**AGCTAA**GCCA**AGGTCT**	2
Fzd8	DR4	-143	**CGGTCA**CCCC**AGGAGA**	6	**CGGTCA**CCCC**AGGAGA**	0	399	**CGGTCG**GGCC**AGGCGA**	2
Hectd3	ER6	-7433	**TGGCCT**GAAGAT**AGGACA** *	-6784	**TGGCCT**CTCCTA**TGGACA**	1	-7570	**TGGCCT**ACAACC**AGGATA**	1
							-6806	**GGGCCA**ATGCTC**AGGACA**	2
Hectd3	DR4	-3516	**AAGTCA**CCTG**AGGAGA**	-5475	**AAGTCA**CCTG**AGGAGA**	0	-2992	**AAGTCA**TTTG**GGGAAA**	2
Ihh	ER6	-5766	**TGACCT**TTATGC**AAGTCA**	-6131	**TGACCT**TTATTC**AAGTCA**	0	-4898	**CCACCT**CTGTTC**AAGTCA**	2
Serpina9	DR4	31	**AGGACA**ACAA**GGGCGA**	31	**AGGACA**ACAA**AGGCGA**	1	167	**AGGACA**GGGC**AGGAGA**	2
Slc25a45	DR4	-4642	**AGGATT**CTAA**GGCCA** *	-5175	**AGGATT**CTAT**GGCCA**	1	-6373	**AGGTTT**GCAA**TGGCCA**	2
Sned1	DR4	409	**AGGTGG**AATG**AGGACA**	317	**AGGTGG**AATG**AGGACA**	0	332	**AGGTGG**AATG**AGGACA**	0
							-864	**AGGTGG**GGGC**AGGACT**	1
Sned1	ER6	217	**TCACCC**CGAAGC**AGGACG**	125	**TCACCC**CGAAGC**AGGACG**	0	125	**TCACCC**CCAAGC**AGGACG**	0
Tbcel	DR4	15	**GGGTCA**GCAT**AGGACA**	-7	**GGGTCA**ATGC**AGGACA**	0	15	**GGGTCA**ATGC**AGGACA**	0
Tbcel	IR0	920	**AGGACAAGTCCC**	891	**AGGACAAGTCCC**	0	649	**AGGACATGTCCC**	1
							1157	**GGGACAAGCCCC**	2
							470	**GGGACCAGTCCC**	2
Tbcel	DR4	1361	**AGGCCA**GCCT**GGGCTA**	1371	**AGGCCA**GCCT**GGGCTA**	0	-230	**AGGACA**ATAG**GGGCTG**	2
Tor1a	DR4	-2364	**AGGACA**GCCA**GGGCTA** *	-4242	**AGGAAA**CACA**CGGCTA**	2	-1610	**AGGATA**CTCC**GGGCTC**	2
Tor1a	DR4	1648	**AGGTTA**GTCT**GGGCTA**	1638	**AGGTTA**GTCT**GGGCTG**	1	552	**CGGTTG**GCTG**GGGCTA**	2
Tor1a	DR4	-2729	**AGGACA**GCCA**GGGCTA**	-4242	**AGGAAA**CACA**CGGCTA**	2	-1610	**AGGATA**CTCC**GGGCTC**	2
Tor1a	DR4	-4783	**AGGCCA**CTTC**AGGTTG**	-6425	**AGGCCA**GAAG**AGGGTG**	1	-6272	**AGGCCA**AGGC**AGGAGG**	2
							-6628	**AGGCCA**GGCA**CGGTGG**	2
Trim24	DR4	295	**AGGACA**ATGG**AGGTGG**	-5	**AGGACA**ATGG**AGGTGG**	0	336	**AGGACA**ATGG**AGGTGG**	0
Txnrd3	IR0	372	**GGGTGATGATCT**	362	**GGGTTATGATCT**	1	1423	**GGGTGGTGATCT**	1
							1876	**GGGTGATAACCT**	2
Previously Characterized									
Klf9 [a]	DR4	-3804	**AGGTGA**AGTG**AGGTCA**	-3819	**AGGTGG**GGCG**AGGTCA**	1	-2875	**AGATTG**TCTG**AGGTTA**	4
Mbp [b]	ER6	-192	**GGACCT**CGGCTG**AGGACA**	-138	**GGACCT**CGGCCG**AGGACA**	0			

TREs were found to be conserved between mice, rats and humans (i.e., within 2 kb of the mouse TRE and with 2 or less mismatches (MM) when compared to the mouse TRE). MMs were only considered in the bolded half-sites. Positions (Pos.) of the TREs are presented in reference to the transcription start site of the associated gene. Two previously characterized TREs are presented at the bottom of the table. * TREs validated by ChIP-PCR. ‡ Corresponds to *2310003H01Rik*. [a] Characterized by (Denver and Williamson, 2009a). [b] Characterized by (Farsetti et al., 1997; Farsetti et al., 1991); bolding of half-sites and positions of TRE were corrected.

ChIP-PCR Analysis

ChIP-PCR, using euthyroid livers, was performed to validate TR-TRE binding of six TREs selected from the list of genes thought to contain conserved TREs (Table 2.4). TRβ-1 antibody was used to precipitate the protein-DNA complexes followed by PCR analysis to compare TI (not precipitated) to IP samples. Antibody specificity has previously been demonstrated (Dong et al., 2009). *Mlxipl* was used as a positive control as it binds TR in its promoter region, whereas *Actb* was used as a negative control. Mean enrichment of *Mlxipl* compared to *Actb* is shown as well as the individual enrichment of the three biological samples (Figure 2.3A). TREs identified in the promoter regions of *Tor1a*, *2310003H01Rik*, HECT domain containing E3 ubiquitin protein ligase 3 (*Hectd3*) and solute carrier family 25, member 45 (*Slc25a45*) were enriched by 4-fold or more in the IP compared to TI (Figure 2.3B-E). Candidate TREs analyzed in the promoter regions of indian hedgehog (*Ihh*) and ADP-ribosylation factor-like 4D (*Arl4d*) showed no apparent enrichment in the IP samples (data not shown).

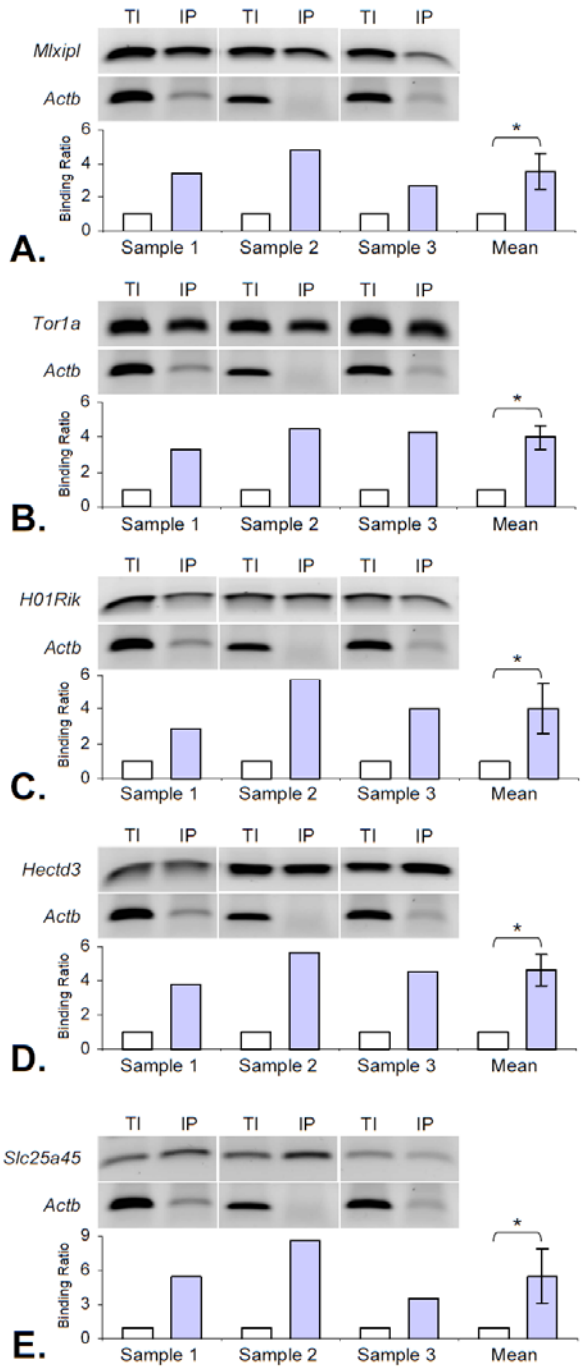

Figure 2.3. Relative enrichment of newly identified TREs determined by ChIP-PCR. The top half of each section shows the amplicons run on an agarose gel, and the bottom half shows relative enrichment of the immunoprecipitated (IP) samples and the total input (TI) samples when compared to *Actb* enrichment. ChIP-PCR validation of negative (*Actb*) and positive

(*Mlxipl*) controls are presented in section (A). Sections (B) to (E) show enrichment of *Tor1a*, *H01Rik* (*2310003H01Rik*), *Hectd3* and *Slc25a45*. Asterisks (*) denote a significant difference, $p \leq 0.05$, determined by Student's t-test. The mean enrichments (± standard deviations) are also presented for each section. All presented immunoprecipitated enrichments were significant ($p \leq 0.05$ determined by Student's t-test) when compared to total input, except for *Actb*.

2.4.5 Electrophoretic Mobility Shift Assays

EMSAs were used to demonstrate the ability of the suspected TREs to bind to the TR. A DR4 containing two perfect half-sites (AGGTCA) was used as a positive control and showed a shift in electrophoretic mobility and a decrease in detection (30-fold decrease) when unlabelled probe was added (Figure 2.4). The DR4 positive control tested with an antibody against TRα/β exhibited a decrease in signal (7-fold decrease) of the shifted bands, and a slightly detectable supershifted band. In contrast, the non-specific mouse IgG antibody showed no reduction in detection of the shifted bands. Probes with sequences of suspected TREs associated with the genes *Slc25a45*, *Hectd3* and *Tor1a* all showed a shift in electrophoretic mobility, as well as a decrease in detection when unlabelled probe (24, 17 and 2.5-fold decrease, respectively) or unlabelled DR4 positive control probe (92, 68 and 20-fold decrease respectively) was added (Figure 2.4). Thus, the EMSA results help to support the idea that the TR can bind to putative TREs in the promoter regions of *Slc25a45*, *Hectd3* and *Tor1a*.

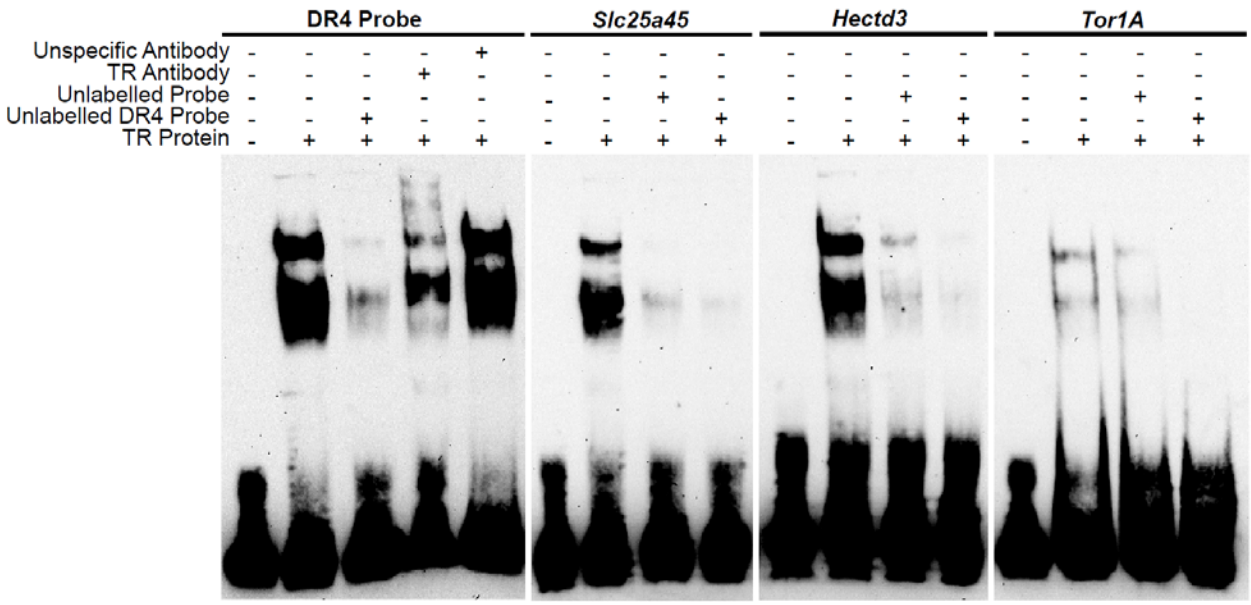

Figure 2.4. Examining the potential binding of candidate TREs by EMSA. The left panel shows results using a classic DR4 TRE with two "AGGTCA" half-sites. The next three panels show gel shifts when using a probe targeting candidate TREs in the promoter regions of *Slc25a45*, *Hectd3* and *Tor1a*.

2.5 Discussion

To identify direct transcriptional targets of TH and genes containing TREs, we produced global gene expression profiles in hypothyroid and hyperthyroid mouse models established by short-term exposure to MMI and perchlorate and/or TH injection. PND 15 livers were studied as animals of this age have circulating T4 levels higher than at any other age (Ahmed et al., 2008) and the liver is widely studied as a model of TH action. In the hypo pups TH levels were altered for three days, whereas in the hyperthyroid pups TH levels were altered for four hours immediately before tissue collection. Concentrations of anti-thyroid agents used in the hypo exposure and concentrations of injected THs were not unusually high when compared to other similar studies (Dong et al., 2009; Flores-Morales et al., 2002). Several hundred genes were responsive to this short-term treatment, with fold-changes as high as 13.8. However, the vast majority of these genes had relatively small fold-changes (i.e., < 3-fold). When filtered on a 2.0 fold-change cutoff, only 31 genes in females and 27 genes in males were perturbed, with an overlap of 14 genes.

PCA confirmed that the microarray data clustered by sex and by treatment type suggesting that there are significant differences at the level of gene expression between i) male and female pups and ii) control, hyper, hypo and hypo+ pups. GO analysis identified multiple pathways involved in oxidative stress and xenobiotic metabolism/signalling, as well as confirming the enrichment of genes in TR/RXR activation. The focus of the present research was to identify direct TH-target genes, rather than conduct a detailed mechanistic analysis. Thus, the data were mined specifically to identify direct TH-regulation and search promoters for putative TREs.

As previously mentioned, studies characterizing TH hepatic gene regulation have been carried out by others (Bungay et al., 2008; Flores-Morales et al., 2002; Weitzel et al., 2003a; Yen et al., 2003) and by our group (Dong et al., 2007). Although these studies were carried out using different experimental designs, animal models, and developmental stages, some important similarities in molecular functions and processes emerge including genes involved in TR and RXR activation (see Supplementary Table 2.3). In addition, several specific genes previously shown to be involved in TH hepatic gene regulation, such as *Me1*, *Thrsp* and *Dio1* were also found in the current study. However, our study design is unique relative to the other work described above because it is a short-term transient perturbation in TH that queries a specific developmental period to identify immediately responsive genes. The overarching goal of the work is to use a robust microarray analysis of gene expression profiling coupled with a novel TRE search algorithm to identify putative TREs. Thus, a detailed functional analysis of the perturbed genes in this study compared to the other studies has not been carried out.

To identify genes under direct TH-regulation we examined the expression of a subset of responsive genes in the hypo+ and hypo++ groups in detail. These groups were rendered hypothyroid for the majority of the 3 day exposure, and then received an *i.p.* TH injection four hours before decapitation and tissue collection. In other words, only a four hour period was allowed for transcriptional response to the TH surge. Where the direction of the transcriptional fold-change in the hypo+ group was the same as in the hyper group, but the opposite of the hypo group, we predicted that the gene in question was under direct TH-regulation. Transcript levels of some of these genes were analyzed by RT-qPCR in the hypo+ and hypo++ groups. RT-qPCR analysis confirmed a significant change in the hypo+ group for four out of the nine genes relative to vehicle controls. Analysis of the hypo++ group, which registered a much higher level of

circulating serum T4 compared to hypo+, showed that seven out of the nine genes had significant fold-changes relative to control. Validation of the transcriptional response in the hypo+ and hypo++ groups help to further support our assumption that the identified genes are under direct TH-regulation. None of the genes identified as being directly regulated by THs have characterized TREs. Although specific genes that are commonly considered to be directly regulated by TH, such as *Me1*, *Thrsp* or *Dio1*, were confirmed to be differentially regulated in our experiment, they did not meet the stringent requirements set for this particular evaluation (i.e., our list of potentially directly regulated genes). As previously described, genes were considered to be directly regulated by TH if they followed a specific expression pattern. Only genes exhibiting fold-changes with FDR-adjusted $p \leq 0.05$ were considered for this analysis. However, the RT-qPCR analysis demonstrated that known TH responsive genes were responding as predicted in the animal model used.

We retrieved the relevant DNA sequences and identified potential TREs within the promoter regions of the responsive genes. We assumed that genes under direct TH-regulation should contain functional TREs in their promoter regions. For practical reasons, our search was limited to the immediate promoter region (from 8 kb upstream to 2 kb downstream of the TSS) even though not all response elements are located in this area. Some studies have shown that transcription factor binding sites can be exceptionally far from the chromosomal location of the genes they regulate. For example, some estrogen response elements (EREs) can be found 50 kb away from of the TSS (Carroll et al., 2006), whereas others can be more than 100 kb away from the TSS (Carroll et al., 2005). In addition, interchromosomal regulatory interactions have also been documented (Spilianakis et al., 2005). Our gene expression profiling analysis identified 28 genes that appeared to be under direct TH-regulation. Within these 28 genes, bioinformatics

mining for three different types of TREs (DR4, IR0 and ER6) revealed 196 candidate TREs. To help identify true TREs, we carried out a local alignment of promoters of these mouse genes with the promoter regions of *Rattus norvegicus* and *Homo sapien*. In the -8 kb to +2 kb promoter regions of these genes we were able to identified 33 TREs in 13 different genes. Thus, within the region examined approximately 46% of the genes possessed potentially conserved TREs that fall within the established half-site criteria.

Conservation of a stretch of DNA between all three species provides evidence of the selective importance of response element functionality. Two previously characterized TREs are presented at the bottom of Table 2.4. The TRE near Kruppel-like factor 9 (*Klf9*) has been characterized in mice, rats, and humans (Denver and Williamson, 2009a). Comparison of the TREs within the orthologous *Klf9* gene of the three species shows that the TREs are within 2 kb of each other relative to the TSS. The TRE located in the myelin basic protein (*Mbp*) gene promoter region has been characterized in mice and rats (Farsetti et al., 1997; Farsetti et al., 1991). The TREs for *Mbp* for both species are within 2 kb of each other relative to the TSS and show very good half-site sequence conservation. Conservation of response elements between species has been previously observed. Similar to the current study, Bourdeau *et al.* identified EREs in 660 different pairs of orthologs between mice and humans (Bourdeau et al., 2004). EREs identified in proximity of these orthologs were within 2 kb of their respective TSSs. Some EREs that were conserved between mice and humans were perfect matches, whereas others had multiple mismatches in their two half-site. EREs are very similar to TREs; they are both made up of AGGTCA half-sites. The classic ERE organization is an IR3, where the two half-sites are arranged in a palindromic organization separated by a 3 bp spacer. The classic TRE, on the other hand, is a DR4 with the two tandem repeated half-sites separated by a 4 bp spacer (Umesono et

al., 1991), although IR0, ER6 and other TREs have also been characterized. The similarities and differences that exist between EREs and TREs suggest that the underlying mechanisms that confer response element specificity are much more complicated than was once thought. A recent paper by Phan *et al.* points out some interesting findings about nuclear receptor DNA recognition specificity (Phan et al., 2010). The authors looked at the half-site recognition for retinoic acid receptor (RAR) and TR, which both bind to the AGGTCA half-site sequences. It was once thought that the spacing between half-sites was the only aspect that conferred specificity (Forman et al., 1992; Naar et al., 1991; Perlmann et al., 1993) although the authors discovered that there were other properties that played an important role, which included naturally occurring non-consensus half-sites, flanking sequences, and auxiliary proteins produced by the cell. These additional properties make the identification of response elements even more complex, especially considering the high degree of degeneracy of TREs; nevertheless, they are important to take into consideration. It is also important to point out that our model did not consider flanking sequences and that the PWM was built with "known" TREs that biased towards the AGGTCA classic DR4 organization. We are hopeful that future response element search tools will be more flexible and take additional details such as those described above into consideration.

Previous studies have primarily used search algorithms that allow very little variation from the classic AGGTCA half-sites. Search algorithms often only allow substitution of a position towards one specific base pair, for example, position one of the half-site would only allow for an A or a G. This is a very restricted approach since TREs can be very degenerated and, based on previously characterized TREs, position one (as well as other positions) could potentially have any of the four nucleotides. Moreover, previous search algorithms often did not allow substitutions to occur at all half-site positions and often limited the number of

"mismatches" when compared to the classic AGGTCA TRE half-site. Our TRE search algorithm was much more flexible when compared to these other approaches, as the PWM scored all possible TREs and applied a score based on the probability for a given base to be located at any position of the half-site based on known functional TREs. A cut-off value was applied to this criterion to minimize false-positives. Since our approach allowed for a great deal of half-site sequence variation, a filtering or refining step was needed to reduce false-positives. We speculate that a cross-species comparison was an effective method to reduce the amount of false-positives, and also increases the potential utility of the new TREs for future research as they may be relevant in multiple species. Although not specifically tested our method appears to have allowed for a larger amount of variability and as a result we identified new candidate TREs that contain some features of the classic TRE, but are substantially different.

ChIP-PCR was used to validate some of the TREs identified by the bioinformatics search. Six candidate TREs were considered for this validation work. Four showed enrichment by TR-immunoprecipitation, whereas the two others did not show enrichment. This suggests that the FDR is approximately 33%, but our sample size for this estimate is quite low. The lack of identification of TREs in certain genes could be attributed to various factors. TREs could be present in the promoter regions of genes thought to be directly regulated by TH but are undetected by the bioinformatics tools currently available (i.e., do not exhibit the classic characteristics). Functional TREs have been described with a high level of degeneration, multiple spacer sizes and various half-site organizations (Dong et al., 2007; Hashimoto et al., 2006; Perez-Juste et al., 2000; Shin et al., 2006; Solanes et al., 2005) with a structure divergent from the models on which our identification algorithm was based. Consequently our model may have been too conservative to identify other functional TREs in these genes. Alternatively, TREs may

truly be absent from the promoter regions of these genes. Expression may be tied to TH action through intermediate regulatory mechanisms. Non-genomic actions of TH have also been characterized (Davis et al., 2008), by which TH activation of plasma membrane receptors induces signal transduction pathways leading to various genomic or cellular responses, although some claim that the non-genomic effects of THs do not play a significant role during vertebrate development (Das et al., 2010). MicroRNAs (miRNAs) could also potentially regulate TH-mediated mRNA expression. We recently identified significant alterations in 40 different miRNAs in the livers of PND 15 hypothyroid mice (Dong et al., 2010). Lastly, within our list of significantly altered genes (FDR adjusted $p \leq 0.05$), several transcription factors are present, including retinoic acid receptor, beta (*Rarβ*), estrogen receptor 1 (*Esr1*) and nuclear receptor subfamily 3, group C, member 1 (glucocorticoid receptor) (*Nr3c1*) (see Supplementary Table 2.1 and 2.2). Thus, genes present within our list may be under the control of other transcription factors that are directly regulated by THs. For example, *Esr1* expression is decreased in hypothyroid female mice. This could lead to many downstream transcriptional effects since ESR1 is a transcription factor that has been shown to interact with 18 different nuclear receptors (Nuclear Receptor Signaling Atlas, www.nursa.org).

ChIP-PCR revealed significant enrichment for some of the stretches of DNA thought to be involved in TR interactions. TRs are thought to be bound in both presence and absence of THs, thus ChIP-PCR was only performed with euthyroid animals. Importantly, the PCR primers targeted a DNA fragment with an average size of 168 bp that includes the putative TRE. In total, four TRE sites were validated by ChIP-PCR. The TREs identified in the promoter regions of *Tor1a* and *Slc25a45* correspond to a DR4 organization. The TRE identified in the promoter region of *Hectd3* corresponds to an ER6 organization, whereas the TRE identified in the

promoter region of *2310003H01Rik* corresponds to an IR0 organization. The genomic locations of these newly identified TREs all fall in upstream promoter regions, -2.3, -4.6, -7.4 and -2.3 kb from their respective TSS. Most TREs identified to date in the mouse genome are located in upstream promoter regions, and more than 70% are within the 0 to -2.5 kb upstream region. The TRE that is the furthest from a TSS that has been characterized to date in mice is in the promoter region Klf9, and is -3.8 kb from its TSS. This information is based on the 14 mouse TREs that we were able to find in the literature (list available on request). Since 50 % of the TREs we have characterized here are outside these bounds, our findings suggest that TREs are not necessarily found more often within the 2 or 3 kb upstream promoter region. The TRE associated with *2310003H01Rik* was not validated by EMSA. This could be due to the fact that recombinant purified protein samples were used, as opposed to tissue or cellular extracts. Extracts would include other transcription factors, such as TR's known heterodimer partner RXR, which may be required for the DNA-protein interaction to occur at a detectable level. In contrast, the TREs associated with *Slc25a45*, *Hectd3* and *Tor1a* were validated by EMSA, each showing a shift in the presence of TR proteins and a decrease in detection when unlabelled probe or DR4 unlabelled probe was added. The addition of unlabelled probe demonstrates the specificity of the shifted band, whereas the addition of the unlabelled DR4 probe demonstrates that the shifted band was caused by an interaction with the TR protein, since a supershift using an antibody against TR was shown for the DR4 positive control probe. A correlation between the ChIP-PCR and EMSA results was observed. *Scl25a45* has the strongest enrichment measured by ChIP-PCR, followed by *Hectd3* and *Tor1a*. *Slc25a45* again showed the strongest decrease in signal intensity when unlabelled specific probe was added in the EMSA, followed by *Hectd3* and *Tor1a*.

SLC25A45 is involved in the transportation of molecules across the mitochondrial membrane (Haitina et al., 2006). THs have been shown to induce mitochondrial biogenesis and enhance ATP production (Weitzel et al., 2003b). The identification of a TRE in the vicinity of the TSS of this transporter could be an indication of its involvement in TH-dependant mitochondrial biogenesis. HECTD3 is a ubiquitin ligase. In humans, it has been shown to directly bind TARA, a guanine nucleotide exchange factor involved in regulating actin cytoskeletal reorganization, cell mobility, and cell growth (Seipel et al., 1999). THs have also been shown to play a role in cytoskeletal protein regulation (Biswas et al., 1997). Thus, a TRE in the promoter region of *Hectd3* could link this gene to cytoskeletal regulation via THs. In mice 2310003H01RIK is the predicted ortholog of FAAP100, Fanconi anemia-associated protein, 100 kDa (Ling et al., 2007). FAAP100 is involved in the Fanconi anemia (FA) core complex, which plays a role in the DNA damage response network (Ling et al., 2007). FA is a genetic disease that results from defects in proteins involved in DNA repair. People affected by FA have physical anomalies, short stature, and are predisposed to cancer arising from chromosomal instability (Eyal et al., 2008). Children with FA have a high risk of endocrine abnormalities including hypothyroidism (Giri et al., 2007). A recent study found that TH therapy could improve the linear growth of children suffering from FA (Eyal et al., 2008). The identification of a TRE in the promoter region of *2310003H01Rik* could shed light on the underlying mechanisms leading to hypothyroidism in FA patients. TOR1A is an adenosine triphosphatase. Mutation of this gene has been linked to early onset dystonia and Parkinsonism (Leung et al., 2001). Dystonia is a disorder characterized by sustained muscle contractions often causing twitching and repetitive movements or abnormal posture. THs are important for proper muscle development

and maintenance (Harrison et al., 1996). Thus, the presence of a TRE in the promoter region of *Tor1a* could suggest a potential role for TH-*Tor1a* interaction in muscle development.

Using transcriptional profiling analysis we were able to identify genes suspected of being directly regulated by THs in male and female mice. Bioinformatics mining of the promoter regions of these genes revealed 33 candidate mouse TREs potentially conserved between rats and humans. ChIP-PCR and EMSAs were employed to validate the mouse TREs. We provide evidence of four new TREs in the promoter regions of *Tor1a*, *Slc25a45*, *Hectd3* and *2310003H01Rik*. The results provide data to develop a stronger model for the TRE sequence motifs that direct TR binding, identify key genes that may be important for TH mediated effects, and help to further characterize the mechanisms by which TH directly regulate gene expression.

CHAPTER 3: THYROID HORMONE MAY REGULATE MRNA ABUNDANCE IN LIVER BY ACTING ON MICRORNAS

Modified from: Hongyan Dong, Martin A. Paquette, Andrew Williams, R.Thomas Zoeller, Mike Wade and Carole Yauk. (2010). *PLoS ONE*, 5(8): e12136.

3.1 Abstract

MicroRNAs (miRNAs) are extensively involved in diverse biological processes. However, very little is known about the role of miRNAs in mediating the action of thyroid hormones (TH). Normal TH levels are known to be critically important for development, differentiation and maintenance of metabolic balance in mammals. We induced transient hypothyroidism in juvenile mice by short-term exposure to methimazole and perchlorate from post natal day (PND) 12 to 15. The expression of miRNAs in the liver was analyzed using Taqman Low Density Arrays (containing up to 600 rodent miRNAs). We found the expression of 40 miRNAs was significantly altered in the livers of hypothyroid mice compared to euthyroid controls. Among the miRNAs, miRs-1, 206, 133a and 133b exhibited a massive increase in expression (50- to 500-fold). The regulation of TH on the expression of miRs-1, 206, 133a and 133b was confirmed in various mouse models including: chronic hypothyroid, short-term hyperthyroid and short-term hypothyroid followed by TH supplementation. TH-regulation of these miRNAs was also confirmed in mouse hepatocyte AML 12 cells. The expression of precursors (pre-) miRs-1, 206, 133a and 133b were examined in AML 12 cells. All three pre-miRNAs decreased in response to TH treatment, while only pre-mir-206 and pre-mir-133b reached statistical significance ($p \leq 0.05$). To identify the targets of these miRNAs, DNA microarrays were used to examine hepatic mRNA levels in the short-term hypothyroid mouse

model relative to controls. We found transcripts from 92 known genes were significantly altered in these hypothyroid mice. Web-based target predication software (TargetScan and Microcosm) identified 14 of these transcripts as targets of miRs-1, 206, 133a and 133b. The vast majority of these mRNA targets were significantly down-regulated in hypothyroid mice, corresponding with the up-regulation of miRs-1, 206, 133a and 133b in hypothyroid mouse liver. To further investigate target genes, miR-206 was over-expressed in AML 12 cells. TH treatment of cells over-expressing miR-206 resulted in decreased miR-206 expression, and a significant increase in two predicted target genes, mitochondrial uncoupling protein (*Mup1*) and glycerol-3-phosphate dehydrogenase 2 (mitochondrial) (*Gpd2*). The results suggest that TH regulation of these genes may occur via miR-206. This study provides novel insight into the role of TH- mediated miRNAs gene regulation.

3.2 Background

Thyroid hormone (TH) is critically important for development, tissue differentiation, and maintenance of metabolic balance in mammals through direct and indirect regulation of expression in target genes (Boelaert and Franklyn, 2005). Severe disruption of TH action during fetal and early neonatal development leads to a suite of permanent deficits in experimental animals and humans (Boelaert and Franklyn, 2005). TH plays a critical role in the liver where it can affect metabolism, serum glucose regulation and lipid regulation. Previous studies using genome wide microarray analyses have shown that TH regulates the expression of genes involved in these important physiological processes (Dong et al., 2007; Stahlberg et al., 2005). However, the mechanisms by which TH regulates target genes, whether by direct actions on mRNA transcription via interation with response elements or by indirect actions on mechanisms that control cellular levels of mRNAs, is not well understood.

MicroRNAs (miRNAs) are small non-coding RNAs of 19-24 nucleotides in length that are important regulators of crucial biological processes, such as metabolism, cell growth, apoptosis and carcinogenesis (Chen, 2009; Lynn, 2009). The number of known miRNAs has rapidly increased over the past years. Recently, the Sanger Institute released the latest version of their database of known miRNAs (miRBase 14.0; Sep 2009, http://microrna.sanger.ac.uk); 786 mature mouse miRNA sequences are currently reported. Long primary miRNAs are transcribed by RNA polymerase II in the nucleus, and then modified by an enzyme complex containing DROSHA and DGCR8 to form pre-miRNA. Subsequent cleavage of pre-miRNA by an RNase III, DICER 1, results in mature miRNA, which suppresses translation and enhances degradation of target gene transcripts by binding to complementary regions within the target transcripts (Chen, 2009; Lynn, 2009).

Considering the importance of TH in regulating fundamental processes governed by hepatic function, and the potential importance of miRNAs in regulating genes coding for proteins essential to these functions, we sought to test the hypothesis that TH regulates specific miRNAs. Therefore, we employed DNA microarrays and TaqMan low density arrays (TLDA) to analyze gene and miRNA expression profiles in a juvenile hypothyroid mouse model induced by short-term TH disruption. TLDA offer a high throughput and sensitive approach for detecting miRNAs (Mees et al., 2009). Selected miRNAs were examined in greater detail using other animal models that also had disrupted TH levels and an *in vitro* system to confirm TH-regulation.MiR-206 target genes were investigated with cell lines stably transfected with miR-206. Analysis of miRNA expression changes in combination with global mRNA levels provides a powerful approach to determine the effect of TH perturbation on miRNA expression and function. These

findings provide new insight into the role of miRNAs in mediating the non-genomic effects of TH action in the liver.

3.3 Methods

3.3.1 Ethics Statement

All animal care and handling was in accordance with Canadian Council for Animal Care Guidelines and was approved by the Health Canada Animal Care Committee. Permit number:2007006.

3.3.2 Animal Models with Altered TH Level

C57BL/6 mice were purchased from Charles River (St. Constant, QC, Canada) and were housed in hanging polycarbonate cages under a 12:12 hour light-dark cycle at 23ºC with food (Purina rodent chow 5010; Ralston-Purina, St. Louis, MO, USA) and sugar water (1%) available *ad libitum*. All cages contained shelters and nesting material. After a 10 day acclimation period breeding was initiated by transferring two sexually mature female mice (8 weeks post natal) into the home cage of a sexually mature (10 weeks) male. After 4 nights of co-housing each female was transferred to a separate cage. Dams were allowed to litter naturally and litter numbers were not adjusted. On post natal day (PND) 12, half of the dams with litters were provided with sugar water containing methimazole (MMI, 0.05%, Sigma Chemical, St. Louis, MO) and perchlorate (1%, Sigma chemical), while other half were provided sugar water. Four hours before sacrifice on PND 15, pups with sugar water were injected with PBS (control group) or T4/T3 (hyper group, 50/5µg/100gbw); MMI and perchlorate treated pups were injected with PBS (hypo group) or T4/T3 (hypo+ group, 20/2µg/100gbw).

For PTU induced hypothyroidism, C57BL/6 time-pregnant mice (gestational day 13, GD 13) were purchased from Charles River (St. Constant) and supplied *ad libitum* with 0.3% diet cherry Kool-aid in water containing 0%(control) or 0.04% PTU (6-propylthiouracil; Sigma Chemical) from GD 13 to PND 15.

On PND 15, a male pup from each litter was sacrificed by exsanguination under isofluorane anaesthesia. Serum, prepared using Serum Separator Tubes (BD Biosciences, Mississauga, ON, Canada) was retained for T4 analysis with RIA kits (MP Biomedicals, Medicorp, Montreal, QC, Canada). Liver was dissected as rapidly as possible, immediately frozen in liquid nitrogen and stored at -80ºC.

3.3.3 Cell Culture and Stable Transfection

Mouse hepatocyte cells AML 12 (ATCC, Manassas, VA,USA) were grown at 37°C in Dulbecco's modified Eagle's medium/Ham's F-12 nutrient mixture with 10% fetal Bovine serum, 100 nM dexamethasone and ITS (insulin, transferrin and selenium, Invitrogen, Burlington, ON, Canada). Stable transfection was performed using 18 µl FuGene (Roche, Indianapolis, IN, USA) with 12 µg miRNASelect pEGP-mir Null Control Vector or pEGP-mmu-mir-206 Expression Vector (Cell Biolabs, Inc., San Diego, CA, USA) in 10-mm Petri dishes. Green clones in the medium containing 2 µg/ml puromycin (Invitrogen) were identified by microscopy, and were picked and cultured in completed medium with puromycin for one week. The over expression of miR-206 was confirmed with qRT-PCR. Ten percent stripped fetal bovine serum (Medicorp, QC, Canada) was added to cultured cells one day before cells were incubated with or without 10 nM T3.

3.3.4 RNA Extraction and Purification

For microarray analysis, total RNA was extracted with TRIzol reagent (Invitrogen) followed by RNeasy Mini Kit (Qiagen, Mississauga, ON, Canada) clean-up according to the manufacturer's instructions. RNA integrity was determined using an Agilent 2100 Bioanalyzer (Agilent Tech. Inc. Mississauga, ON, Canada) and only high quality RNA (RIN>9.0) was used for microarray analysis. For other analyses (miRNA expression, qRT-PCR), total RNA was extracted with *mir*Vana miRNA Isolation Kits (Ambion, Inc., Applied Biosystems, Foster city, CA, USA) according to the manufacturer's instructions.

3.3.5 Microarray Hybridization

Relative transcript levels were determined using a 2 colour reference hybridization design where each RNA sample was labelled with Cyanine 5-CTP (Cy5) and universal mouse reference total RNA (Stratagene, Cedar Creek, TX, USA) was labelled with Cyanine 3-CTP (Cy3) using Agilent Quick Amp Labelling kits (Agilent Tech. Inc.). Labelled sample and common reference cRNA were hybridized to Agilent mouse oligo microarrays (product number G4122F; 4X44K arrays) according to the manufacturer's instructions. Slides were washed and scanned on an Agilent G2505B microarray scanner and data were acquired with Agilent Feature Extraction software version 10.1.1.1.

3.3.6 Microarray Normalization and Analysis of Differential Gene Expression

Background fluorescence was measured using the (-)3xSLv1 probes. Probes exhibiting median signal intensities less than the trimmed mean (trim = 5%) plus three trimmed standard deviations of the (-)3xSLv1 probe were flagged as absent (within the background signal). Data

were normalized using the transform.madata function in the MAANOVA library in R using a global lowess with a span of 0.2 (Team, 2008; Wu H, 2003). Genes that were differentially expressed as a result of treatment were determined using the MAANOVA library in R. The Fs statistic (Nitto et al., 2008) was used to test for treatment effects. P-values were estimated by the permutation method using residual shuffling, followed by adjustment for multiple comparisons using the false discovery rate (FDR) approach (Benjamini Y, 1995). The fold-change calculations were based on the least-square means. Significant genes were identified as those where the Fs statistic had a Benjamini-Hochberg corrected $p < 0.05$. All data are MIAME compliant and available through the Gene Expression Omnibus (GEO, accession number GSE21277).

3.3.7 MiRNA Expression Analysis with TLDA

Four male mice from each of the control and hypo groups respectively were used to comprehensively analyze miRNA expression. Samples containing 750 ng RNA were used to perform reverse transcription with the Taqman miRNA Reverse Transcription kit and Megaplex RT Primers Rodent Pool A and B (Applied Biosystem). RT-PCR reactions were performed with TaqMan Rodent miRNA Array A and B (containing up to 600 rodent miRNAs) by the Institut de Recherche en Immunologie et en Cancérologie (IRIC), University de Montreal, with the 7900 HT system. Using the log2 of the delta Ct values, differentially expressed miRNAs were identified using an F-test with U6 as a housekeeping miRNA. The critical value of the F-test statistic was determined by bootstrapping the residuals from the one way ANOVA model (Kerr MK, 2001) using the R (Team, 2008) software. Residuals were re-sampled within each treatment condition to avoid making the common variance assumption (Higgins, 2003). Multiple

comparison adjustment was applied to the final results using the FDR approach (Benjamini Y, 1995). The dataset is available through GEO (accession number GSE21277).

3.3.8 MiRs-1, 206, 133a and 133b Expression in Animal Models or Cultured Cell Lines

Taqman miRNA Reverse Transcription kits (Applied Biosystem) were used for reverse transcription reactions with 10 ng total RNA as template and specific primers from the Taqman miRNA Assay Kits. PCRs were performed with Taqman universal PCR Master Mix according to the manufacturer's instructions. Three animals from each group or 3 batches of cultured cells were used. Relative miRNA expression was analyzed using the ΔΔCt method with U6 as a housekeeping miRNA and one of the control samples as the calibrator. Significant differences in expression were determined using a Student's t-test and called significant if $p < 0.05$.

3.3.9 MiRNA Target Predictions

TargetScan mouse 5.1 (http://www.targetscan.org/mmu_50/) and MicroCosm Targets Version 5 (http://www.ebi.ac.uk/enright-srv/microcosm/cgi-bin/targets/v5/search.pl) were used to predict the targets of miRs-1, 206, 133a and 133b. Genes predicted by either of algorithm were considered to be the targets. These softwares apply different algorithms to identify the highly complementary sites and are widely used for miRNA target prediction (Friedman et al., 2009; Grimson et al., 2007; Lewis et al., 2005).

3.3.10 QRT-PCR Analysis of Target Genes and Precursors of miRNAs

Reverse transcription was carried out with SuperScript III (Invitrogen) using SYBR-Green and a GFX system (BioRad, Mississauga, ON, Canada). Primers were designed using Beacon design 2.0 (Premier BioSoft International, Palo Alto, CA, USA). PCR reactions were performed in duplicate, and the values of the threshold cycles were averaged. Gene expression levels were normalized to *Hprt*. PCR efficiency was examined using the standard curve for each gene. The primer specificity was assured by the melting curve for each gene. A Student's t-test was used for statistical evaluation. The sequences of primers are available upon request.

3.4 Results

3.4.1 Validation of the Short-term MMI/perchlorate-induced Hypothyroid Juvenile Mouse Model

Serum T4 levels in PND 15 male pups of dams treated from PND 12 to 15 with drinking water containing 0.05% MMI and 1% perchlorate were significantly reduced ($p < 0.001$, Figure 3.1A). RT-qPCR analysis of malic enzyme (*Me1*) (a known TH-regulated gene in liver (Dong et al., 2007)) in hypothyroid mouse liver revealed a significant 2-fold down-regulation (Figure 3.1B).

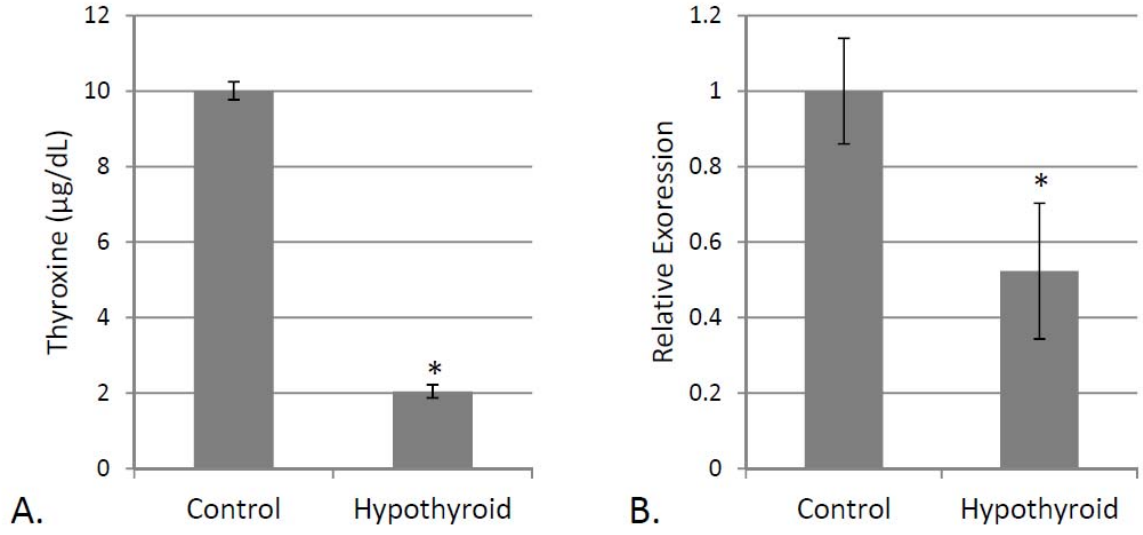

Figure 3.1. Serum T4 levels and liver *Me1* mRNA levels in mouse pups rendered hypothyroid by three day exposure of dams and their litters to drinking water containing MMI and perchlorate from PND 12 to 15. A. Serum T4 data are expressed as mean ± standard error (standard error, n =10) and * indicates a significant difference ($p < 0.001$). B. RT-qPCR for *Me1* mRNA (positively regulated by direct TH action) was performed with RNA derived from male pups. Data are presented as mean ± SE (n =5). A two-tailed Student's t-test was used to calculate significance; * indicates $p = 0.03$.

3.4.2 MiRNA Expression in Hypothyroid Mice

TLDA analysis revealed that 40 miRNAs were significantly altered ($p < 0.1$) in the liver of hypothyroid mice compared to euthyroid controls. Eleven miRNAs exhibited a fold-change greater than four (Table 3.1); eight of these 11 (70%) were up-regulated in hypothyroid mice. Three miRNA families (miRs-1 and 206, miRs-133a and 133b as well as miRs-135a and 135b) exhibited very large increases in expression (ranging from 50- to 500-fold). Data for these findings are available through GEO, accession number GSE21277.

Table 3.1. Differentially expressed miRNAs in hypothyroid mouse liver ($p < 0.1$, Fold-change > 4)

Gene Name	Fold-change	p-value	Clustered miRNAs	Function
MiR-133 family				
mmu-miR-133b	501.39	0.05	mmu-miR-206	Apoptosis[a] and muscle development[b,c]
mmu-miR-133a	100.36	0.02	mmu-miR-1	Apoptosis[a] and muscle development[b,c]
MiR-1/206 family				
mmu-miR-1	92.11	0.01	mmu-miR-133a	Apoptosis[a] and muscle development[b,c]
mmu-miR-206	58.9	0.07	mmu-miR-133b	Apoptosis[a] and muscle development[b,c]
MiR-135 family				
mmu-miR-135b	85.11	0.09		Colorectal cancer[d]
mmu-miR-135a	14.62	0.09		Colorectal cancer[d]
Others				
mmu-miR-138*	27.77	0.08		Squamous cell carcinoma[e]
mmu-miR-199b*	4.96	0.05		Choriocarcinoma[f]
mmu-miR-148a*	-4.2	0.04		DNA methyltransferase[g]
mmu-miR-582-5p	-5.14	0.07		Malignant mesothelioma[h]
mmu-miR-200a*	-5.49	0.10		Cervical cancer[i]

[a](Valencia-Sanchez et al., 2006), [b](Lewis et al., 2005), [c](Visser et al., 2009), [d](Xu et al., 2007), [e](Jiang et al., 2010), [f](Chao et al., 2010), [g](Duursma et al., 2008), [h](Guled et al., 2009), [i](Hu et al., 2010)

* indicates they are in the same chromosome and apart less than 10kb (based on TargetScan database)

3.4.3 The Expression of MiRs-1, 206, 133a, 133b in Other Animal Models with Altered TH Levels

To further investigate the effect of TH on hepatic miRNA expression, we examined the expression of the most differentially regulated miRNAs (miRs-1, 206, 133a, 133b) in the livers of i) hypothyroid mice induced by PTU treatment (PTU hypothyroid); ii) hyperthyroid mice created by injecting T3/T4 four hours before sacrifice (hyperthyroid); and iii) hypothyroid mice induced by MMI/perchlorate treatment but receiving T4/T3 injection four hours before sacrifice (corrected hypothyroid). Three mice were chosen from each group and their serum T4 levels are shown in Table 3.2. As shown in Figure 3.2A, all four selected miRNAs were significantly increased in the livers of PTU induced hypothyroid mice and significantly decreased in the livers of hyperthyroid mice. Corrected hypothyroid animals had serum T4 levels intermediate between control and hyperthyroid animals although these were only significantly different from the hyperthyroid T4 levels ($p = 0.046$ vs hyperthyroid and 0.067 vs control; Table 3.2). Similarly, hepatic expression of all four miRNAs was also intermediate between control and hyperthyroid mice with only miR-206 being significantly reduced compared to control animals (Figure 3.2B).

Table 3.2. Serum T4 levels of male pups in the various animal models (n = 3).

Mouse models	T4 (µg/dL)	p-value
Chronic Model		
Control	9.9	
Hypothyroid (PTU)	0.6	<0.001
Transient Model		
Control	9.6	
Hyperthyroid	39.4	<0.001
Hypothyroid +	16.6	0.067 (to control) 0.046 (to hyper)

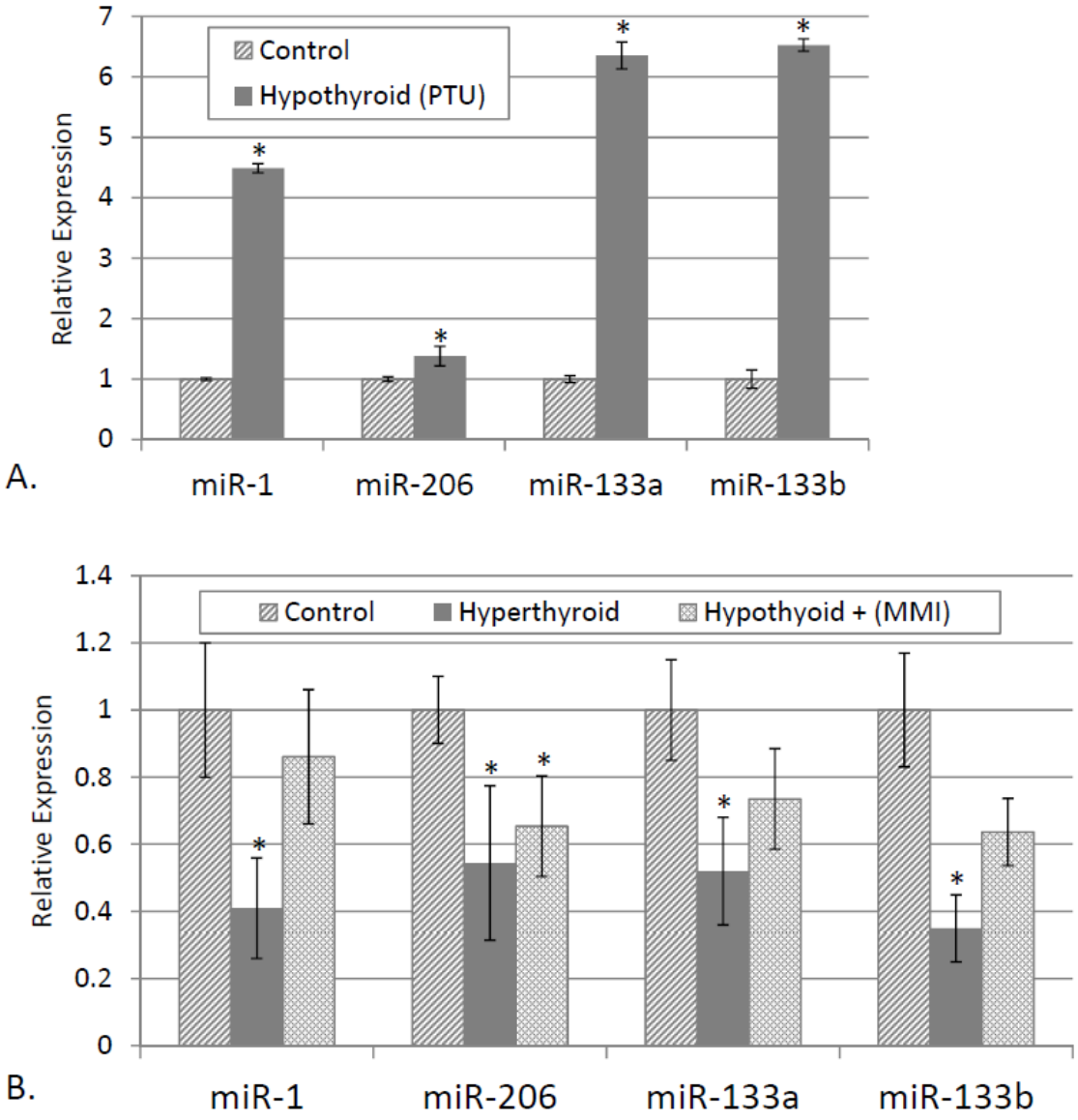

Figure 3.2. Expression of miRs-1, 206, 133a and 133b in other animal models with altered TH levels. A. Hepatic miRNA expression in livers of PND 15 mouse pups rendered hypothyroid by treatment with drinking water containing 0.04% (wt/vol) of PTU from GD 13 to PND 15. RT-qPCR was performed with the Taqman miRNA Assay with RNA derived from male pups (3 per group). B. Hepatic miRNA expression in livers of PND 15 mice whose TH levels were modulated as follows: hyperthyroid pups (hyper) received an injection of T4 + T3 (50 µg + 5 µg, respectively per 100g bw) four hours prior to sacrifice and corrected hypothyroid pups received

drinking water containing MMI and perchlorate (0.05 and 1% wt/vol, respectively) from PND 12 to 15 and an injection of T4 + T3 (20 μg + 2 μg, respectively per 100g bw) four hours prior to sacrifice, while control mice received an injection of PBS only. RT-qPCR was performed with the Taqman miRNA Assay with RNA derived from male pups (3 per group). Data are presented as mean ± SE (n = 3). A two-tailed Student's t-test was used to calculate significance. * indicates $p < 0.05$.

3.4.4 The Expression of MiRs-1, 206, 133a and 133b in AML 12 Cells Treated with TH

To further investigate the effects of TH on miRNA regulation in liver, we treated AML 12 cells (derived from mouse hepatocytes) with 10 nM T3 for 1 hour or 24 hours. The expression of miRs-1, 206, 133a and 133b were examined with the Taqman miRNA Assay. TH treatment caused a down-regulation of all miRNAs examined at both 1 and 24 hours, although this effect was only statistically significant for miRs-1, 206 and 133b at 24 hours (Figure 3.3A).

Since mature miRNAs are derived from precursors, we investigated the effects of TH on the levels of the precursors of the selected miRNAs in AML 12 cells. As significant decreases of mature miRNAs were only found at 24 hours, we therefore examined pre-miRNAs at 24 hours as well. Precursors of all four miRNAs were reduced by at least 50% and this reduction was statistically significant ($p<0.05$) for mir-206 and mir-133b (Figure 3.3B) even with small sample sizes (n=3).

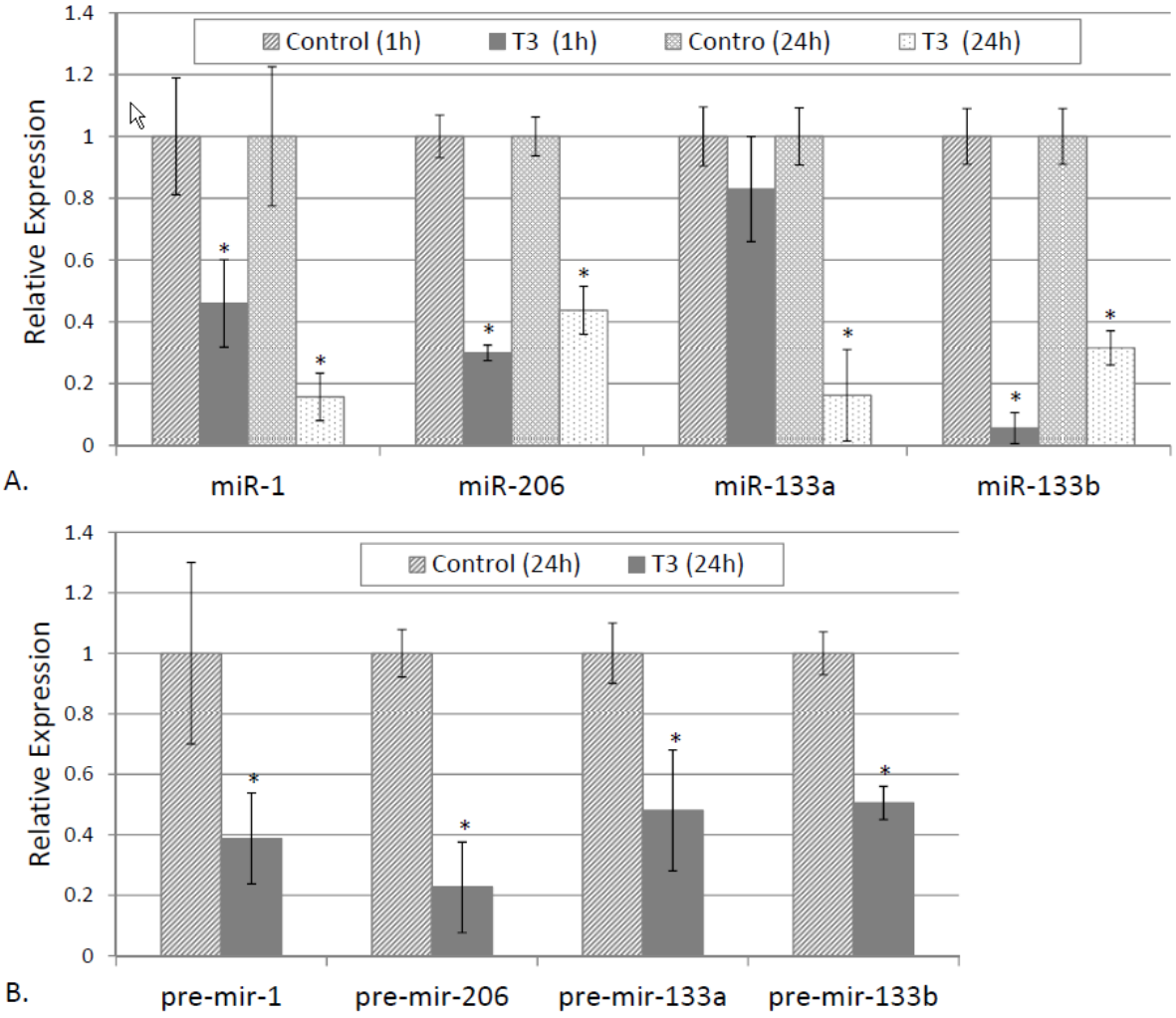

Figure 3.3. Expression of miRs-1, 206, 133a and 133b as well as their precursors in the AML 12 cells. A. AML 12 cells were treated with 10 nm T3 for 1 hour or 24 hours. The expression of miRs-1, 206, 133a and 133b was examined with the Taqman miRNA Assay. U6 was used as an internal control. Five batches of cultured cells were considered as 5 biological replicates. B. The expression of the precursors of miRs-1, 206, 133a and 133b was examined in AML 12 cells treated with 10 nm T3 for 24 hours using RT-qPCR. *Hprt* was used as internal control. Three batches of cultured cells were used as 3 biological replicates. Data are presented as mean ± SE. A two-tailed Student's t-test was used to calculate significance. * indicates $p < 0.05$.

3.4.5 Target Genes of miRs-1, 206, 133a and 133b in Hypothyroid Mouse Liver

The livers of five male pups from the transient hypothyroid model (exposed to MMI/perchlorate) were analyzed using Agilent gene expression microarrays alongside controls. Analysis revealed that 103 transcripts were significantly altered ($p < 0.05$) in hypothyroid samples compared to euthyroid samples. Among these, 92 genes have known functions and include genes known to be regulated by TH, such as deiodinase, iodothyronine, type I (*Dio1*), thyroid hormone responsive SPOT14 (*Thrsp*) and very low density lipoprotein receptor (*Vldlr*) (Dong et al., 2007). The expression of *Me1* was also decreased in these hypothyroid mice (1.4-fold, unadjusted p-value = 0.005), consistent with RT-qPCR results (Figure 3.1B). Detailed analysis of the expression profiles of these mice is presented as part of another publication (Chapter 2). The dataset is available through GEO (accession number GSE21277). Because miRs-1and 206 as well as miRs-133a and 133b families exhibited such large fold-changes, the targets of these miRNAs were predicted using TargetScan and MicroCosm. The overlap between predicted target genes and significantly changed genes with fold-change ≥ 1.5 and $p \leq 0.05$ in hypothyroid mice is shown in Table 3.3. Of the 14 predicted targets, 11 were significantly down-regulation in hypothyroid pups, corresponding with the up-regulation of miRs-1, 206, 133a and 133b. None of the targets of miRs-1, 206, 133a and 133b that were curated in TarBase (http://diana.cslab.ece.ntua.gr/tarbase/) were altered in the hypothyroid mouse livers.

Table 3.3. Targets of miRs-1, 206, 133a and 133b that were significantly altered in hypothyroid mouse liver ($p \leq 0.05$, Fold-change ≥ 1.5).

Accession Number	Gene Symbol	p-value	Fold-Change	Description
Targets of miR-1/206				
NM_013703[a]	Vldlr*	0.001	1.7	very low density lipoprotein receptor
NM_001013785[a]	Akr1c19	<0.001	1.6	aldo-keto reductase family 1, member C19
NM_029692[a]	Upp2	0.008	-1.6	uridine phosphorylase 2
NM_010274[b]	Gpd2	<0.001	-1.7	glycerol phosphate dehydrogenase 2, mitochondrial
NM_031188[a]	Mup1	0.003	-1.8	major urinary protein 1
NM_008737[b]	Nrp1*	<0.001	-2.0	neuropilin 1
NM_026460[a]	Serpini2	0.001	-3.1	serine (or cysteine) peptidase inhibitor, clade I, member 2
Targets of miR-133a/b				
NM_016919[a,b]	Col5a3	<0.001	1.8	procollagen, type V, alpha 3
NM_182959[a]	Slc17a8	<0.001	-1.6	solute carrier family 17
NM_025989[a]	Gp2	0.002	-1.7	zymogen granule membrane glycoprotein 2
NM_009344[a]	Phlda1*	<0.001	-1.8	pleckstrin homology-like domain, family A, member 1
NM_008693[a]	Klk1b3	0.002	-2.1	kallikrein 1-related peptidase b3
NM_010639[a]	Klk1	0.001	-2.1	kallikrein 1
NM_007769[a]	Dmbt1	0.004	-4.2	deleted in malignant brain tumors 1

[*] indicates genes that were found in chronic hypothyroidism in our previous study (Dong et al., 2007);

[a] indicates genes predicted by the MicroCosm database

[b] indicates genes predicted by theTargetScan database.

To provide direct evidence of the regulation of the expression of target genes by miRNAs in response to TH, we established AML 12 cells that over-expressed mir-206 by stable transfection of vector containing mir-206 precursor. The expression of miR-206 was approximately 1500 times higher in miR-206 over-expressing cells than in miR-null control vector transfected cells (Figure 3.4A). We selected four down-regulated genes uridine phosphorylase 2 (*Upp2*), glycerol-3-phosphate dehydrogenase 2 (mitochondrial) (*Gpd2*), mitochondrial uncoupling protein 1 (*Mup1*) and neuropilin 1 (*Nrp1*)) from miR-206 predicted targets in Table 3.3. The expression of these genes was examined in the cell line (Figure 3.4B). Expression of *Gpd2*, *Mup1* and *Nrp1*was significantly decreased in miR-206 over expressed cells suggesting that these three genes are true targets of miR-206.

To investigate whether these three true target genes are regulated by TH, we examined their expression and that of miR-206 in miR-206 transfected AML 12 cells treated with T3 for 24 hours. T3 treatment decreased the expression of miR-206 by roughly 50% ($p < 0.05$) in miR-206 transfected AML 12 cells (Figure 3.4C), while the expression of target genes *Gpd2* and *Mup1* significantly increased (Figure 3.4D).

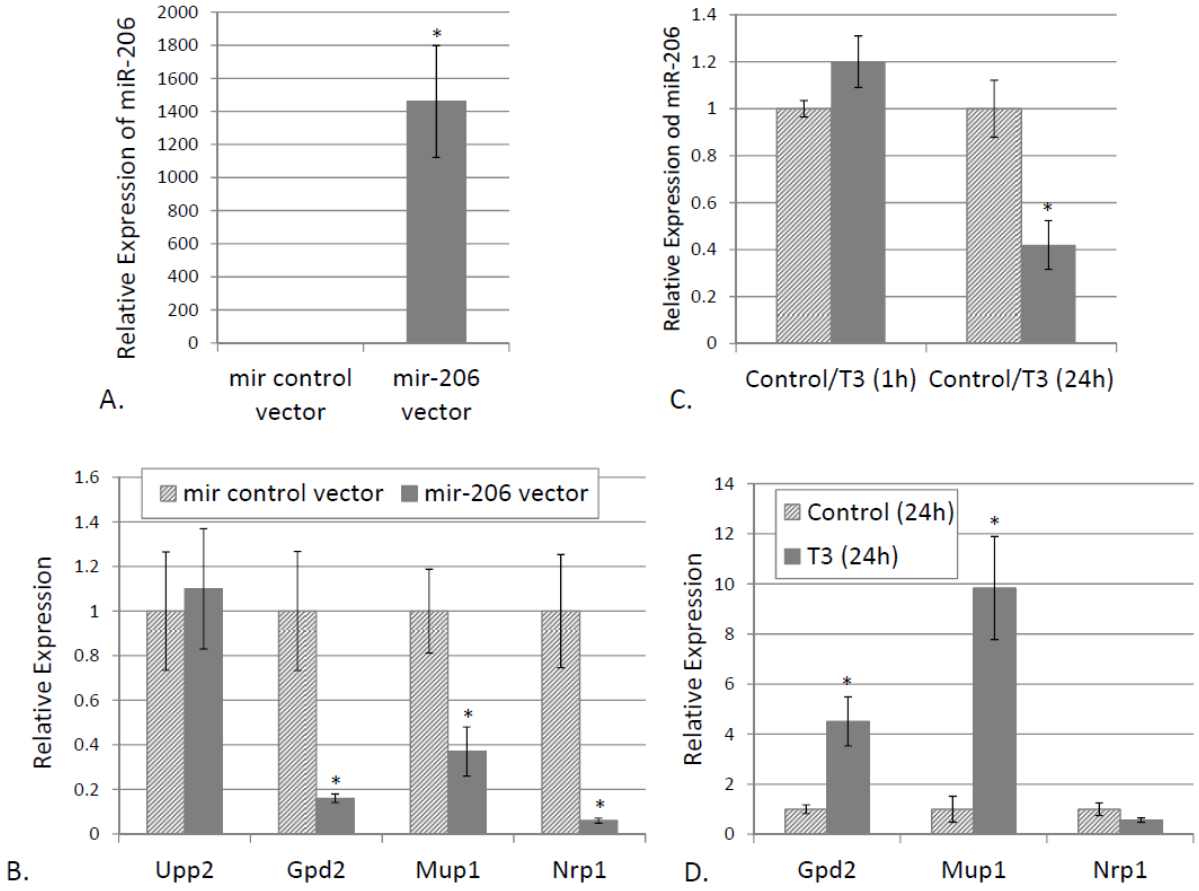

Figure 3.4. Identification of the target genes of miR-206 regulated by TH. A. Levels of miR-206 in AML 12 cells stably transfected to ectopically express miR-206. The expression of miR-206 was examined with the Taqman miRNA Assay (n = 5). B. The expression of genes that are putative targets of miR-206 in the two cell types shown in figure 3.4A was examined with RT-PCR (n = 3). C. The effects of TH on the expression of miR-206 in the transfected cells. The miR-206 transfected cells were treated with 10 nM T3 for 24 hours. MiR-206 expression was analyzed with Taqman miRNA Assay (n = 3). D. The effect of TH on the expression of the miR-206 target genes in the transfected cells. The miR-206 transfected cells were treated with 10 nM T3 for 24 hours. The expression of target genes was examined using RT-qPCR (n = 3). Data are presented as mean ± SE. A two-tailed Student's t-test was used to calculate significance; * indicates $p < 0.05.3$

3.5 Discussion

In both early development and throughout adulthood, THs have profound effects on metabolism. Recent studies on the effects of a TRβ-selective drug that targets the liver indicate that activation of TRβ can lower serum lipids, decrease global fat reserves, and improve insulin tolerance in *ob/ob* mice (Bryzgalova et al., 2008). Thus, liver is an important target of TH in regulating energetic metabolism and physiology (Dong et al., 2007; Stahlberg et al., 2005). TH primarily exert their effects through interaction with TR, which, upon heterodimerization with the retinoic X receptor (RXR), acts as ligand–activated transcription factors to initiate or block target gene expression by binding to TH response elements (TREs) (Lazar, 2003). Indeed, much of the focus of our work has been on the identification of TREs associated with promoters (Dong et al., 2009). However, a direct TR-TRE mechanism may not explain all TH actions. For example, non-genomic action of TH, which is often related to activation of signalling pathways, is another well characterized TH response (Iordanidou et al., 2010). MiRNAs represent an additional mechanism by which TRs may regulate or coordinate TH responsive genes. MiRNAs are involved in many biological processes and functions that control protein expression through mRNA degradation , translational suppression and directing chromatin structure (reviewed in (Valencia-Sanchez et al., 2006)). As such, in the current work we explored the role of miRNAs in governing TH response.

To examine the possibility that TH action may influence miRNA expression which could, in turn, alter mRNA levels, we generated hypothyroid mice by short-term treatment with MMI and perchlorate. Global expression of miRNAs and mRNAs were studied with TLDA and DNA microarray technologies. TLDA (a modified RT-qPCR method) was applied to generate miRNA profiles. This high throughput method has increased sensitivity and accuracy relative to

microarrays, and demonstrates a 100% miRNA expression validation rate against standard RT-qPCR (Mees et al., 2009). We detected 40 significantly altered miRNAs ($p < 0.1$) in the livers of hypothyroid mice. Among these, 11 miRNAs were altered by over four-fold, including eight up-regulated and three down-regulated miRNAs. Remarkably, miRs-1, 206, 133a and 133b exhibited fold-changes in excess of 50-fold. MiR-1 and miR-133a cluster on chromosome 2 within 10 kb, while miR-206 and miR-133b cluster on chromosome 1 within 4 kb. The results demonstrate a highly robust induction of miRNAs in response to hypothyroidism for specific genomic sites.

To demonstrate that the increased miRNA expression was induced by TH deficiency, not the toxicity of MMI and perchlorate, we examined the expression of miRs-1, 206, 133a and 133b in chronic hypothyroid, short-term hyperthyroid and a TH-supplemented transient hypothyroid animal models using RT-qPCR. All of the miRNAs significantly increased in the chronically hypothyroid mouse liver, although the fold-changes were smaller than in the transient hypothyroid model. This may be attributed to the different animal models or different detection systems used. Alternatively, there may be some adaptation following chronic hypothyroidism, or the miRNAs may exhibit a large initial response to the TH perturbation. This increased miRNA expression was not seen in TH corrected transient hypothyroidism, while miR-206 was significantly decreased. In addition, all selected miRNAs were significantly decreased in hyperthyroid mouse livers. Both serum T4 and hepatic expression of these miRNAs in the corrected hypothyroid animals are intermediate between control and hyperthyroid animal suggesting an inverted dose dependant regulation of miRNAs by TH. These observations were confirmed in an *in vitro* model of mouse hepatocytes (AML 12 cells), where treatment with T3 caused a rapid (1 hour) reduction in the levels of miRs-1, 206, 133a and 133b. Further reduction

of miRs-1 and 133a was found 24 hours post-treatment. The expression of pre-miRNA decreased with T3 treatment at 24 hours. Although some of these changes were not significant at $p < 0.05$ (only three biological replicates were used in these analyses), the data *in vitro* provide more evidence to support that TH down-regulates miRs-1, 206, 133a and 133b at the transcript level.

TH-regulation of these miRNAs is also supported by recent studies on muscle miRNA expression in hypothyroid humans (Visser et al., 2009). In this work Visser *et al*. collected skeletal muscle biopsies from clinically hypothyroid patients who were being treated with TH. TH induced a large down-regulation of primary miRs-206 and 133b. Levels of the primary (pri-) transcript associated with pri-miRs-1 and 133a were also reduced but to a lesser extent. Together these findings provide evidence that TH has the ability to down-regulate the expression of miRs-1, 206, 133a and 133b. However, the targets of these miRNAs and the potential biological implications remain unknown.

In order to explore the correlation between miRNA and mRNA levels, gene expression microarrays were used to quantify transcript abundance in the livers of the same mice (hypothyroid and euthyroid). Significant alterations in mRNA levels ($p < 0.05$) were found for 92 transcripts with known functions between euthyroid and hypothyroid pups. Changes in gene expression may be regulated by TH through TR-TRE, miRNAs, non-genomic signalling or other mechanisms. Targets of miRs-1, 206, 133a and 133b were predicted using TargetScan and MicroCosm. The analysis predicted that these miRNAs may target 14 genes that also exhibited changes in mRNA levels in hypothyroid mice relative to controls. The vast majority of these mRNA targets (11/14) were down-regulated under hypothyroid conditions, corresponding with an increased expression of miRs-1, 206, 133a and 133b. Three targets (*Vldlr*, *Nrp1* and pleckstrin homology-like domain, family A, member 1 (*Phlda1*)) have previously been found to be

differentially expressed following alterations in TH levels in mouse livers (Dong et al., 2007). We further validated the targets of miR-206 by establishing an AML 12 cell line that over-expresses miR-206. The expression of miR-206 was approximately 1500 times higher in the transfected cells relative to control cells. The expression of four predicted targets of miR-206 that were down-regulated in hypothyroid livers was examined; three of these genes were significantly down-regualted in miR-206 transfected cells. These findings strongly suggest that these three genes are putative targets of miR-206. To further demonstrate that miR-206 targets are regulated by TH, we treated the miR-206 transfected cells with TH for 24 hours and found that the expression of miR-206 decreased significantly and was accompanied by an increase in the expression of two of the miR-206 target genes (*Mup1* and *Gpd2*, Figure 3.4D). *Mup1* mediates chemical signalling by acting as pheromone ligand and regulates systemic glucose and lipid metabolism (Logan et al., 2008; Zhou et al., 2009), while *Gpd2* plays a role in thermogenesis (DosSantos et al., 2003). Our current findings provide possible mechanisms by which TH regulates target genes via post-transcriptional control through miR-206.

These findings suggest that TH may regulate the cellular levels of several species of miRNA which, in turn, regulate the mRNA levels of certain genes. To our knowledge, this represents the first observation of miRNA mediating the physiological action of a hormone in the developing liver. At present, it is not clear if TH reduces the levels of these specific miRNAs by blocking transcription of primary genes or through some other mechanisms

In conclusion, the present study applied global miRNA and mRNA expression profiling to reveal a potential regulatory role for miRNAs in response to TH in the developing mouse liver. Two target genes of miR-206 affected by TH were confirmed *in vitro*. These findings provide new insight into the role of miRNAs in mediating the non-genomic effects of TH action in the liver.

CHAPTER 4: GLOBAL ANALYSIS OF THYROID HORMONE RECEPTOR BINDING SITES REVEALS INTERACTION WITH THE *DDX54* AND *THRSP* PROMOTER IN JUVENILE MOUSE LIVER

In preparation for submission: Martin A. Paquette, Rémi Gagné, Hongyan Dong, Ella Atlas, Mike G. Wade and Carole L. Yauk.

4.1 Abstract

Thyroid hormones (THs) play a critical role in development and throughout adulthood. THs act through the thyroid receptor (TR), which binds to the TH response element (TRE) to regulate the expression of target genes. Although TH action has been studied for decades, surprisingly few TREs have been well validated and characterized. In this study we used chromatin immunoprecipitation followed by microarray analysis (ChIP-chip) to identify TR-binding sites in juvenile (postnatal day 15) mice liver. Microarray analysis revealed twelve TR-binding sites consistent between all analyzed samples. *In silico* analysis was carried out to search for moderately conserved classic TRE sequences within these novel binding regions, which led to the identification of six candidate TREs within three binding regions. Luciferase reporter assays confirmed the presence of a TRE in the promoter region of DEAD (Asp-Glu-Ala-Asp) box polypeptide 54 (*Ddx54*) and thyroid hormone responsive SPOT14 (*Thrsp*). The TR/retinoid X receptor (RXR) heterodimer and RXR homodiner were shown to bind the promoter region of *Ddx54* and drive gene expression in the presence of 9-cis-retinoic acid (9cRA). The promoter region of *Thrsp* was shown to allow binding of the TR/RXR heterodimer, and both T3 and 9cRA were able to significantly increase luciferase activity. The RXR homodimer was also able to bind the response element in the promoter region of *Thrsp* and increase luciferase activity. Overall,

ChIP-chip analysis revealed a relatively limited number of TR-binding sites in juvenile mouse liver despite previous studies showing that numerous genes can be affected by TH disruption at that developmental stage, suggesting that TH action may also be mediated through other intermediates. Collectively the results provide an important step towards characterizing TR-binding sites and identifying the underlying drivers of TR-gene regulation.

4.2 Background

Thyroid hormones (THs - triiodothyronine (T3) and thyroxine (T4)) are key messengers that play fundamental roles in directing early development and in throughout adulthood. THs are crucial for proper development and maturation of neurons, as well as overall growth (Bernal, 2005; Williams et al., 1998). Slight alterations in TH levels during pregnancy have long term adverse neurodevelopmental effects (Haddow et al., 1999). THs have also long been characterized as master regulators of the basal metabolic rate, and imbalances can cause various metabolic disorders that can lead to deleterious long-term effects (Boelaert and Franklyn, 2005; Kaptein, 1996).

TH mainly exerts its effects through transcriptional regulation of target genes. THs bind to thyroid receptors (TRs) that interact with DNA response elements (TREs: thyroid response elements) and activate nearby target genes (Brent, 2012). Unlike steroid hormone receptors, TRs (as well as retinoic acid receptor (RAR), retinoid X receptor (RXR) and peroxisome proliferator-activated receptor (PPAR)) are thought to bind DNA response elements in the presence or absence of their ligand (Zhang and Lazar, 2000). TRs can bind DNA as homodimers, although they are primarily thought to heterodimerize with other nuclear receptors, particularly RXR (Bugge et al., 1992).

Although research on the fundamental mechanisms by which THs regulate gene expression has been ongoing for decades, surprisingly few *bona fide* TREs have been identified. This may be due in part to the functional complexity of TREs that includes, but is most likely not limited to: i) the effects of variability in flanking sequence surrounding the TRE; ii) half-site orientation; iii) the degenerate nature of the TRE half-sites; and iv) the variability in TRE half-site spacing. The classic half-site of a TRE is made up of an AGGTCA hexamer (Glass et al., 1988), although it is well known that nucleotide variation at different positions of the half-sites can still produce a functional TRE. Some nucleotide positions appear to be more conserved than others; for example, the GG dinucleotide at position 2 and 3 are frequently unchanged in characterized TREs when compared to the classic TRE half-site. Flanking sequence and spacer composition can play an important role in the transcriptional strength of a TRE (Phan et al., 2010). The most commonly identified TRE is a direct-repeat with a 4 bp spacer (DR4), although inverted repeats with no spacer (IR0) and everted repeats with a 6 bp spacer (ER6) have also been characterized as functional TREs (Glass, 1994).

Given the vital importance of TH-TR physiology in normal development, a thorough characterization of the genes under direct TH-regulation and their TR-binding sites (TRE sequences) would assist in understanding the downstream effects of perturbations in the TH signalling cascade. In our past work we used DNA microarrays to investigate hepatic transcriptional response in a mouse model of transient hyper- and hypothyroidism (Paquette et al., 2011). Using transcriptional profiling we were able to identify genes potentially under direct TH-regulation. This was followed by *in silico* identification of TREs and validation by electrophoretic mobility shift assay (EMSA). We also characterized TR-binding sites in the developing mouse cerebellum and validated various TREs using EMSA and luciferase reporter

assays (Dong et al., 2009; Gagne et al., 2013). These studies helped to develop a stronger model for the TRE sequence motifs that directs TR binding, and identified several genes that may be important for TH mediated effects.

In the present study we use chromatin immunoprecipitation (ChIP) to isolate DNA regions bound by TR in liver samples from juvenile mice collected on postnatal day (PND) 15. This period coincides with a period where TH concentrations are higher than any other age (Ahmed et al., 2008) suggesting that this may be a notable time to evaluate TR-binding. Mouse promoter microarrays were used to identify the genomic sequences associated with TR-binding. *In silico* analyses were carried out to associate the bound DNA sequences to the transcription start site (TSS) of the nearest genes. TR-binding in samples was confirmed by ChIP-PCR and luciferase reporter assays. Additionally, regulation of genes associated with these TR-binding sites was investigated using RT-qPCR. The results provide an important step towards characterizing TR-binding sites and identifying the underlying drivers of TR-gene regulation.

4.3 Methods

4.3.1 Animals, Exposures and Tissue Collection

All of the mice used in our study were produced as part of previous experiments in our laboratories (referenced and briefly described below). We refer the reader to the original sources for more detailed methodologies. All animal care and handling was in accordance with Canadian Council for Animal Care Guidelines and was reviewed by the Health Canada Animal Care Committee prior to commencement of the study.

The mice used in this experiment were also used in three previous studies (Dong et al., 2010; Dong et al., 2009; Paquette et al., 2011). Females were cohoused for 4 days with sexually

mature males and singly housed post-mating. Dams were allowed to litter naturally (day of birth = PND 0) and pup numbers were not adjusted. To produce hypothyroid (hypo) pups, dams were provided with drinking water containing methimizole (MMI, 0.05 % wt/vol) and perchlorate (1 % wt/vol) for three days (PND 12 to 15). Hyperthyroid (hyper) pups were generated with intraperitoneal injections (*i.p.)* of THs (50 μg of T4 + 5 μg of T3 in saline per 100 g body weight), four hours before decapitation and tissue collection on PND15. Both control and hypo groups received a saline *i.p.* four hours before decapitation and tissue collection.

For propylthiouracil (PTU) induced hypothyroidism, C57BL/6 pregnant mice gestational day (GD) 13 were supplied *ad libitum* with 0.3% diet cherry Kool-aid in water containing 0% (control) or 0.04% PTU (Sigma Chemical) from GD 13 to PND 15. Pups were sacrificed by decapitation. Livers were rapidly dissected and flash frozen in liquid nitrogen. These mice were also used in two previous studies (Dong et al., 2009; Dong et al., 2007).

For all studies, serum prepared from trunk blood using serum separator tubes (BD Biosciences, Mississauga, ON, Canada) was used for T4 analyses by radioimmunoassay (RIA) kits (MP Biomedicals, Medicorp, Montreal, QC, Canada) as per the manufacturer's instructions. Serum T4 concentrations have been previously published (Dong et al., 2007; Paquette et al., 2011). The detection limit or sensitivity of the RIA is 0.76 μg/dL, as determined by the manufacturer (MP Biomedicals, Medicorp).

4.3.2 Chromatin Immunoprecipitation

DNA isolated from the livers of female euthyroid and hypothyroid groups was used for ChIP analysis. ChIP was performed using an EZ ChIP kit (Millipore Corporation, Toronto, ON, Canada) according to the manufacturer's instructions. Briefly, a small piece of liver was

homogenized with a hand-held homogenizer in 250 µL phosphate buffered saline (PBS) containing broad-spectrum protease inhibitors, and was then cross-linked with 1 % formaldehyde. Cross-linking was stopped with glycine and nuclei were collected by using the lysis buffer provided in the kit. To ensure that DNA fragments ranged from 200 to 600 bp, the nuclear solution was sonicated in an ice bath with 30 second bursts at 27 % amplitude. Fifteen bursts were completed, each separated by a 60 second rest period. DNA fragment size was verified by agarose gel electrophoresis. Six percent (about 100 µL) of the sonicated solution was stored at -20 ºC as total input (TI), while the remainder was incubated with anti-TRβ polyclonal antibody (PA1-213, clone TRβ-62, Affinity BioReagents, Golden, CO, USA) overnight with agitation at 4 ºC. Antibody-bound chromatin was precipitated with Protein G conjugated agarose beads, washed with gradient stringent buffers, and eluted with elution buffer as per the manufacturer's instructions. Both the eluted solution and the stored TI were incubated at 65 ºC overnight to reverse cross-links. Immunoprecipitated (IP) DNA and TI DNA were purified by treatment with RNase, proteinase K and multiple phenol:chloroform:isoamyl alcohol (25:24:1) extractions. Equivalent amounts (~ 50 ng) of IP DNA and TI DNA were subjected to two rounds of whole-genome amplification, using GenomePlex Complete Whole Genome Amplification Kit (Sigma-Aldrich, Oakville, ON, Canada). Amplified DNA was purified using GenElute PCR Clean-Up kit (Sigma-Aldrich).

4.3.3 Microarray Hybridization

TR-binding sites were identified using Agilent 1 x 1M mouse promoter arrays that cover the promoter regions of approximately 19 000 genes. The overall median probe spacing on the array is approximately 200 bp, and the region of the promoter spanned ranges from -8.1 to 2.5 kb

from the TSS (as per our sampling of a few promoter regions). The Agilent Mammalian ChIP-on-chip protocol (version 10.2, Agilent Technologies, Mississauga, ON, Canada) was used for sample labelling, hybridization, washes and scanning. Briefly, amplified TI and IP DNA samples (2 μg) were labelled with cyanine 3-dUTP and cyanine 5-dUTP respectively, using the Genomic DNA Enzymatic Labelling Kit (Agilent Technologies) as per the manufacturer's instructions. Labelled genomic DNA was then cleaned using Microcon YM-30 filter units (Millipore Corporation). TI and IP samples (5 μg each) were then hybridized to Agilent SurePrint G3 Mouse Promoter Microarray, 1x1M (G4875A) at 65 ºC, 20 RPM for 40 hours. Slides were scanned on an Agilent Microarray Scanner (G2565CA). The data were acquired using Agilent Feature Extraction software version 10.7.3.1. Prior to analysis, the scans were inspected using the Agilent Quality Control report. Only microarrays that passed Agilent's quality control standards were used in subsequent analyses.

4.4.4 ChIP-chip Data Analysis

The log2 ratio(IP/TI) median probe intensity for each array was subtracted from its median and then divided by the standard deviation. Data for each array were then submitted to Splitter (Shulha et al., 2007) for peak discovery. Splitter uses the extreme right section of the log2 ratio intensity distribution to find binding events. A cut-off median +2.35 standard deviations (98^{th} percentile assuming normal distribution) was selected. From this high log2 ratio distribution section, a peak would be identified if a minimum of two consecutive probes were present at a genomic distance of less than 420 bp. A reduced cut-off median of the 93^{rd} percentile was applied to identify a peak in the promoter region of *Thrsp*, which served as a positive

control. The conservative 98th percentile cut-off was used to reduce the probability of false positive peaks, but would result in a higher level of potentially false negative findings.

4.4.5 ChIP-PCR Analysis

Primers targeting the enriched peaks were designed using Beacon Designer 7 and NCBI Primer-BLAST. PCRs were performed using Taq DNA Polymerase (Roche, Laval, QC, Canada). Actin, beta (*Actb*) (NM_007393), hypoxanthine phosphoribosyltransferase 1 (*Hprt*) (NM_013556) and hydroxymethylbilane synthase (*Hmbs*) (NM_013551) were used as a negative control. Gel analyses and band quantifications were carried out using GeneTools (Syngene, Frederick, MD, USA). Binding ratios were calculated by dividing the ratio of IP/TI from the gene of interest by the ratio of IP/TI from the reference genes. Mean enrichment, standard deviations, and p-values were calculated using log ratios and were then back-transformed.

4.4.6 RT-qPCR Analysis

Total RNA was isolated using TRizol (Invitrogen Burlington, ON, Canada). RNA quality and quantity were examined by Nanodrop (Thermo Scientific, Billerica, MA, USA). All samples had a 260/280 ratio ≥ 1.8 and 260/230 greater than ≥ 1.8. RT-qPCR analysis was carried out using a CFX96 Real-Time PCR Detection Systems (BioRad Laboratories, Mississauga, ON, Canada). RNA integrity numbers was determined to be over 9.

Custom PCR arrays were purchased from SABiosciences (Qiagen Missisauga, ON, Canada) and were run as per the manufacturer's recommendations. *Hprt* expression was used as a reference since its expression was not affected by changes in TH. Raw Ct values were

uploaded to the RT^2 Profiler PCR Array Analysis, version 3.5 (SABiosciences) web-based program for ΔΔCt based fold-change and p-value calculation.

For DEAD (Asp-Glu-Ala-Asp) box polypeptide 54 (*Ddx54*) analysis, total RNA was reverse transcribed into cDNA using SuperScriptIII (Invitrogen) as per the manufacturer's instructions. iQ SYBR Green Supermix (BioRad Laboratories) was used with a reaction volume of 50 μL. *Hprt* was used as the reference gene because it was stable across all groups in this analysis. Reactions were carried out in 96-well plates. PCRs were done in duplicate and each plate contained all samples for the gene of interest and the reference gene for one sex. Melting curves were performed for each reaction to ensure primer specificity.

4.4.7 Plasmid Construction

Primers were designed using Primer-BLAST (http://www.ncbi.nlm.nih.gov/). Endonuclease restriction sites were added to each primer to allow for directional cloning into pGL4.10[*luc2*] Vector (Promega, Madison, WI, USA). Plasmids were transformed into Mach1-$T1^R$ chemically competent *E. coli* bacteria (Invitrogen) as per the manufacturer's recommendations, and spread onto LB ampicillin plates to be grown overnight. A number of colonies were selected to be grown in LB+amp, followed by plasmid isolation using QIAprepr Spin Miniprep kit (Qiagen). Plasmid insertions were verified by endonuclease mapping and sequencing.

Mutant plasmid containing the promoter of Thsrp was produced using QuikChange II Site-Directed Mutagenesis Kit (Agilent). Briefly, primers were designed using the Agilent web-based QuikChange Primer Design Program (2013). The mutant strand was synthesized using *PfuUltra* HF DNA polymerase in a thermal cycler, followed by *Pdn I* digestion and

transformation into XL1-Blue competent cells as per the manufacturer's recommendations. Plasmid DNA from a number of colonies were selected to be verified by sequencing.

4.4.8 Cell Culture, Transfection and Luciferase Reporter Assays

AML12 cells and COS-7 cells were maintained at 37^{o}C with 5% CO_2. For RT-qPCR AML12 cells were seeded at a density of 1.2 x 10^5 in 6-well plates DMEM/F12 (1:1) medium with 10% charcoal stripped fetal bovine serum supplemented with dexamethasone, insulin, transferrin and selenium. Twenty-four hours after seeding, cells were treated with 1nM T3 and harvested 3 hours later for RNA isolation to be used for RT-qPCR analysis. Experiments were run in triplicate and repeated at least three times independently.

For luciferase assays COS-7 cells were seeded in 12-well plates at a density of 4 x 10^4 cells per well. Cells were grown in Dulbecco's Modified Eagle Medium containing 5% charcoal stripped fetal bovine serum and 0.5 mg/ml penicillin-streptomycin. Twenty four hours after seeding cells were transfected using FUGENE HD (Promega) with 100 ng of the reporter plasmid of interest, and co-transfected with 10 ng pRL-CMV and 50 ng TRα or TRβ with and without 50 ng RXRα. Twenty four hours post-transfection cells were treated with T3 (5 nM) and/or 9-cis-retinoic acid (9cRA) (1 μM). Twenty four hours after hormone treatment cells were harvested and luciferase activity was determined using a Veritas luminometer with Dual-Luciferase Reporter Assay System (Promega). Firefly luciferase activity was normalized to renilla luciferase activity. Experiments were run in triplicates and repeated at least three times independently (i.e., on separate days). Fold changes were calculated by using the average of triplicates to calculate ratios. These ratios were then log transformed to calculate an average and

then reverse log-transformed. Statistical significance was determined using a two-tailed, paired Student's t-test.

4.4.9 Bioinformatics Search for TREs

The TRE search was limited to the genomic region under the peak identified by the microarrays analysis, plus 50 bp on each side. Using a list of validated mouse TREs gathered from the literature, a position weight matrix (PWM) was developed to score the information content (bits) for position one to six of TRE half-sites. In this way, each TRE half-site was assigned a 'score' against the PWM. The score for each TRE half-site was obtained iteratively by leaving the subject out of the PWM construction. Cross-validation of the TREs from the literature was carried out with each half-site analyzed separately. This analysis revealed that a low threshold score of greater or equal than 3.76 (sum of log odd values) for one half-site and a high threshold score greater or equal than 6 (sum of log odd values) for the second half site (regardless of half-site order) allowed minimization of type I and type II errors (Gagne et al., 2013). We therefore used the cut-off scores identified in this cross-validation analysis and scanned the promoter regions for putative TREs. The scan searched for three different types of TREs: direct repeats with a four nucleotide spacer (DR4); inverted repeats with no spacer (IR0); and everted repeats with a spacer of six nucleotides (ER6).

4.5 Results

4.5.1 Identification of TR Binding Sites in the Livers of Mouse Pups

ChIP analysis of TRβ1 binding was carried out on PND 15 pup livers using Agilent 1 x 1M mouse promoter microarrays. Antibody specificity has previously been demonstrated (Dong

et al., 2009). Although the original experiment was initiated using six samples, the final analysis was conducted on three samples, one from a euthyroid pup and two from hypothyroid pups. Other samples had to be excluded due to technical difficulties either at the ChIP level or because of poor microarray quality as identified using feature extraction quality assessment/quality control reports. Thus, a comparison could not be made between euthyroid and hypothyroid samples and the analysis focused on binding sites that would confer to the consensus model that TR is bound to DNA similarly under both conditions. When looking at peaks consistent between at least two of the samples, our analysis revealed 791 peaks (see Supplementary Table 4.1). We focused validation work on peaks that were found in all three samples, to further reduce false positives. Twelve peaks were found in every sample and we refer to these as our top TR-binding sites. Peaks were mapped to the nearest TSS for neighbouring genes. Gene ontology (GO) analysis of all peaks (found in two or more samples) using Database for Annotation, Visualization and Integrated Discovery (DAVID) (Huang da et al., 2009a, b) revealed that the top GO terms for these genes were associated with development, apoptosis/cell death, metabolism, cytoskeleton and transcriptional regulation. Table 4.1 shows the twelve genes that were in closest proximity to our top TR-binding sites, and also presents the associated function of each gene. The genes encompass a range of functions from repressing transcriptional activity to cellular membrane trafficking and signalling.

Table 4.1. Genes associated with TR-binding site peaks found in all liver samples.

Gene Symbol	Location	Distance to TSS (kb)	Description	Function
Cpne4	Upstream	4.9	copine IV	May be involved in membrane trafficking; Phospholipid binding properties
Ctbp2	Downstream	0.4	C-terminal binding protein 2	Corepressor targetting transcription factors; May act as scaffold for specialized synapses
Ddx54	Upstream	0.3	DEAD (Asp-Glu-Ala-Asp) box polypeptide 54	RNA-Depedent ATPase activity; Represses the transcriptional activity of nuclear receptors
Duoxa2	Downstream	0.3	dual oxidase maturation factor 2	Required for maturation of DUOX2; May play a role in thyroid hormone synthesis
Gm364	Upstream	4.9	predicted gene 364	Unknown
Mir449c	Upstream	2.9	microRNA 449c	No experimentally validated targets
Pde8a	Upstream	1.7	phosphodiesterase 8A	Hydrolyzes the second messenger cAMP; May be involved in maintaining cAMP basal levels
Plekhb2	Upstream	0.7	pleckstrin homology domain containing, family B member 2	Involved in retrograde transport of recycling endosomes
Ptprn	Upstream	5.6	protein tyrosine phosphatase, receptor type, N	Implicated in neuroendocrine secretory processes
Ston2	Upstream	1.6	stonin 2	Adapter protein involved in endocytic machinery; May be involved in the vesicle recycling
Tpst1	Downstream	1.4	tyrosylprotein sulfotransferase 1	Catalyzes the O-sulfation of tyrosine residues within acidic motifs of polypeptides
Tuba1b	Upstream	3.0	tubulin, alpha 1b	Major constituent of microtubules

The location of the peak relative to the TSS, distance of the peak relative to the TSS, description or full name of the gene, and a summary of the UniProt/Swiss-Prot functions are presented.

4.5.2 ChIP-PCR Validation of TR Binding Sites

ChIP-PCR using the same three liver samples as those used in the ChIP-chip experiment was performed to confirm TR binding within the region of the identified top TR-binding site peaks in these samples. ChIP using the TRβ-1 antibody was performed to precipitate the protein-DNA complexes followed by PCR analysis and quantification of bands comparing TI (not precipitated) to IP samples. *Thrsp* was used as a positive control as it is often differentially regulated in mice liver when TH-levels are altered (Dong et al., 2007; Paquette et al., 2011; You et al., 2010). Although no TREs have been specifically identified and validated in the mouse *Thrsp* locus, there is a well-defined TRE in the promoter of this gene in humans (Campbell et al., 2003) as well as multiple potential TREs that have been identified in the rat *Thrsp* promoter region (Zilz et al., 1990). Even though the rat *Thrsp* TREs have not been well validated, we utilized its genomic location to base our region of interest in the mouse *Thrsp* promoter region. *Hprt* was used as the negative control although *Atcb* and *Hmbs* were also included as negative controls (data not shown) and showed similar results; that is, amplification was observed in the TI samples and there was little to no amplification in the IP samples. By testing all three negative controls we further reduced the possibility of discovering false-positives. The mean enrichment of TRβ-1 near the mouse *Thrsp* gene was compared to *Hprt*; there was clear evidence for enrichment in all three biological samples (Figure 4.1A). TR-binding sites identified in the promoter regions of *Ddx54*, dual oxidase maturation factor 2 (*Duoxa2*), microRNA 449c (*Mir449c*) and tubulin, alpha 1b (*Tuba1b*) were enriched by 4-fold or more in the IP samples compared to TI samples, and exhibited a mean enrichment of at least 7-fold (Figure 4.1B-E). Candidate TR-binding sites in the promoter regions of stonin 2 (*Ston2*) and phosphodiesterase

8A (*Pde8a*) were also investigated and showed no significant enrichment in the IP samples when compared to TI samples (data not shown).

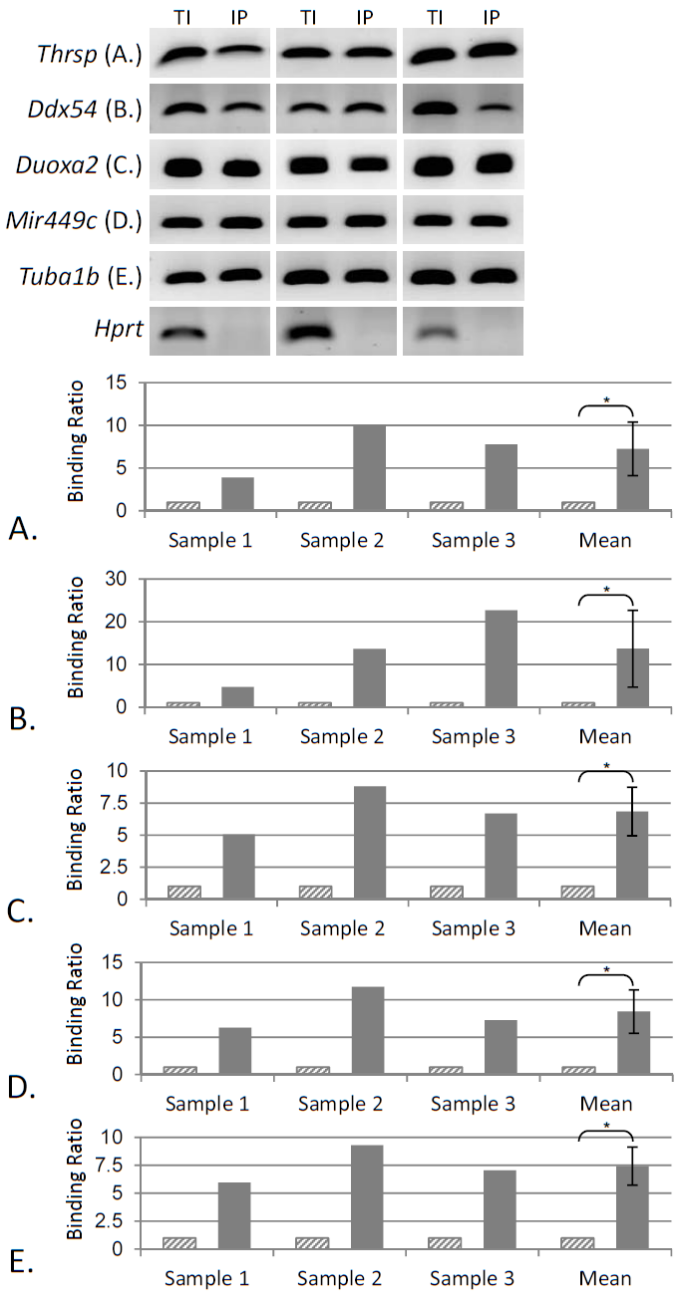

Figure 4.1. Relative enrichment of TR binding sites identified by ChIP-chip using ChIP-PCR and gel quantification. The top portion shows the amplicons run on an agarose gel, and the bottom portion shows relative enrichment of the immunoprecipitated (IP - red) samples and the total input (TI – blue) samples when compared to *Hprt* enrichment. ChIP-PCR validation of positive control (*Thrsp*) relative to negative control (*Hprt*) is presented in (A). (B) through (E)

show enrichment of peaks associated with *Ddx54*, *Duoxa2*, *Mir449c* and *Tuba1b*. Asterisks (*) denote a significant difference, $p \leq 0.05$, determined by Student's t-test. The mean enrichments (± standard deviations) across all three samples are also presented for each gene. All immunoprecipitated enrichments were significant ($p \leq 0.05$ determined by a two-tailed, paired Student's t-test) when compared to total input, except for *Hprt*.

4.5.3 In Silico Search for TREs within TR Binding Peaks

To investigate the presence of TREs within the top TR-binding sites peaks, we utilized an *in silico* bioinformatics search based on a PWM built from all known TREs in mice (Gagne et al., 2013). The analysis identified six TREs in three different genes found within the 12 peaks (plus 50 bp on each side) of the top TR-binding sites (Table 4.2). DR4, IR0 and ER6 TRE organizations were all considered.

Table 4.2. Putative TREs identified within top TR-binding sites peaks.

Gene Symbol	Position (bp)	Type	TRE Sequence
Gm364	-5265	DR4	**AGGGCA**GTGT**AGGGCT**
Gm364	-5227	DR4	**AGGAGT**TCTA**AGGGCA**
Plekhb2	-1111	IR0	**AGGGCAACACCC**
Plekhb2	-1117	ER6	**TCTCCT**TCCCAC**AGGGCA**
Plekhb2	-1062	ER6	**TTTCCT**GGTAGG**AGGGCA**
Tuba1b	-3114	DR4	**AGGCCA**CCCC**AGGCTA**

Positions relative to the TSS of the closest associated genes, the type of half-site organization, and the putative TRE sequences with bolded half-sites are also presented.

4.5.4 TH-Response in Genes Associated with Top TR-Binding Site Peaks

We investigated the transcriptional response of genes thought to be associated with top TR-binding sites identified by ChIP-chip in mice rendered hypothyroid by chemical treatment or hyperthyroid by injection of T3 relatives to euthyroid controls (Table 4.3). Serum T4 levels were determined by radioimmunoassay. In hyperthyroid samples, serum T4 levels were 4.5 fold higher than controls. Hypothyroid (MMI) samples had 5.0 fold lower T4 levels than control. Hypothyroid (PTU) samples had even lower levels of serum T4, approximately 20 fold lower than control euthyroid samples. More details regarding hyperthyroid and hypothyroid (MMI) serum T4 levels can be found in (Paquette et al., 2011). Details regarding the hypothyroid (PTU) serum T4 levels can be found in (Dong et al., 2005). A 10 fold decrease (or 90%) in T4 levels would be maximum that could be detected due to the limitations of the RIA.

The top part of Table 4.3 shows changes in the genes used as controls in this experiment. *Hprt* was used as a negative control and showed no significant changes in any of the treated groups relative to euthyroid controls. *Thrsp*, deiodinase, iodothyronine, type I (*Dio1*) and malic enzyme 1, NADP(+)-dependent, cytosolic (*Me1*) were included as positive controls because they have previously been shown to be responsive to TH changes in the liver at PND 15 (Dong et al., 2007; Paquette et al., 2011). In hyperthyroid samples, *Dio1* was significantly up-regulated relative to euthyroid samples. In hypothyroid (MMI) samples all three positive control genes were significantly down-regulated relative to euthyroid samples. *Thrsp* was the only positive control gene to show significant down-regulation in the hypothyroid (PTU) group despite the fact that the serum samples from these mice had even lower levels of serum T4 compared to euthyroid controls.

The bottom part of Table 4.2 shows fold-change values determined by RT-qPCR (normalized to *Hprt*) for all genes associated with the top peaks in Table 4.1. *Pde8*a and *Ston2* were the only two genes to exhibit significant responses to TH changes compared to euthyroid samples under the treatment and sampling regimens analyzed. *Ston2* was significantly up-regulated in hyperthyroid samples and significantly down-regulated in hypothyroid (MMI) samples, indicative of a positively regulated gene. *Pde8a* was significantly up-regulated in hypothyroid (PTU) samples, suggesting negative regulation by TH.

Table 4.3. Fold changes determined by RT-qPCR for gene expression in the livers of juvenile mice rendered hyperthyroid by T3 injection or hypothyroid by chemical treatment relative to euthyroid controls is shown for the genes in closest proximity to the top TR-binding site peaks.

Gene Symbol	Hyperthyroid (T3 Injected)		Hypothyroid (MMI Treated)		Hypothyroid (PTU Treated)	
	Fold-Change	P-Value	Fold-Change	P-Value	Fold-Change	P-Value
Dio1	**1.38**	**0.04**	**-12.5**	**0.00**	-50.0	0.07
Me1	1.19	0.26	**-1.6**	**0.03**	-3.6	0.10
Thrsp	1.56	0.50	**-14.3**	**0.05**	**-9.1**	**0.04**
Hprt	1.07	0.49	-1.0	0.82	-1.0	0.88
Cpne4	-1.05	0.50	1.12	0.19	1.05	0.70
Ctbp2	-1.11	0.25	1.07	0.50	-1.18	0.35
Ddx54	-1.20	0.17	-1.14	0.48	-1.08	0.43
Duoxa2	-1.05	0.50	1.12	0.19	1.05	0.70
Gm364	-1.05	0.50	1.12	0.19	1.05	0.70
Pde8a	-1.01	0.84	1.10	0.16	**1.29**	**0.02**
Plekhb2	1.03	0.76	-1.01	0.93	0.94	0.37
Ptprn	-1.16	0.22	1.05	0.68	1.06	0.68
Ston2	**1.28**	**0.05**	**-1.35**	**0.05**	-1.30	0.24
Tpst1	1.08	0.81	1.20	0.40	-1.30	0.40
Tuba1b	1.01	0.88	1.10	0.32	1.02	0.91

The top section shows three positive control genes: *Dio1*, *Me1* and *Thrsp*; as well as a negative control: *Hprt*. Fold-changes are presented for treated animals relative to control animals; n = 4 for all groups. P-values are in bold when $p \leq 0.05$.

4.5.5 TH-Responsiveness of Ddx54 in AML12 Cells

Ddx54 response to TH was further investigated in mouse hepatocyte AML12 cells. *Ddx54* was specifically selected for this analysis because this gene has previously been shown to interact with various nuclear receptors in a hormone-dependant manner (Rajendran et al., 2003), and TR interaction with this gene has never been investigated. Cells were exposed to T3 and RT-qPCR was used to analyze transcriptional response compared to untreated cells (Figure 4.2). *Ddx54* was up-regulated by 1.8 fold ($p < 0.0001$) following exposure to 1 nM of T3 compared to control cells. *Hprt* expression was examined and showed no response to the T3 treatment. Cytochrome P450, family 17, subfamily A, polypeptide 1 (*Cyp17a1*) was used as a positive control because it has previously been identified as TH-responsive in Aml12 cells (Ventura-Holman et al., 2007). *Cyp17a1* expression was increased by 4.3 fold relative to control cells following exposure to T3 ($p < 0.0001$).

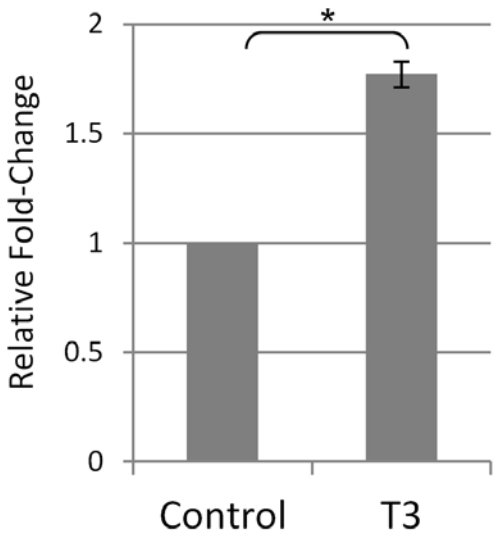

Figure 4.2. *Ddx54* expression in response to T3 in AML12 cells measured by RT-qPCR. Cells we treated with 1nM T3 for 3 hours. Asterisks (*) denote a significant difference, $p \leq 0.05$, determined by Student's t-test. Means are presented ± standard deviations for T3 treated samples.

4.5.6 Validation of Ddx54 and Thrsp by Luciferase Reporter Assay

We initially used a DR4 TRE to validate our reporter assay and confirm the ability of TR to regulate gene expression following exposure to T3 for a known TRE (Figure 4.3A). Our DR4 plasmid consisted of two DR4s separated by a 16 bp spacer. We observed a significant 2.9 fold increase when DR4 was co-transfected with TR and treated with T3. A significant 2.7 fold increase was also observed when DR4 was co-transfected with TR and RXR and treated with T3+9cRA.

After the establishment of our positive control and confirmation that our reporter system could effectively measure TR/T3 induced gene expression, we investigated the ability of TR to regulate gene expression for peaks identified in four promoter regions: *Tuba1b*, *Pde8*, *Thrsp* and *Ddx54*. We note that constructs corresponding to peaks in the promoter region of *Tuba1b* and *Pde8*a did not show any response (data not shown).

We evaluated luciferase expression driven by a region of the *Thrsp* promoter (Figure 4.3B). A segment of DNA in the promoter region of this gene in rats has been shown to regulate the expression of *Thrsp* in response to T3 (Campbell et al., 2003); the exact location of the TRE in rats has not been fully investigated although a portion of the promoter region appears to contain multiple putative TREs and half-sites (Zilz et al., 1990). This region of the promoter is well conserved between rat and mouse (~90% similarity) and is within the peak that was identified in our ChIP-chip analysis. The genomic region corresponding to the TR-binding site peak, in addition to part of the surrounding region (-2982 to -3676 bp from the TSS), was cloned into an expression vector. No significant up-regulation in luciferase activity was observed when the *Thrsp* plasmid was co-transfected with TR and treated with T3. However, when co-transfected with TR and RXR, treatment with T3+9cRA, T3 alone, or 9cRA alone resulted in

significant increases in luciferase production (2.7, 2.5 and 2.1 fold-increases, respectively). In addition, RXR alone was able to drive transcription in response to 9cRA treatment with a significant 2.8 fold-increase.

Finally, we investigated the potential TRE found in *Ddx54*. Examination of the sequence did not reveal a putative classical TRE in this region; however, we proceeded to examine a potential regulatory region. A plasmid containing -933 to +33bp of the *Ddx54* promoter region was cloned into the reporter vector. This segment included the regions of DNA underlying the peaks identified in the ChIP-chip analysis. No significant effect on luciferase expression was observed when the vector containing regions of the *Ddx54* promoter was co-transfected with TR and treated with T3 (Figure 4.3C). However, when co-transfected with TR and RXR, treatment with T3+9cRA, or 9cRA alone resulted in a significant increases in luciferase activity (2.2 and 1.4 fold increases, respectively). Interestingly, treatment with T3 alone did not increase the transcriptional activity of the reporter and RXR alone in the presence of 9cRA was sufficient to enhance the luciferase activity by a significant 2.9 fold.

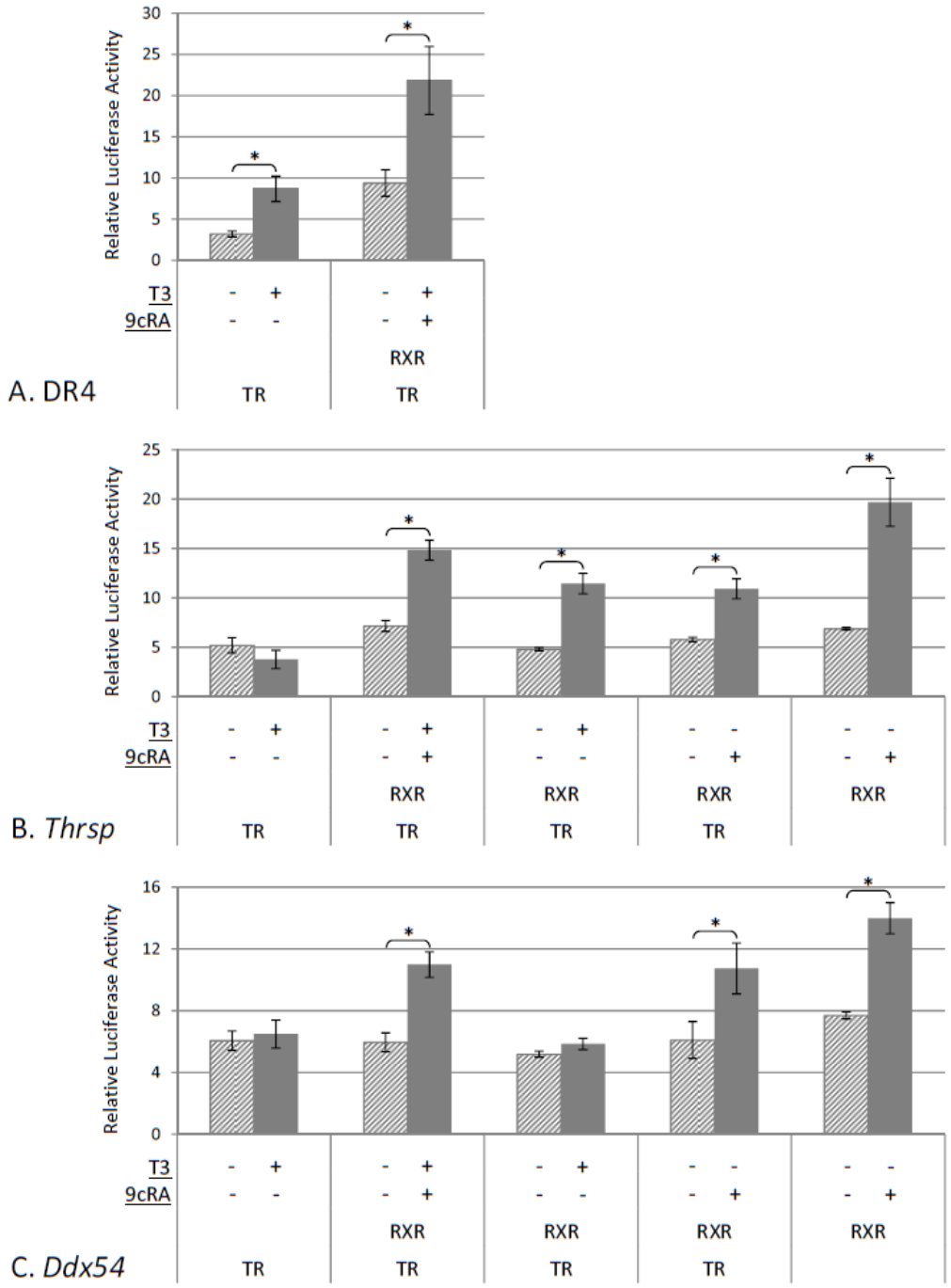

Figure 4.3. Transcriptional activity determined by luciferase reporter assay for DR4 (A), *Thrsp* (B) and *Ddx54* (C). COS-7 cells were co-transfected with a TRα and/or RXRα expression vectors. Some experiments included treatment with 5 nM T3 and/or 1 μM 9cRA as indicated at the bottom half of each panel. Data for each condition are shown separately since each

experiment is paired and was run independently. Firefly luciferase expression was normalized to renilla luciferase expression. Experiments were run in triplicate and repeated at least three times. Means are presented ± standard error of the mean. Asterisks (*) denote a significant difference, $p \leq 0.05$, determined by a two-tailed, paired Student's t-test.

4.5.7 Analysis of the Mouse Thrsp Promoter Region

Alignment of the rat and mouse *Thrsp* promoter regions was carried out to identify regions of high similarity, since the rat has been reported to potentially have multiple putative TREs (Figure 4.4). Peaks identified in our ChIP-chip analysis fall within this mouse genomic region. Some of the sequence of the mouse promoter region contained within the peak region shows perfect conservation with the rat sequence, whereas other regions are slightly diverged. Of the putative TREs included in our plasmid, only one resembled a DR4 configuration and had 100% similarity to the rat sequence. We therefore pursued further functional analysis of this specific TRE by producing an additional vector containing four mutated nucleotides when compared to the original *Thrsp* plasmid. Similar to the analysis carried out for the human *THRSP* TRE (Campbell et al., 2003), we mutated positions 2 and 3 of both of the DR4 half-sites from CC to AA. Since *Thrsp* is on the negative strand, and we are presenting the positive strand, this caused a GG to TT mutation in the DR4 TRE (confirmed by sequencing). When transfected into COS-7 cells, no transcriptional repression relative to the original *Thrsp* plasmid was observed in luciferase assays (data not shown). That is, the mutated and non-mutated versions of the *Thrsp* plasmid performed identically in this experiment.

Figure 4.4. Alignment of the mouse and rat *Thrsp* promoter regions. Mm9 corresponds to mouse genome build 9 and Rn5 corresponds to rat genome build 5. Genomic location is indicated for each DNA sequence. The arrow indicates the beginning of the amplicon that was inserted into the expression vector for *Thrsp*. The underlined sequences in the rat DNA are half-sites of two putative DR4 TREs indicated in (Campbell et al., 2003). The bolded sequence in the rat DNA are regions thought to act as TREs as observed by (Zilz et al., 1990). The boxes indicate nucleotides that have been mutated to produce a second *Thrsp* plasmid. The positive DNA strand is shown. Asterisks (*) denote conserved regions between the two alignments. The alignment was accomplished by ClustalW2 and subsequently modified manually.

4.6 Discussion

In this study TR-binding sites were isolated with ChIP using a TRβ1 antibody on PND 15 mouse liver samples, followed by hybridization of immunoprecipitated DNA to mouse Agilent promoter arrays. ChIP-PCR, gene expression analysis of hyper- and hypothyroid mouse models, gene expression analysis in cells in culture treated with T3, bioinformatics, and luciferase reporter assays were carried out to confirm TR binding and to study the activation or repression of genes by TR. We specifically investigated the role of the liganded/unliganded nuclear receptor TR and/or RXR to determine their ability to drive gene expression for four promoter regions bound by TR. This work provides new insight into TR-binding sites, genes targeted by TR/T3 regulation and the role of RXR in the regulation of expression.

Twelve TR-binding sites were identified in all samples studied using our conservative thresholds. Although this number is relatively low, this type of work has never been done in the liver and thus it was unclear how many peaks we might have expected to occur reproducibly in every sample. In previous work, our laboratory identified 91 TR-binding sites using ChIP-chip on mouse cerebellum (Dong et al., 2009). An *in vitro* study using a cerebellum cell line and chromatin affinity purification (ChAP), which is similar to ChIP but uses a tagged protein instead of an antibody, identified fifteen TR-binding sites (Chatonnet et al., 2012). Thus, the number of detectible TR-binding sites in our study is comparable to previous work. No overlap in TR-binding sites was observed between all three studies, this may be due to differences in tissue, developmental stage and technology used to identify binding sites. Our findings suggest that there are a relatively limited number of TR-binding sites in PND 15 mouse liver, suggesting that TR may not extensively bind DNA in this tissue at this developmental period. However, we note that several well-established genes that are regulated by T3 in the liver were not found in

our analysis. This may be the result of the conservative filtering thresholds applied to identify peaks, which likely reduced false positives but increased false negatives. Alternatively, we associated the TR-binding sites with the nearest TSS. It has been reported that response elements can be far away from target genes (Bourdeau et al., 2004). Thus, the assumption that the regulatory region would control the gene with the nearest TSS may have resulted in us mistakenly assigning some of the peaks to the incorrect gene. Additionally, it is important to note the small sample size (n=3) that limited the power of this study. Technical difficulties related to the ChIP and microarray analyses lead to the removal of other samples.

Transcriptional response for genes identified by ChIP-chip to contain TR-binding sites was assessed by RT-qPCR. Positive controls (*Thrsp*, *Dio1* and *Me1*) showed the expected responses to perturbations in TH levels in the hypothyroid groups, demonstrating that our mouse models and PCR conditions were appropriate. The smaller (or lack of) response observed for *Me1* and *Thrsp* in the T3 injected group may be because of the short period of time between injection and sacrifice. Of the 11 novel genes analyzed that contained TR binding peaks in nearby regions, only *Pde8a* and *Ston2* were affected by changes in TH. *Pde8a* was significantly induced in the hypothyroid (PTU) samples, suggesting negative regulation, whereas *Ston2* was significantly supressed in the hypothyroid (MMI) group and significantly induced in the hyperthyroid group, suggesting positive regulation. It is peculiar that *Ston2* was not also significantly altered in the hypothyroid PTU group. This is most likely due to the differences in exposure periods - hypothyroid (PTU) treatment went from GD 13-PND 15 (23 days), whereas the hypothyroid (MMI) exposure went from PND 12-PND 15 (3 days). The time period associated with hypothyroidism may influence the developmental trajectory leading to differences in transcriptional regulation. The lack of response in genes associated with our top

TR-binding sites may be explained by: i) low power because of a small sample size used in the *in vivo* component of this study; ii) the subtle changes in T3 levels caused by the short-term exposures to low levels of TH-disruptor or T3; iii) physiological differences in TH levels that exist between mice contributing to biological variance; or iv) assignment of a peak to the incorrect gene (as described above).

A search for TREs within the sites bound by TR in all three samples analyzed by ChIP led to the identification of three promoter regions that contained TREs, as defined by our bioinformatics search algorithm (Gagne et al., 2013). We previously used this approach to search for TREs in the promoter regions of genes identified to be differentially expressed in hypo and hyperthyroid mouse livers (Paquette et al., 2011). The lack of TREs found among the genes bound by TR may indicate a high amount of degenerateness in the TREs located within these promoter regions. This is a stringent approach that is used to minimize the rate of false positives; if TREs diverge too much from the classic TRE sequence they would be missed by this approach. It is possible that non-classic TRE-like response elements are present within these regions and that TR may bind an entirely different DNA sequence. Some investigators have suggested that TRs could be indirectly interacting with DNA through other proteins such as jun proto-oncogene (JUN) and FBJ murine osteosarcoma viral oncogene homolog (FOS) that can bind to AP-1 sites (Lazar, 2003). Future work from our group will mine the TR-binding peaks to search for commonalities, such as known and novel DNA motifs, that may suggest direct or indirect TR binding to novel motifs.

We produced constructs that contained the promoter regions of *Thrsp* and *Ddx54* to dissect the molecular mechanisms involved in the control of gene expression by TR for these promoters. DR4 was used as a positive control and showed a response to T3, or T3 and 9cRA, in

the presence or absence of RXR. The results indicate that DR4 TREs allow binding of TR homodimers and RXR heterodimers. The data shown were produced using the TRα isoform, although experiments using the TRβ isoform were also conducted for all luciferase experiments and produced similar responses (data not shown).

Thrsp expression is limited to the liver and adipose tissue where it plays an important role in regulating lipogenesis (Grillasca et al., 1997). This gene was first identified in the liver as a gene that was rapidly induced by T3 (Liaw and Towle, 1984), and has been used in multiple studies as an indicator of TH disruption in the liver (Dong et al., 2007; Paquette et al., 2011; You et al., 2010). The *Thrsp* plasmid that corresponds to the genomic location of the identified TR-binding site was tested for its ability to drive gene expression in a luciferase reporter assay. The active TRE(s) in the specified promoter region of *Thrsp* does not seem to behave similarly to the DR4 plasmid; in contrast, this TRE requires RXR to enable expression of the nearby luciferase gene. Interestingly, both T3 and 9cRA appear to be able to bind the heterodimer and drive expression. In addition, the RXR homodimer is also able to drive expression in the presence of 9cRA. The inability of the *Thrsp* promoter region to regulate expression in the presence of TR homodimers suggests that the TRE found in this region does not closely resemble the classic DR4 motif. *Thrsp* was not initially detected in our ChIP-chip analysis possibly because of the highly stringent filtering that was applied. By slightly reducing the cut-off median peak signal from the 98th to the 93rd percentile we were able to detect a peak in the promoter region of *Thrsp* in all three samples. Thus, the thresholds that we set were very stringent, and the 12 genomic sites that we identified should have a very high probability of being bound by TR.

Binding of TR to the promoter region of *Thrsp* was confirmed by ChIP-PCR. A segment of DNA under the peak identified in our study matched the genomic region where a TRE has

been identified in the rat *Thrsp* gene (see Figure 4.4 – underlined sequence). To determine whether this sequence is the TRE/TR-binding site at this specific location in the mouse genome we cloned this region into an expression vector for quantification in a luciferase report assay. In addition, a mutated *Thrsp* plasmid was used to attempt to localize the TRE. Although the DNA fragment used was effective in regulating gene expression by TH/TR, the luciferase expression produced by the mutated *Thrsp* plasmid was not affected by the altered base pairs. Thus, the long fragment analyzed contains a TRE, but it is not consistent with the consensus DR4 TRE sequence that is the region proposed to be the site of the TRE in rats. This region contains various proposed TREs in rats (see Figure 4.4 – bolded sequence) determined by bioinformatics. These TREs are not consistent with the classic TRE half-site motifs. Further investigation, such as regional point mutations, into this genomic region would be required to precisely localize the TRE sites in the mouse and rat promoter regions of *Thrsp*.

DDX54 (previously referred to as Dp97) is an RNA helicase with RNA-dependent ATPase activity that has been found to interact with nuclear receptors in a hormone-dependent manner (Rajendran et al., 2003). DDX54 was determined to contain an amino acid sequence highly similar to that of a repression domain of a nuclear receptor co-repressor and was also shown to interact with estrogen receptor (ERα and β), retinoic acid receptor (RARα), progesterone receptor (PRb) and glucocorticoid receptor (GR) (Rajendran et al., 2003). Interaction with TR has never been investigated. Previous work has also shown that DDX54 can associate with myelin basic protein (MBP) and in some cases cause an increase in MBP expression (Ueki et al., 2012). MPB is mostly expressed in the brain and is the primary constituent of the electrical insulating myelin sheath which forms around axons and neurons (Sternberger et al., 1978). We determined that *Ddx54* was positively regulated in AML12 cells in

the presence of T3. Using luciferase reporter assays we investigated the TR-binding site that was identified in the *Ddx54* promoter. We were unable to confirm that the TR homodimer binds to the area in the promoter region that we identified. However, we were able to conclude that the TR/RXR heterodimer can drive expression in the presence of 9cRA and possibly T3. RXR alone was also able to significantly induce gene expression in the presence of 9cRA. These results suggest that the response element within the isolated promoter region acts as an RXR response element (RXRE) in the constraints of luciferase assays. However, we hypothesize that given the right conditions (such as the appropriate co-activators), the response element may act as a TRE in light of our evidence that it is positively regulated by TH in cells in culture, and that its promoter region is bound by TR *in vivo*.

In conclusion, our stringent analysis revealed a number of TR-binding sites that are reproducibly observed in juvenile mouse liver. We found that only a small number of the associated genes were TH-responsive or contained an apparent TRE within the identified promoter region. We provide evidence to show that the *Thrsp* promoter region can bind TR/RXR heterodimers and regulate gene expression, but that this is not likely to be controlled by one of the TREs that align with TREs speculated to regulate the rat *Thrsp* gene. Additional work is required to characterize the exact location of the TRE(s) in the mouse and rat *Thrsp* promoter regions. Finally, we demonstrate that *Ddx54* is responsive to TH and that its promoter region contains nuclear receptor response elements. Collectively the findings suggest that there is surprisingly little TR-DNA binding in the liver of developing mice, despite the fact that a previous study from our group found that hundreds of genes were altered following TH disruption (Paquette et al., 2011). This suggests that TH action may also be mediated through other intermediates such as microRNA or other receptors.

CHAPTER 5: THYROID HORMONE RESPONSE ELEMENT HALF-SITE ORGANIZATION AND ITS EFFECT ON THYROID HORMONE MEDIATED TRANSCRIPTION

In preparation for submission: Martin A. Paquette, Ella Atlas, Mike G. Wade and Carole L. Yauk.

5.1 Abstract

Thyroid hormone (TH) disruption can have detrimental health effects, especially during early development. TH exerts its effects by binding to the thyroid hormone receptor (TR), which binds to TH response elements (TREs) to regulate target gene expression. A number of TRE organizations have been identified and include: i) direct repeats with a 4 base pair (bp) spacer (DR4), ii) inverted repeat with no spacer 0 (IR0); and iii) everted repeats with a 6bp spacer (ER6). However, the precise molecular mechanics of TH action to control target genes at these diverse TREs is unclear. In this study we investigate the relative ability of liganded homodimers TR and retinoid X receptor (RXR), and the heterodimer TR/RXR, to regulate gene expression for the TRE half-site organizations: DR4, IR0 and ER6. Luciferase reporter assays using a DR4 construct revealed that TR homodimer and TR/RXR heterodimer were able to increase luciferase expression in the presence of their respective ligands, although the presence of RXR in the heterodimer TR/RXR partially inhibited TH-mediated activation relative to TR homodimer. In the presence of the IR0 TRE, TR/RXR heterodimer and RXR homodimer increased luciferase activity. For IR0, the presence of 9-cis-retinoic acid (9cRA) was necessary for luciferase expression, whereas TH treatment alone was insufficient, suggesting that IR0 may act as a RXR response element. For ER6, TR/RXR heterodimer, TR homodimer and RXR homodimer (in the

presence of their respective ligands) all caused a significant increase in luciferase activity. Interestingly, we found that the TR/RXR heterodimer can be activated by T3 or 9cRA for ER6, although when both ligands are present significantly more activation occurs suggesting that there may be an additive effect. Finally, we investigated the efficacy of the TR-antagonist 1-850 in inhibiting transcription by TR or TR/RXT at DR4 and ER6 TREs. 1-850 effectively inhibited transcription driven by the TR homodimer for DR4. In contrast, TR/RXR heterodimer-mediated activation was only inhibited when bound to the DR4 TRE. No effect of 1-850 on T3 induced luciferase activity for the ER6 TRE was observed, suggesting that the ligand binding domain of the TR could have different conformational or chemical properties when bound to ER6 that cause a change in affinity to TH or TH-mimicking compounds. Collectively, the findings indicate that there are fundamental differences between TRE configurations that affect nuclear receptor interactions with the response element and the ability to specifically bind their ligands.

5.2 Background

Thyroid hormones (THs) regulate genes involved in many different functions, from metabolism to neuronal development. Disruption of TH signalling can lead to detrimental effects, especially during gestation where minor alterations in TH levels can cause long-term neurophysiological impairment to the child (Haddow et al., 1999). Iodine deficiency is the most common cause of hypothyroidism and affects almost one-third of the world's population (Zimmermann, 2009). TH levels can also be altered by exposure to environmental contaminants such as bisphenol A, polychlorinated biphenyls and polybrominated diphenyl ethers (Boas et al., 2006; Brucker-Davis, 1998; Jugan et al., 2010; Zoeller, 2010). Understanding the molecular

mechanics of TH action to control gene expression will facilitate the identification and mitigation of environmental factors that impair TH signalling.

Gene regulation by TH is achieved through activation of the TH receptor (TR). TR is bound to thyroid hormone response elements (TREs) in DNA in the presence or absence of TH. Interaction of triiodothyronine (T3) with TR causes conformational changes in TR and activation (or sometimes suppression) of target genes (see (Brent, 2012) for review). TREs are generally composed of two half-sites; the classic half-site is an AGGTCA hexamer (Harbers et al., 1996; Velasco et al., 2007). However, the TREs that have been identified and characterized thus far are often not composed of perfect classic half-sites, but instead tend to be degenerated. The orientation and spacing of the half-sites can also vary across TREs, although three types of TREs are the most well-known: i) direct repeat 4; ii) inverted repeat 0; and iii) everted repeat 6. Although most characterized TREs have been shown to positively regulate gene expression, negative TREs (nTREs) have also been observed (Carr and Wong, 1994; Chin et al., 1998; Decherf et al., 2010; Dong et al., 2007). This adds an additional layer of complexity in the identification and characterization of TREs.

The most frequently characterized TRE consists of a direct repeat of the half site with a 4bp spacer (DR4) between half sites. This can also be described as head to tail organization. A good example of a DR4 TRE is found in the promoter region of kruppel-like factor 9 (*Klf9*), and has been characterized in mouse, rats and humans (Denver and Williamson, 2009b) as AGGTGAagtgAGGTCA (mouse sequence). A second type of TRE is composed of an inverted repeat (or palindrome – Pal0) with no spacer between half sites in a head to head organization (IR0). This is the least well characterized TRE and very few IR0s have been identified. One of the first TREs to be characterized was the rat growth hormone 1 (*Gh1*) promoter TRE. This TRE

is comprised of a combination of organizations including an IR0 TRE (Brent et al., 1989a; Brent et al., 1989b). A third type of TRE is an everted repeat with a 6bp spacer (ER6 – sometimes referred to as F2 or IP6), referred to as a tail to tail organization. The myelin basic protein (*Mbp*) promoter regions in the mouse and rat have ER6 TREs (Farsetti et al., 1997); the mouse *Mbp* TRE sequence is GGACCTcggctgAGGACA.

The TR can operate as a homodimer to drive gene expression but it is also frequently heterodimerized with the retinoid X receptor (RXR) (Bugge et al., 1992). The ligand-binding domain (LBD) of TR primarily binds to T3, the most active form of TH, whereas the RXR LBD binds 9-cis-retinoic acid (9cRA) (Leid et al., 1992; Mangelsdorf et al., 1992; Mangelsdorf et al., 1990). In the TR/RXR heterodimer, RXR was once considered to be non-permissive; i.e., 9cRA was not able to transactivate target gene expression (Mangelsdorf and Evans, 1995). In this model, RXR was thought of as a silent partner. Further investigation led to the discovery that RXR was not a silent partner and could, in fact, bind its ligand and affect transcription (Li et al., 2002). More importantly, it is now understood that RXR and its ligand participate in regulatory activities of the TR/RXR heterodimer (Li et al., 2004).

In this study we investigate the relative ability of liganded homo- or heterodimers TR, RXR and TR/RXR to drive gene expression in respect to TRE half-site organization – DR4, IR0 and ER6. We also investigate the efficacy of a TR-antagonist in relation to TRE half-site organization in the presence TR homodimers and TR/RXR heterodimers. Our results reveal that there are important differences between the TRE organizations that relate to the presence of binding partners and their ability to drive gene expression. The results also suggest that TRE organization may affect the ability of TR-antagonists to inhibit transcription.

5.3 Methods

5.3.1 Plasmid Construction

Endonuclease restriction sites were added to each custom oligonucleotide (Eurofins MWG Operon, KY, USA) to allow for directional cloning into pGL4.10[luc2] vector (Promega, Madison, WI, USA). Oligonucleotides were annealed, followed by phenol chloroform cleaning. Oligonucleotides and plasmids were digested by XhoI and HindIII (New England Biolabs, ON, Canada) for 1h and ligated overnight using T4 Ligase (New England Biolabs). Plasmids were then transformed into Mach1-T1R chemically competent *E. coli* bacteria (Invitrogen, Burlington, ON, Canada) as per the manufacturer's recommendations, and spread onto ampicillin plates to be grown overnight. A number of colonies were selected to be grown in Luria-Bertani broth + ampicillin, followed by plasmid isolation using QIAprepr Spin Miniprep kit (Qiagen, Missisauga, ON, Canada). Plasmids containing DR4, IR0 or ER6 TREs were verified by sequencing (see Figure 5.1 for oligonucleotide sequence).

The DR4 half-site spacer "CTTC" was chosen because this spacer is present in the human thyroid hormone responsive SPOT14 (*Thrsp*) TRE, which is one of the most well characterized TRE. The ER6 half-site spacer "CGGCTG" was chosen because it appears in the mouse *Mbp* TRE and is almost completely identical (5 out of the 6 bp are conserved) to the rat *Mbp* TRE spacer "CGGCCG". Each plasmid contains two TREs separated by the same 16 bp spacer. The 16 bp space was randomly generated although it was verified not to contain GG dinucleotides since they appear to play an important role in TRE half-site functionality.

5.3.2 Cell Culture, Transfection and Luciferase Reporter Assays

COS-7 cells were seeded in 12-well plates at a density of 4 x 10^4 cells per well. Cells were grown in Dulbecco's Modified Eagle Medium containing 5% charcoal stripped fetal bovine serum and 0.5 mg/ml penicillin-streptomycin and were maintained at 37^{o}C with 5% CO2. Twenty-four hours after seeding, cells were transfected using FUGENE HD (Promega) with 100 ng of the reporter plasmid of interest (see Table 5.1), and co-transfected with 10 ng pRL-CMV(Promega) and 50 ng TRα (SC307938, Origene, MD, USA) with and without 50 ng RXRα (MC216284, Origene). Twenty-four hours post-transfection cells were treated with T3 (5 nM) (3,3',5-triiodo-L-thyronine, Sigma Chemical, Oakville, ON, Canada) and/or 9cRA (1 μM) (Santa Cruz Biotechnology Inc., CA, USA). Twenty-four hours after hormone treatment cells were harvested and firefly luciferase activity was determined using a Veritas luminometer with Dual-Luciferase Reporter Assay System (Promega). Firefly luciferase activity was normalized to renilla luciferase activity. Experiments were run in triplicates and repeated at least three times independently (i.e., on separate days). Fold changes were calculated by taking the average of triplicates to calculate ratios. These ratios were then log transformed to calculate an average and then reverse log-transformed. Statistical significance was determined using a two-tailed, paired Student's t-test.

For TR antagonist 1-850 (EMD Milipore, MA, USA) exposures, cells were transfected (as described above) 5h after seeding. Twenty-four hours after transfection, cells were treated with 10 μM 1-850 in DMSO. Twenty-four hours after 1-850 exposure, cells were treated with T3 (5 nM), and harvested 24h later.

All of the experiments described above were run in triplicates and repeated at least three times. Fold-changes were calculated by taking the average of triplicates to calculate ratios. These

ratios were then log transformed to calculate an average and then reverse log-transformed. Statistical significance was determined by a two tailed, paired Student's t-test or one way ANOVA followed by Tukey's HSD test (as indicated in figure legends).

Table 5.1. Half-site organization for TRE constructs.

TRE	Sequence (5' to 3')
DR4	CTCGAG**AGGTCA**CTTC**AGGTCA**TCTACGTAACTGATGT**AGGTCA**CTTC**AGGTCA**AAGCTT
IR0	CTCGAG**AGGTCATGACCT**TCTACGTAACTGATGT**AGGTCATGACCT**AAGCTT
ER6	CTCGAG**TGACCT**CGGCTG**AGGTCA**TCTACGTAACTGATGT**TGACCT**CGGCTG**AGGTCA**AAGCTT

Half-sites are in bold and the arrows show the orientation of each half-site. Underlined sequences are the endonuclease sites (Xho I on left and Hind III on right) showing where the oligonucleotide was inserted into the plasmid.

5.4 Results

5.4.1 TH and 9cRA Response for Three TRE Configurations

Three different TRE configurations - DR4, IR0 and ER6 were investigated for their potential to drive gene expression in the presence or absence of TR and/or RXR when treated with T3 and/or 9cRA. Oligonucleotides were designed to contain two TREs separated by an identical 16 bp spacer (Table 4.1) and were cloned into the same two restriction sites to allow for directional cloning into pGL4.10. COS-7 cells were selected for this experiment due to their ease of use and high transfection efficiency. Additionally, the TRE expression plasmids do not respond to their respective ligands in the absence of TR and/or RXR co-transfection, indicating very low levels of TR and RXR; these findings confirm that COS-7 cells are a good choice for evaluating TRE activation in response to specific nuclear receptor binding.

When evaluating the DR4 plasmid, co-transfection with TR resulted in a significant 3.6-fold increase in luciferase activity in the presence of T3 (Figure 5.1A). Cells co-transfected with RXR in addition to TR exhibited a significant 2.3-fold and 2.0-fold increase in luciferase activity in the presence of T3+9cRA or T3 alone, respectively, when compared to vehicle control. When cells were transfected with TR+RXR or RXR alone, no significant changes to luciferase activity were observed when treated with 9cRA.

The organization of the IR0 construct is shown in Table 4.1, and the experimental results are summarized in Figure 5.1B. When co-transfected with TR only or TR+RXR, T3 treatment did not induce luciferase activity. However, when co-transfected with TR+RXR and treated with T3+9cRA, a significant 3.2-fold increase in activity was observed. A 1.7-fold increase was observed for cells treated with 9cRA alone when compared to baseline. When co-transfected

with RXR only and treated with 9cRA, a significant 1.7 fold increase in luciferase activity was noted.

Results for the ER6 are shown in Figure 5.1C. When co-transfected with TR only and treated with T3 we observed a significant 2.5-fold increase in luciferase activity over non-T3 treated cells. When co-transfected with TR+RXR we observed a significant increase of 4.0-fold in the presence of T3+9cRA, 1.6-fold in the presence of T3, and 2.1-fold in the presence of 9cRA. In addition, when co-transfected with RXR alone and treated with 9cRA, a significant 2.5-fold increase in luciferase activity was detected.

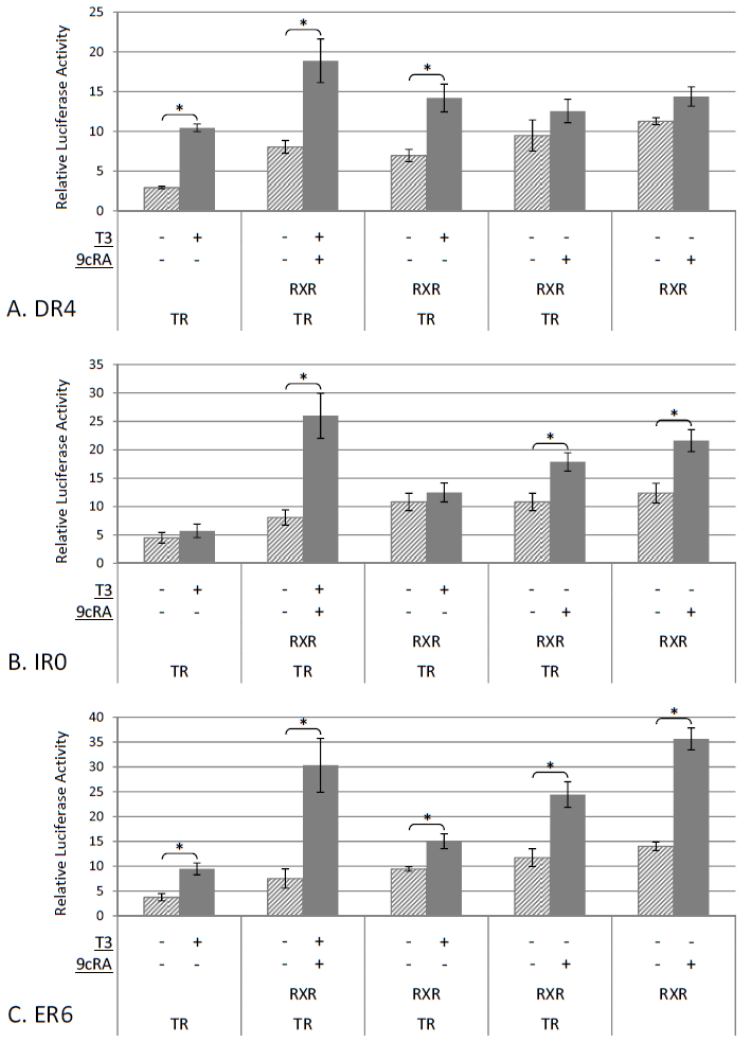

Figure 5.1. Transcriptional activity determined by luciferase reporter assay for DR4 (A), IR0 (B) and ER6 (C). COS-7 cells were co-transfected with a TRα and/or RXRα expression vectors. Cells were treated with 5 nM T3 and/or 1μM 9cRA alongside untreated controls. Firefly luciferase expression was normalized to renilla luciferase expression. Experiments were run in triplicate and repeated at least 3 times. Data for each condition are shown separately since each experiment is paired and was run independently. Data are presented as means ± standard error of the mean. Asterisks (*) denote a significant difference, $p \leq 0.05$, determined by a two-tailed, paired Student's t-test.

5.4.2 Effects of the TR Antagonist 1-850 on TH-driven Expression in the DR4 and ER6 Plasmids

The chemical 1-850 has been shown to act as a TR antagonist under certain conditions (Schapira et al., 2003). Here, we examined the effect of 1-850 on two different TRE organizations in the presence of TR alone, or with TR+RXR. The IR0 TRE organization was not included in the analysis since we previously found that it was not responsive to T3 treatment alone. We observed a significant 3.2-fold increase in luciferase expression in DR4 plasmids in the presence of T3 (Figure 5.2A). However, in the presence of 1-850 (10 μM), this increase was inhibited by 48% compared to the T3 treatment alone. When co-transfected with TR+RXR, a significant 2.8-fold increase in luciferase expression was observed in the presence of T3, whereas in the presence of 1-850 a 1.3 fold increase was observed, which translates to a significant 75% inhibition when compared to T3 treatment alone.

Experiments were repeated with the ER6 plasmid (Figure 5.2B). When co-transfected with TR, T3 induced a significant 3.4-fold increase in luciferase activity, whereas, with the addition of 1-850 a 1.6 fold increase was observed. Thus, 1-850 treatment caused a significant 48% reduction in luciferase activity compared to T3 treatment alone. Co-transfection of ER6 with TR+RXR and treatment with T3 induced a significant 2.1 fold increase in luciferase activity. However, there was no inhibitory effect of 1-850 on luciferase activity for ER6 when co-transfected with TR+RXR in the presence of T3 (i.e., fold increase remained consistent at a 2.1-fold increase).

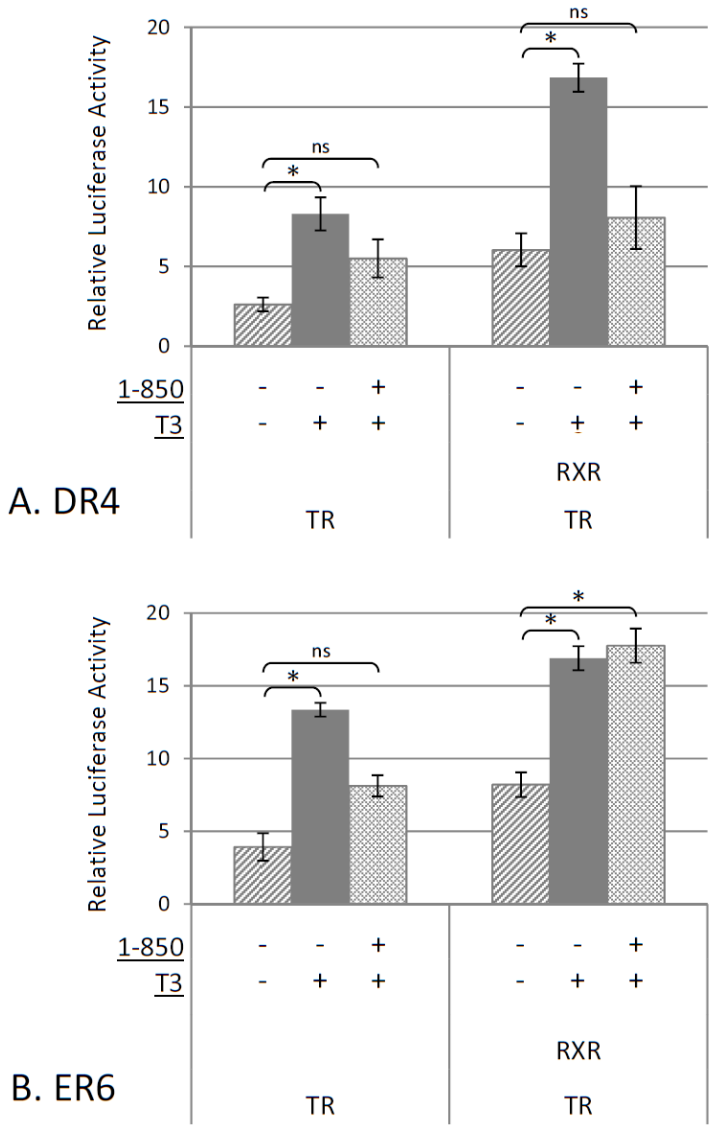

Figure 5.2. Antagonistic effects of 1-850 determined by luciferase reporter assay for DR4 (A) and ER6 (B). COS-7 cells were co-transfected with a TRα and/or RXRα expression vectors. Cells were treated with or without 5 nM T3, or with T3 in the presence of 10 μM 1-850. Firefly luciferase expression was normalized to renilla luciferase expression. Experiments were run in triplicate and repeated at least 3 times. Data are presented as means ± standard error of the mean. Asterisks (*) denote a significant difference, $p \leq 0.05$, determined by one way ANOVA followed by Tukey's HSD test.

5.5 Discussion

We investigated variables involved in TR-regulated gene expression for three established TRE sequence motifs. It is known that TRs can operate as monomers or in a complex as hetero- or homodimers to regulate the expression of TH-responsive genes. How sequence motif may influence the type and/or function of the nuclear receptor dimer that will form to control transcription has not been explored in detail. Thus, we examined whether TR and/or RXR, when treated with their respective ligands, were required for transcriptional activation when bound to the DR4, IR0 and ER6 TREs. Collectively, the results indicate that the three TRE organizations behave quite differently, that they do not all bind the same homo- or heterodimers, and that there may be both inhibitory and additive effects of co-activators and their ligands.

Using the DR4 TRE construct, TR activated gene expression in the presence of T3 based on luciferase activity (Figure 5.1A). When co-transfected with RXR and treated with T3+9cRA, or T3 alone, significant induction of transcription also occurred although fold-changes were significantly reduced ($p = 0.004$) when compared to TR alone. This finding is consistent with a previous study that determined that RXR in the heterodimer TR/RXR can inhibit T3-mediated transactivation (Li et al., 2002; Li et al., 2004); this was shown using chloramphenicol acetyltransferase (CAT) reporter assays with a Gal4-TR chimera/Gal4 reporter model, as well as with a DR4 plasmid. The Li et al. 2004 study also found that inhibition by RXR was further enhanced in the presence of 9cRA, although this was not consistent with our experiments. We found that when using the DR4 construct, 9cRA was unable to increase luciferase activity in the presence of TR/RXR heterodimer or RXR homodimer. Our findings suggest that when acting on a DR4 TRE, TR and T3 are more effective in driving gene expression on their own than in the presence of RXR and 9cRA.

In the presence of the IR0 TRE, TR and T3 were not able to activate gene expression (Figure 5.1B). Even when co-transfected with RXR, T3 alone did not significantly induce luciferase activity. However, RXR alone in the presence of 9cRA caused a significant increase in luciferase activity, suggesting that this type of half-site may act as a RXR response element (RXRE). This is supported by the fact that when co-transfected with TR and RXR, 9cRA alone caused a significant increase in luciferase activity. In the presence of 9cRA and T3, a marginal increase in gene expression was observed when compared to TR+RXR in the presence of 9cRA only ($p=0.14$) or compared to RXR in the presence of 9cRA ($p=0.11$). P-values are only approaching significance due to the variability of some of the experiments. Our results suggest that the IR0 response element allows binding of the RXR homodimer to activate gene expression, and provides some evidence that the binding of the TR/RXR heterodimer may occur and operate on gene expression when both respective ligands are present. Additional work would be needed to validate these findings and confirm that TR interacts with this IR0. The work certainly shows that 9cRA is critical for gene expression activation by a TR/RXR heterodimer when bound to the IR0 TRE. The IR0 remains one of the least understood response element. In previous studies, the IR0 response element was found to allow binding of: i) retinoic acid receptor/RXR (RAR/RXR) heterodimer (Lee and Wei, 1999); ii) farnesoid X receptor/pregnane X receptor (FXR/PXR) heterodimer (Echchgadda et al., 2004); and iii) vitamin D receptor/RXR (VDR/RXR) heterodimer (Echchgadda et al., 2004). Clearly further research on the IR0 response element is required to determine how specificity of nuclear receptor binding is achieved. Flanking sequence and the specific expression co-activator and co-repressors may play an important role in determining this specificity.

In the presence of the ER6 TRE, TR and T3 treatment caused a significant increase in luciferase activity (Figure 5.1C). Co-transfection with RXR and treatment with T3 and 9cRA appeared to cause a greater effect on transcription, although this was not statistically significant when compared to the induction caused by TR+T3 (possibly due to large standard errors). This result is in contrast to the DR4 TRE, for which a repression of TH-induced luciferase activity was noted in the presence of RXR. For ER6, both T3 and 9cRA on their own were able to induce gene expression in the presence of the heterodimer TR/RXR. Fold changes for these experiments were significantly lower than when T3 and 9cRA were administered together ($p=0.02$ for both comparisons). In addition, cells transfected with RXR and treated with 9cRA was also able to induce gene expression. The findings suggest TR homodimers, RXR homodimers and TR/RXR heterodimers are all able to effectively bind to the ER6 TRE and activate the target gene. The results also suggest that T3 and 9cRA may have an additive effect on transcriptional activation in the presence of TR/RXR heterodimer. In other words, the heterodimer can be activated by T3 or 9cRA although when both ligands are present significantly more activation occurs. Although we did not assess this possibility, we assume that TR and RXR may also be acting as monomers. A previous study on the prolactin (*Prl*) promoter region revealed similar findings (Castillo et al., 2004). These authors used a CAT reporter assay in Hela cells that was co-transfected with TR and RXR. CAT activity was increased in the presence of T3 or 9cRA. Interestingly, in the presence of both ligands an even higher transcriptional activation was observed. The active TRE in the promoter region of *Prl* has not been completely characterized and the half-site organization remains unconfirmed; our findings suggest that the TRE in question could be an ER6 since none of the other TRE organizations respond in this specific manner to these ligands.

An overarching goal in our laboratory is to apply these TRE constructs to identify potential chemical TR agonists and antagonists. Thus, we explored the ability of a proposed TR antagonist (1-850) to inhibit TH-induced gene expression across the two TREs that responded to T3 (DR4 and ER6), to determine if chemical effects may also be specific to TRE sequence context. Specifically, we examined the effects of 1-850 on TR homodimer and TR/RXR heterodimer promotion of gene expression when bound to a DR4 or ER6 TRE. The chemical 1-850 was previously identified through a virtual screening tool that searched for chemicals that could potentially bind the TR LBD (Schapira et al., 2003). When tested using a CAT reporter assay in Hela cells, 1-850 was found to inhibit TR transactivation by 80% at 5 μM concentration using a TRα expression plasmid and a reporter plasmid containing an IR0 TRE (Schapira et al., 2003). We note that we were unable to directly compare our findings with the results of Schapira et al. (2003) since our IR0 TRE plasmid when bound by TR homodimer or TR/RXR heterodimer was not significantly induced by T3.

In our experiments on COS-7 cells, 10 μM of 1-850 was used to inhibit TR activity. Much higher levels could not be used due to cellular toxicity. Viability tests using 10 μM of 1-850 did not significantly affect cellular growth (data not shown). Both DR4 and ER6 TREs that were co-transfected with a TRα expression plasmid in the presence of T3 exhibited comparable inhibition of T3 mediated transactivation in the presence of 1-850. However, inhibition caused by 1-850 in the presence of TR/RXR in DR4 plasmids was stronger than inhibition in the presence of TR only. This indicates that the TR/RXR heterodimer on DR4 may be more vulnerable to the inhibitory effects of 1-850, which may be due to differences in the structure of the LBD caused by heterodimerization. Surprisingly, inhibition by 1-850 in the presence of TR/RXR in the ER6 plasmid was not observed. This suggests that TR/RXR heterodimerization

when associated with ER6 causes modifications to the LBD that permit T3 binding but inhibit 1-850 binding. Similar to other receptors, the TR LBD contains the specific region involved in dimerization (Au-Fliegner et al., 1993). The TR/RXR heterodimer binds to TREs that are composed of half-sites in various orientations with different sized spacers; therefore, it is reasonable to speculate that due to dimer configurations resulting from TRE organization, the LBD of the TR could have slightly different conformational or chemical properties that would cause a change in affinity to TH or TH-mimicking compounds. The overall results support the notion that TRE motifs govern the type and function of complexes formed on DNA to promote TH-driven gene expression.

Understanding TR-TRE mediated gene expression has remained a challenging task. This is in part due to the degenerate nature of these response elements. Our data demonstrate that the organization of the sequence motif is critical to TH activation of gene expression. The sequence motif adds a further layer of complexity to how the expression of a specific gene may be modified by changes in TH (or 9cRA) levels. We show that TRE configuration is likely to account for some of the differences observed between genes in the way that they respond to TH perturbations or exposures to chemicals that interact with TR. The effects of nucleotide substitution in the TRE half-site, alterations to flanking sequence and changes in half-site spacer composition would be interesting avenues to explore for future work in this area. These experiments are necessary to build stronger models for the different TREs to determine more precisely the genes and functions controlled by TH. Previous studies investigating the effects of various polychlorinated biphenyl (PCB) congeners on TH action have found that known positively TH-regulated genes such as RC3/neurogranin (*Nrgn*), *Thrsp*, and deiodinase 1(*Dio1*) respond differently in the presence of specific TH disruptors (Bansal and Zoeller, 2008; Giera et

al., 2011). Our findings in combination with those above suggest that in addition to 1-850, various PCB congeners may selectively inhibit TR/RXR heterodimers due to LBD differences that are caused by variations of TR-RXR interactions, which are specific to TRE half-site organization.

In conclusion, we have characterized the transcriptional responses of three different types of TREs to TH, 9cRA and a TR antagonist. We provide evidence that supports the hypothesis that RXR may be acting as a repressor when heterodimerized to TR bound to a DR4 TRE. We show that under the given conditions the IR0 TRE cannot be induced by T3 alone in the presence of TR homodimer or TR/RXR heterodimer. We provide evidence of additive effects of T3 and 9cRA in the presence of TR/RXR for the ER6 TRE. Finally, we demonstrate that the TR-antagonist 1-850 selectively inhibits TR/RXR heterodimers when bound to DR4 TREs but not ER6 TREs. Our findings are of critical importance for the development of *in vitro* chemical screening tools for TR-agonists or antagonists. These assays must take TRE organization into consideration. Cumulatively, these findings indicate that there are fundamental differences in TRE half-site organization that affect nuclear receptor interactions with response elements and ability to specifically bind their ligand and ligand mimics.

CHAPTER 6: RESEARCH SUMMARY AND CONCLUSIONS

6.1 Hypothesis Testing and Summary of Study Outcomes

The overall objectives of this Ph.D. thesis were to: i) characterize global gene and miRNA expression in early response to TH perturbation in order to identify candidate genes that may be directly controlled by TH; ii) identify and characterize TREs found in the promoter regions of directly regulated TH-mediated genes; iii) identify TR binding sites found throughout the genome through the use of ChIP-chip; iv) compare TRE half-site organization and its ability to drive gene expression in the presence and absence of TH and/or its dimerization partner retinoic acid; and v) investigate the effects of TR-antagonists on gene expression for different TRE half-site organization. An overview of the outcomes relating to the hypotheses and objectives is presented below, as well as conclusions based on the findings for each chapter.

Chapter 2

Hypotheses: Short-term TH perturbation causes alteration to transcripts directly regulated by TH. Genes directly regulated by TH contain TREs in their promoter regions.

Outcome: These hypotheses were supported. Short-term TH perturbation disrupts hundreds of genes in juvenile mouse liver. Transcriptional profiling enabled the identification of 28 genes that appear to be under direct TH regulation. A bioinformatics search identified 33 candidate TREs in the promoter regions of 13 different genes that appear to be regulated by TH. TREs found in the promoter regions of *Tor1a*, *2310003H01Rik*, *Hect3d* and *Slc25a45* were validated by confirming that the TR is associated with these sequences *in vivo* and that it can bind directly to these sequences *in vitro*.

Conclusions: The results support the hypothesis that short-term perturbation of TH during critically sensitive periods leads to transcriptional changes to genes under the control of nearby TRE(s).

Chapter 3

Hypothesis: TH regulates transcript levels via effects on specific miRNAs.

Outcome: This hypothesis was supported. Analysis revealed 40 miRNAs that are significantly altered in the livers of hypothyroid juvenile mice compared to controls. Notably, miR-1/206/133 expression is substantially increased in response to low levels of TH. MiR-206 targets *Mup1* and *Gpd2*. *Mup1* and *Gpd2* are down-regulated *in vitro* in the presence of mir-206, whereas in the presence of TH *Mup1* and *Gpd2* are up-regulated.

Conclusion: TH disruption affects miRNA expression, which in turn leads to changes in mRNA expression.

Chapter 4

Hypotheses: (This chapter is discovery-based rather than hypothesis driven.)

Outcome: In this chapter, TR-binding sites were identified in juvenile mouse livers. However, only a few TR-binding sites were consistently identified in every sample. An *in silico* search identified TREs in only a small portion of these TR-binding sites. *Ddx54* and *Thrsp* contain TREs in their promoter regions that are capable of binding the TR/RXR heterodimer to drive target gene expression.

Conclusion: Compared to previous findings in cerebellum and *in vitro* neural cells, a relatively limited number of TR-binding sites are reproducibly observable in juvenile mouse liver. Very few apparent TREs are detectable within the identified TR-binding site promoter regions. Technological approaches used in this chapter may have limited the ability to detect TR-binding

Chapter 5

Hypotheses: TRE half-site organization dictates binding partners and their ability to drive gene expression. TR-antagonist binding to the TR is affected by TRE half-site organization and the dimerization partner.

Outcome: These hypotheses were supported. Different TRE organizations mediate specific binding of nuclear receptors, which in turn drive gene expression in the presence of their respective ligands. Ligand-binding is also dictated by TRE half-site organization. The TR-antagonist 1-850 selectively inhibits gene expression. This antagonistic action is dependent on the specific TR binding partner and the TRE half-site organization.

Conclusion: The TR homodimer, RXR homodimer and TR/RXR heterodimer selectively and differentially bind TREs of different half-site organizations. The TR-antagonist 1-850 selectively inhibits gene expression depending on TR binding partner and the TRE half-site organization.

6.2 Contributions to Scientific Knowledge

Overall, the results of this thesis significantly increase our knowledge of the mechanisms by which TH regulates mRNA levels in the livers of developing rodents. In addition, the thesis

clearly demonstrates that the DNA sequence of the TRE is a critical mediator of the potential regulatory activity by TH on gene expression. Finally, the thesis provides a first step towards the development of *in vitro* tools to screen for chemicals that directly interfere with the TR to perturb TH-mediated gene expression. Below I describe the specific advances that have emerged from the work in this thesis.

6.2.1 TH Mediated Gene Expression

Transcriptional profiling of hyper, hypo and hypo+ groups allowed for the identification genes directly regulated by THs in male and female mice. A bioinformatics search based on a PWM built from known TREs was applied to analyse promoter regions of genes directly regulated by TH and identified 33 candidate mouse TREs potentially conserved between rats and humans. We provide evidence of four new TREs in the promoter regions of *Tor1a*, *Slc25a45*, *Hectd3* and *2310003H01Rik*. The results provide data to develop a stronger model for the TRE sequence motifs that direct TR binding, identify key genes that may be important for TH mediated effects, and help to further characterize the mechanisms by which TH directly regulate gene expression. The addition of these four TREs, given that prior to this thesis there were only 13 genes with characterized TREs in the mouse genome (as per our literature search), provides a stronger dataset on which to build future PWM.

This thesis also clearly demonstrates the significant role that miRNAs likely play in mediating TH- driven gene expression. The magnitude of the changes observed in miRNA transcription far exceeded the mRNA response, indicating a major modulating role of these non-coding RNAs. In total, analysis of hypothyroid and euthyroid mice liver identified the disruption

of 40 different miRNA. We also provide specific evidence to show that TH down regulates miR-206, which in turn alleviates miR-206-mediated suppression of its downstream targets *Mup1* and *Gpd2*. These findings provide new insight into the role of miRNAs in mediating the non-genomic effects of TH action in the liver.

6.2.2 TR-binding Sites

Although TH action has been studied for decades, surprisingly few TREs have been validated and characterized. Our ChIP-chip analysis identified TR-binding sites in juvenile mouse livers. The investigation revealed that a relatively limited number of TR-binding sites are likely in juvenile mouse liver DNA despite previous studies showing that numerous genes can be affected by TH disruption at that developmental stage, suggesting that TH action must also be mediated through other intermediates. TREs in the promoter region of *Thrsp* and *Ddx54* were confirmed. The ability of TR, RXR homodimer and TR/RXR heterodimer to bind and drive gene expression in the presence of their ligands for these genes was demonstrated for the first time in detail. Collectively the results provide an important step towards characterizing TR-binding sites and identifying the underlying drivers of TR-gene regulation.

6.2.3 TRE Half-site Organization

The precise molecular mechanisms of TH action in controlling target genes at diverse TREs is unclear. We used luciferase reporter assays to demonstrate important differences between homodimers of TR and RXR, and the TR/RXR heterodimer, in their ability to drive gene expression when bound to different TRE half-site organizations: DR4, IR0 and ER6. We

show that a TR-antagonist can selectively bind the TR depending on the half-site organization of the TRE, demonstrating that the LBD of the TR may have different conformational or chemical properties when bound to TREs that are composed of different half-site organizations. The findings indicate that there are fundamental differences between TRE configurations that affect nuclear receptor interactions with the response element and the ability to specifically bind their ligands.

6.3 Critiques and Limitations of Findings

Our investigation of transcriptional response to TH disruption and TR-binding sites employed DNA microarray analysis. As with all technologies, DNA microarrays have their limitations. Microarrays have numerous sources of variability including the microarray platform, dye labelling, reverse transcription efficiency, and hybridization. There are different experimental designs that must be considered to reduce false positive discoveries and allow for appropriate array comparison. In our gene expression experiments we used a two-colour reference design because this allows for easy comparison to other experiments using the same common reference. An alternative method to microarray analyses would be RNA-sequencing (RNA-seq), which is becoming more affordable and accessible. RNA-seq would ultimately lead to higher quality quantitative data since the technology is based on a digital output that reveals the precise transcript that is changing, rather than analogue read-outs that rely on probe hybridization.

ChIP-chip has become widely used for genome-wide analyses of protein-DNA interactions although there are well known concerns about this method, such as high background

signal and high false positive rates. There are many factors that can contribute to these effects, including incomplete crosslinking/reverse-crosslinking, or protein/RNA contamination. Additionally, the ChIP method often yields very little DNA, which needs to go through whole genome amplification, and which can contribute to a high background signal. PCR artefacts can also potentially cause false positives. The antibody used for ChIP should be of very high quality and specificity, although very few antibodies are considered "ChIP grade". To help minimize false positive findings we concentrated our work on peaks that were consistent between all analyzed samples. An alternative method that could be beneficial when there is a lack of "ChIP grade" antibodies would be to run a ChAP-chip, which utilizes a tagged protein (such as the TR) and affinity purification, although this technique is also not without drawbacks. Using a tagged protein can lead biochemical changes that may alter the native form and function of the studied protein.

6.4 Future Directions

The findings in this thesis raise many interesting questions that could be the subject of future work. Specific recommendations are proposed below:

- In chapter 2 we investigated the transcriptional response to TH changes and discovered hundreds of gene responding to the exposures, although only a few were found to fit the profile of genes directly regulated by TR/TH. Our findings on miRNAs revealed that there are alternative regulatory mechanisms involved in TH response that should be explored. An additional alternative mechanism that would be interesting to investigate is genomic methylation changes in response to TH disruption. This could be achieved by

methylated DNA immunoprecipitation followed by sequencing (MeDIP-seq) or by whole genome bisulfite sequencing. A previous study has shown that hypothyroidism can cause an increase in methylation in brain-derived neurotrophic factor (*Bdnf*) and reelin (*Reln*) in rat hippocampus (Sui and Li, 2010) although no genome-wide analyses have been performed.

- Based on our miRNA findings, a detailed analysis of the genomic location of each identified miRNA that responds to TH disruption should be performed to search for TREs or novel-motifs. Some miRNAs are found within genes and can be transcribed by the same promoters as the host genes, whereas others will have their own promoters. These experiments would also shed light on the mechanisms regulating miRNA expression. Additionally, our analysis was only performed on hypothyroid and euthyroid animals; including hyperthyroid animals in the analysis would enhance the findings by supporting the role of TH in the response.
- The potential role of miRNAs as *in vivo* biomarkers of TH disruption during development should be explored. Exposures should be repeated with chemicals that have different modes of action but that ultimately alter TH levels. A dose-response study could also be beneficial to characterize miRNA response to changing TH levels by determining the TH levels at which measurable miRNA perturbations arise.
- A previous study on EREs investigated the effects of substituting, one nucleotide at a time across each position of the response element (Bourdeau et al., 2004). For each substituted position an EMSA was conducted using ERα and ERβ to document binding efficiency compared to an unchanged ERE. This type of experiment should be conducted for the TREs DR4, IR0 and ER6. Luciferase reporter assays should be used instead of

EMSAs in order to produce higher quality, more quantitative data. These experiments could reveal which degenerated response elements are able to act as TREs and which half-site positions are most important for an active TRE to bind the TR homodimer or TR/RXR heterodimer. This could ultimately lead to more accurate and robust TRE search algorithms.

- A more in depth analysis of other TR-antagonist and agonists would help strengthen the TRE half-site organization investigation. NH3 is another synthetic TR-antagonist that has been previously shown to inhibit binding of TH to the TR and also inhibit cofactor recruitment (Grover et al., 2007). Analysis of NH3 with the established DR4, IR0 and ER6 reporter constructs would permit a comparison to the 1-850 results. In addition, the chemical structures of NH3 and 1-850 could be used to compare and identify the structural similarities that might be useful for bioinformatics programs that attempt to predict antagonistic properties.
- Repeating the luciferase work using a different cell line would also help strengthen the TRE half-site organization investigation. Since the 1-850 was initially established as an inhibitor of TR in Hela cells, it would be interesting to compare inhibitory capacity in this cell line using our DR4, IR0 and ER6 reporter constructs. In addition, repeating the work in primary hepatocytes could yield interesting findings. Variation in results between these cell lines will most likely be because of differences in co-activator and co-repressor expression; it would therefore be important to quantify the expression of main TR/RXR cofactors in all tested cell lines.
- This study has shown the importance of TRE half-site organization in mediating gene expression. Future work surrounding the identification of TR-agonists and antagonist

should take these findings into consideration by investigation effects on various TRE half-site organizations. In addition, these findings have provided new insight that may explain peculiar (i.e., seemingly discordant) findings for gene expression changes in response to different chemicals that cause hypothyroidism. It would be worth exploring the possibility that TRE half-site organization is involved in these effects.

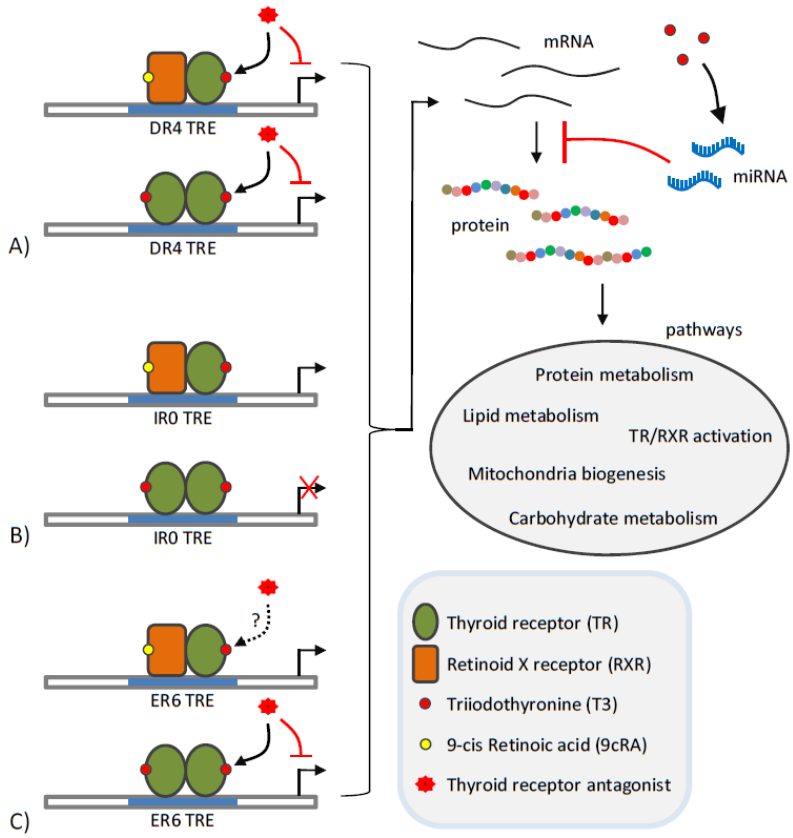

Figure 6.1. Summary of molecular mechanisms controlling TH-induced changes in mRNA levels revealed in this thesis. (A) The DR4 TRE operates via both the TR/RXR heterodimer and TR homodimer to regulate gene expression. TR antagonist 1-850 is effective at suppressing this regulation in both the TR/RXR heterodimer and the TR homodimer. (B) The IR0 TRE operates only through the TR/RXR heterodimer, although 9cRA appears to be the required ligand for activation. Antagonistic effect for the IR0 TRE could not be assessed since T3 on its own was not found to drive gene expression. (C) The ER6 TRE operates via both the TR/RXR heterodimer and TR homodimer to regulate gene expression. TR antagonist 1-850 is effective at suppressing regulation in the TR homodimer only; activation by the TR/RXR heterodimer appears to be unaffected. TH mediated miRNA action on target genes is also shown although the molecular mechanisms for this regulation remain unclear.

6.5 Concluding Remarks

This thesis explores the underlying molecular biology governing how TH controls mRNA levels. We have identified key characteristics of TRE half-site organization and its effects on binding partner and LBD configuration, as well as the critical role of miRNAs in post-transcriptional processes (see Figure 6.1). We believe that this investigation of the key molecular mechanisms dictating TH action will ultimately lead to better understanding of toxicological responses triggered by TH disruption and enable the development of more biologically relevant *in vitro* tools for screening, identifying and characterizing TDC.

The past decade has seen widespread international endorsement and uptake of a shift in the toxicological testing paradigm away from animal-intensive traditional toxicological testing. Thus, there is an urgent need for the development of effective *in vitro* screening tools for endocrine disrupting chemicals in general, but in particular for the identification of chemicals that perturb TH signalling (an important gap in the existing battery of *in vitro* assays). The underlying biology explored in this thesis relates directly to the development of *in vitro* assays that detects alterations in TR ligand binding. Specifically, our results lead us to speculate that configurational differences in TREs are primary factors governing differences between endogenous genes following TH disruption. We argue that consideration of TRE characteristics in the development of *in vitro* screening tools is critical to assay predictivity (i.e., ability to correctly predict in vivo effects). For example, based on our findings, an *in vitro* screening tool that utilized an ER6 TRE half-site organization might not identify a TR-antagonist depending on the presence (or absence) of TR homodimer and TR/RXR heterodimer (as illustrated in Figure 6.1). Thus, we specifically recommend that the development of *in vitro* screening tools should incorporate the use of both DR4 and ER6, as well as exploring response in both monomeric and

dimeric states. Additional work, possibly in a different cell line, would be required to assess the functionality of the IR0 TRE and to determine whether it should be included for assessment of chemical interaction with TR.

Overall, the molecular biology experiments conducted in this thesis provide important insights into critical mechanisms by which TH governs mRNA levels that must be considered in the development of toxicological testing methods for TH-disrupting chemicals. The findings raise concerns about the suitability of existing *in vitro* methods applied to identify TDC (i.e. that lack of considering TRE half-site organization and its effect on LBD) and suggest key features that should be considered for the development of improved *in vitro* screens to identify chemicals that interact with TR.

REFERENCES

Ahmed, O.M., El-Gareib, A.W., El-Bakry, A.M., Abd El-Tawab, S.M., and Ahmed, R.G. (2008). Thyroid hormones states and brain development interactions. International journal of developmental neuroscience : the official journal of the International Society for Developmental Neuroscience *26*, 147-209.

Alvarez-Garcia, I., and Miska, E.A. (2005). MicroRNA functions in animal development and human disease. Development *132*, 4653-4662.

Au-Fliegner, M., Helmer, E., Casanova, J., Raaka, B.M., and Samuels, H.H. (1993). The conserved ninth C-terminal heptad in thyroid hormone and retinoic acid receptors mediates diverse responses by affecting heterodimer but not homodimer formation. Molecular and cellular biology *13*, 5725-5737.

Auso, E., Lavado-Autric, R., Cuevas, E., Del Rey, F.E., Morreale De Escobar, G., and Berbel, P. (2004). A moderate and transient deficiency of maternal thyroid function at the beginning of fetal neocorticogenesis alters neuronal migration. Endocrinology *145*, 4037-4047.

Bansal, R., and Zoeller, R.T. (2008). Polychlorinated biphenyls (Aroclor 1254) do not uniformly produce agonist actions on thyroid hormone responses in the developing rat brain. Endocrinology *149*, 4001-4008.

Benjamini, Y., Drai, D., Elmer, G., Kafkafi, N., and Golani, I. (2001). Controlling the false discovery rate in behavior genetics research. Behav Brain Res *125*, 279-284.

Benjamini Y, H.Y. (1995). Controlling the False Discovery Rate: a Practical and Powerful Approach to Multiple Testing. Journal of the Royal Statistical Society *57*, 289-300.

Bernal, J. (2005). Thyroid hormones and brain development. Vitamins and hormones *71*, 95-122.

Bertrand, S., Brunet, F.G., Escriva, H., Parmentier, G., Laudet, V., and Robinson-Rechavi, M. (2004). Evolutionary genomics of nuclear receptors: from twenty-five ancestral genes to derived endocrine systems. Molecular biology and evolution *21*, 1923-1937.

Bianco, A.C., Salvatore, D., Gereben, B., Berry, M.J., and Larsen, P.R. (2002). Biochemistry, cellular and molecular biology, and physiological roles of the iodothyronine selenodeiodinases. Endocrine reviews *23*, 38-89.

Biswas, S.C., Pal, U., and Sarkar, P.K. (1997). Regulation of cytoskeletal proteins by thyroid hormone during neuronal maturation and differentiation. Brain research *757*, 245-253.

Blount, B.C., Pirkle, J.L., Osterloh, J.D., Valentin-Blasini, L., and Caldwell, K.L. (2006). Urinary perchlorate and thyroid hormone levels in adolescent and adult men and women living in the United States. Environmental health perspectives *114*, 1865-1871.

Boas, M., Feldt-Rasmussen, U., and Main, K.M. (2012). Thyroid effects of endocrine disrupting chemicals. Molecular and cellular endocrinology *355*, 240-248.

Boas, M., Feldt-Rasmussen, U., Skakkebaek, N.E., and Main, K.M. (2006). Environmental chemicals and thyroid function. European journal of endocrinology / European Federation of Endocrine Societies *154*, 599-611.

Boas, M., Main, K.M., and Feldt-Rasmussen, U. (2009). Environmental chemicals and thyroid function: an update. Current opinion in endocrinology, diabetes, and obesity *16*, 385-391.

Boelaert, K., and Franklyn, J.A. (2005). Thyroid hormone in health and disease. The Journal of endocrinology *187*, 1-15.

Bourdeau, V., Deschenes, J., Metivier, R., Nagai, Y., Nguyen, D., Bretschneider, N., Gannon, F., White, J.H., and Mader, S. (2004). Genome-wide identification of high-affinity estrogen response elements in human and mouse. Molecular endocrinology (Baltimore, Md *18*, 1411-1427.

Brent, G.A. (2008). Clinical practice. Graves' disease. The New England journal of medicine *358*, 2594-2605.

Brent, G.A. (2012). Mechanisms of thyroid hormone action. The Journal of clinical investigation *122*, 3035-3043.

Brent, G.A., Harney, J.W., Chen, Y., Warne, R.L., Moore, D.D., and Larsen, P.R. (1989a). Mutations of the rat growth hormone promoter which increase and decrease response to thyroid hormone define a consensus thyroid hormone response element. Molecular endocrinology (Baltimore, Md *3*, 1996-2004.

Brent, G.A., Larsen, P.R., Harney, J.W., Koenig, R.J., and Moore, D.D. (1989b). Functional characterization of the rat growth hormone promoter elements required for induction by thyroid hormone with and without a co-transfected beta type thyroid hormone receptor. The Journal of biological chemistry *264*, 178-182.

Brent, G.A., Williams, G.R., Harney, J.W., Forman, B.M., Samuels, H.H., Moore, D.D., and Larsen, P.R. (1992). Capacity for cooperative binding of thyroid hormone (T3) receptor dimers defines wild type T3 response elements. Molecular endocrinology (Baltimore, Md *6*, 502-514.

Brucker-Davis, F. (1998). Effects of environmental synthetic chemicals on thyroid function. Thyroid : official journal of the American Thyroid Association *8*, 827-856.

Bryzgalova, G., Effendic, S., Khan, A., Rehnmark, S., Barbounis, P., Boulet, J., Dong, G., Singh, R., Shapses, S., Malm, J.*, et al.* (2008). Anti-obesity, anti-diabetic, and lipid lowering effects of the thyroid receptor beta subtype selective agonist KB-141. The Journal of steroid biochemistry and molecular biology *111*, 262-267.

Buchholz, D.R., Paul, B.D., and Shi, Y.B. (2005). Gene-specific changes in promoter occupancy by thyroid hormone receptor during frog metamorphosis. Implications for developmental gene regulation. The Journal of biological chemistry *280*, 41222-41228.

Bugge, T.H., Pohl, J., Lonnoy, O., and Stunnenberg, H.G. (1992). RXR alpha, a promiscuous partner of retinoic acid and thyroid hormone receptors. The EMBO journal *11*, 1409-1418.

Bungay, A., Selden, C., Brown, D., Malik, R., Hubank, M., and Hodgson, H. (2008). Microarray analysis of mitogenic effects of T3 on the rat liver. Journal of gastroenterology and hepatology *23*, 1926-1933.

Campbell, M.C., Anderson, G.W., and Mariash, C.N. (2003). Human spot 14 glucose and thyroid hormone response: characterization and thyroid hormone response element identification. Endocrinology *144*, 5242-5248.

Carr, F.E., and Wong, N.C. (1994). Characteristics of a negative thyroid hormone response element. The Journal of biological chemistry *269*, 4175-4179.

Carroll, J.S., Liu, X.S., Brodsky, A.S., Li, W., Meyer, C.A., Szary, A.J., Eeckhoute, J., Shao, W., Hestermann, E.V., Geistlinger, T.R*., et al.* (2005). Chromosome-wide mapping of estrogen receptor binding reveals long-range regulation requiring the forkhead protein FoxA1. Cell *122*, 33-43.

Carroll, J.S., Meyer, C.A., Song, J., Li, W., Geistlinger, T.R., Eeckhoute, J., Brodsky, A.S., Keeton, E.K., Fertuck, K.C., Hall, G.F*., et al.* (2006). Genome-wide analysis of estrogen receptor binding sites. Nat Genet *38*, 1289-1297.

Castillo, A.I., Sanchez-Martinez, R., Moreno, J.L., Martinez-Iglesias, O.A., Palacios, D., and Aranda, A. (2004). A permissive retinoid X receptor/thyroid hormone receptor heterodimer allows stimulation of prolactin gene transcription by thyroid hormone and 9-cis-retinoic acid. Molecular and cellular biology *24*, 502-513.

Chao, A., Tsai, C.L., Wei, P.C., Hsueh, S., Chao, A.S., Wang, C.J., Tsai, C.N., Lee, Y.S., Wang, T.H., and Lai, C.H. (2010). Decreased expression of microRNA-199b increases protein levels of SET (protein phosphatase 2A inhibitor) in human choriocarcinoma. Cancer letters *291*, 99-107.

Chatonnet, F., Guyot, R., Benoit, G., and Flamant, F. (2013). Genome-wide analysis of thyroid hormone receptors shared and specific functions in neural cells. Proceedings of the National Academy of Sciences of the United States of America *110*, E766-775.

Chatonnet, F., Guyot, R., Picou, F., Bondesson, M., and Flamant, F. (2012). Genome-wide search reveals the existence of a limited number of thyroid hormone receptor alpha target genes in cerebellar neurons. PloS one *7*, e30703.

Chen, X.M. (2009). MicroRNA signatures in liver diseases. World J Gastroenterol *15*, 1665-1672.

Chin, S., Apriletti, J., and Gick, G. (1998). Characterization of a negative thyroid hormone response element in the rat sodium, potassium-adenosine triphosphatase alpha3 gene promoter. Endocrinology *139*, 3423-3431.

Cook, C.B., Kakucska, I., Lechan, R.M., and Koenig, R.J. (1992). Expression of thyroid hormone receptor beta 2 in rat hypothalamus. Endocrinology *130*, 1077-1079.

Crane, H.M., Pickford, D.B., Hutchinson, T.H., and Brown, J.A. (2005). Effects of ammonium perchlorate on thyroid function in developing fathead minnows, Pimephales promelas. Environmental health perspectives *113*, 396-401.

Crofton, K.M. (2008). Thyroid disrupting chemicals: mechanisms and mixtures. International journal of andrology *31*, 209-223.

Crofton, K.M., Craft, E.S., Hedge, J.M., Gennings, C., Simmons, J.E., Carchman, R.A., Carter, W.H., Jr., and DeVito, M.J. (2005). Thyroid-hormone-disrupting chemicals: evidence for dose-dependent additivity or synergism. Environmental health perspectives *113*, 1549-1554.

Cui, X., Hwang, J.T., Qiu, J., Blades, N.J., and Churchill, G.A. (2005). Improved statistical tests for differential gene expression by shrinking variance components estimates. Biostatistics (Oxford, England) *6*, 59-75.

Dai, G., Levy, O., and Carrasco, N. (1996). Cloning and characterization of the thyroid iodide transporter. Nature *379*, 458-460.

Das, B., Heimeier, R.A., Buchholz, D.R., and Shi, Y.B. (2009). Identification of direct thyroid hormone response genes reveals the earliest gene regulation programs during frog metamorphosis. The Journal of biological chemistry *284*, 34167-34178.

Das, B., Matsuda, H., Fujimoto, K., Sun, G., Matsuura, K., and Shi, Y.B. (2010). Molecular and genetic studies suggest that thyroid hormone receptor is both necessary and sufficient to mediate the developmental effects of thyroid hormone. General and comparative endocrinology *168*, 174-180.

Davis, P.J., and Davis, F.B. (1996). Nongenomic actions of thyroid hormone. Thyroid : official journal of the American Thyroid Association *6*, 497-504.

Davis, P.J., and Davis, F.B. (2002). Nongenomic actions of thyroid hormone on the heart. Thyroid : official journal of the American Thyroid Association *12*, 459-466.

Davis, P.J., Davis, F.B., and Cody, V. (2005). Membrane receptors mediating thyroid hormone action. Trends in endocrinology and metabolism: TEM *16*, 429-435.

Davis, P.J., Davis, F.B., Mousa, S.A., Luidens, M.K., and Lin, H.Y. (2011). Membrane receptor for thyroid hormone: physiologic and pharmacologic implications. Annual review of pharmacology and toxicology *51*, 99-115.

Davis, P.J., Leonard, J.L., and Davis, F.B. (2008). Mechanisms of nongenomic actions of thyroid hormone. Frontiers in neuroendocrinology *29*, 211-218.

Davis, P.J., Tillmann, H.C., Davis, F.B., and Wehling, M. (2002). Comparison of the mechanisms of nongenomic actions of thyroid hormone and steroid hormones. Journal of endocrinological investigation *25*, 377-388.

Dayan, C.M., and Daniels, G.H. (1996). Chronic autoimmune thyroiditis. The New England journal of medicine *335*, 99-107.

Decherf, S., Seugnet, I., Kouidhi, S., Lopez-Juarez, A., Clerget-Froidevaux, M.S., and Demeneix, B.A. (2010). Thyroid hormone exerts negative feedback on hypothalamic type 4 melanocortin receptor expression. Proceedings of the National Academy of Sciences of the United States of America *107*, 4471-4476.

Denver, R.J., and Williamson, K.E. (2009a). Identification of a thyroid hormone response element in the mouse Kruppel-like factor 9 gene to explain its postnatal expression in the brain. Endocrinology.

Denver, R.J., and Williamson, K.E. (2009b). Identification of a thyroid hormone response element in the mouse Kruppel-like factor 9 gene to explain its postnatal expression in the brain. Endocrinology *150*, 3935-3943.

DeVito, M., Biegel, L., Brouwer, A., Brown, S., Brucker-Davis, F., Cheek, A.O., Christensen, R., Colborn, T., Cooke, P., Crissman, J.*, et al.* (1999). Screening methods for thyroid hormone disruptors. Environmental health perspectives *107*, 407-415.

Dong, H., Paquette, M., Williams, A., Zoeller, R.T., Wade, M.G., and Yauk, C.L. (2010). Thyroid hormone may regulate mRNA abundance in liver by acting on microRNAs. PloS one *5(8)*.

Dong, H., Wade, M., Williams, A., Lee, A., Douglas, G.R., and Yauk, C. (2005). Molecular insight into the effects of hypothyroidism on the developing cerebellum. Biochemical and biophysical research communications *330*, 1182-1193.

Dong, H., Yauk, C.L., Rowan-Carroll, A., You, S.H., Zoeller, R.T., Lambert, I., and Wade, M.G. (2009). Identification of thyroid hormone receptor binding sites and target genes using ChIP-on-chip in developing mouse cerebellum. PLoS ONE *4*, e4610.

Dong, H., Yauk, C.L., Williams, A., Lee, A., Douglas, G.R., and Wade, M.G. (2007). Hepatic gene expression changes in hypothyroid juvenile mice: characterization of a novel negative thyroid-responsive element. Endocrinology *148*, 3932-3940.

DosSantos, R.A., Alfadda, A., Eto, K., Kadowaki, T., and Silva, J.E. (2003). Evidence for a compensated thermogenic defect in transgenic mice lacking the mitochondrial glycerol-3-phosphate dehydrogenase gene. Endocrinology *144*, 5469-5479.

Dudek, K.M., Suter, L., Darras, V.M., Marczylo, E.L., and Gant, T.W. (2013). Decreased translation of Dio3 mRNA is associated with drug-induced hepatotoxicity. The Biochemical journal *453*, 71-82.

Duursma, A.M., Kedde, M., Schrier, M., le Sage, C., and Agami, R. (2008). miR-148 targets human DNMT3b protein coding region. Rna *14*, 872-877.

Echchgadda, I., Song, C.S., Roy, A.K., and Chatterjee, B. (2004). Dehydroepiandrosterone sulfotransferase is a target for transcriptional induction by the vitamin D receptor. Molecular pharmacology *65*, 720-729.

Eyal, O., Blum, S., Mueller, R., Smith, F.O., and Rose, S.R. (2008). Improved growth velocity during thyroid hormone therapy in children with Fanconi anemia and borderline thyroid function. Pediatric blood & cancer *51*, 652-656.

Farsetti, A., Lazar, J., Phyillaier, M., Lippoldt, R., Pontecorvi, A., and Nikodem, V.M. (1997). Active repression by thyroid hormone receptor splicing variant alpha2 requires specific regulatory elements in the context of native triiodothyronine-regulated gene promoters. Endocrinology *138*, 4705-4712.

Farsetti, A., Mitsuhashi, T., Desvergne, B., Robbins, J., and Nikodem, V.M. (1991). Molecular basis of thyroid hormone regulation of myelin basic protein gene expression in rodent brain. The Journal of biological chemistry *266*, 23226-23232.

Flamant, F., Poguet, A.L., Plateroti, M., Chassande, O., Gauthier, K., Streichenberger, N., Mansouri, A., and Samarut, J. (2002). Congenital hypothyroid Pax8(-/-) mutant mice can be rescued by inactivating the TRalpha gene. Molecular endocrinology (Baltimore, Md *16*, 24-32.

Flint, S., Markle, T., Thompson, S., and Wallace, E. (2012). Bisphenol A exposure, effects, and policy: a wildlife perspective. Journal of environmental management *104*, 19-34.

Flores-Morales, A., Gullberg, H., Fernandez, L., Stahlberg, N., Lee, N.H., Vennstrom, B., and Norstedt, G. (2002). Patterns of liver gene expression governed by TRbeta. Molecular endocrinology (Baltimore, Md *16*, 1257-1268.

Forman, B.M., Casanova, J., Raaka, B.M., Ghysdael, J., and Samuels, H.H. (1992). Half-site spacing and orientation determines whether thyroid hormone and retinoic acid receptors and related factors bind to DNA response elements as monomers, homodimers, or heterodimers. Molecular endocrinology *6*, 429-442.

Friedman, R.C., Farh, K.K., Burge, C.B., and Bartel, D.P. (2009). Most mammalian mRNAs are conserved targets of microRNAs. Genome research *19*, 92-105.

Gagne, R., Green, J.R., Dong, H., Wade, M.G., and Yauk, C.L. (2013). Identification of thyroid hormone receptor binding sites in developing mouse cerebellum. BMC genomics *14*, 341.

Gauger, K.J., Kato, Y., Haraguchi, K., Lehmler, H.J., Robertson, L.W., Bansal, R., and Zoeller, R.T. (2004). Polychlorinated biphenyls (PCBs) exert thyroid hormone-like effects in the fetal rat brain but do not bind to thyroid hormone receptors. Environmental health perspectives *112*, 516-523.

Gauthier, K., Chassande, O., Plateroti, M., Roux, J.P., Legrand, C., Pain, B., Rousset, B., Weiss, R., Trouillas, J., and Samarut, J. (1999). Different functions for the thyroid hormone receptors TRalpha and TRbeta in the control of thyroid hormone production and post-natal development. The EMBO journal *18*, 623-631.

Giera, S., Bansal, R., Ortiz-Toro, T.M., Taub, D.G., and Zoeller, R.T. (2011). Individual polychlorinated biphenyl (PCB) congeners produce tissue- and gene-specific effects on thyroid hormone signaling during development. Endocrinology *152*, 2909-2919.

Gilbert, M.E., Hedge, J.M., Valentin-Blasini, L., Blount, B.C., Kannan, K., Tietge, J., Zoeller, R.T., Crofton, K.M., Jarrett, J.M., and Fisher, J.W. (2013). An animal model of marginal iodine deficiency during development: the thyroid axis and neurodevelopmental outcome. Toxicol Sci *132*, 177-195.

Giri, N., Batista, D.L., Alter, B.P., and Stratakis, C.A. (2007). Endocrine abnormalities in patients with Fanconi anemia. The Journal of clinical endocrinology and metabolism *92*, 2624-2631.

Glass, C.K. (1994). Differential recognition of target genes by nuclear receptor monomers, dimers, and heterodimers. Endocrine reviews *15*, 391-407.

Glass, C.K., Holloway, J.M., Devary, O.V., and Rosenfeld, M.G. (1988). The thyroid hormone receptor binds with opposite transcriptional effects to a common sequence motif in thyroid hormone and estrogen response elements. Cell *54*, 313-323.

Goodman, J.H., and Gilbert, M.E. (2007). Modest thyroid hormone insufficiency during development induces a cellular malformation in the corpus callosum: a model of cortical dysplasia. Endocrinology *148*, 2593-2597.

Goodnight, J.H., and Harvey, W.R. (1978). SAS Technical Report R-103, Least-Squares Means in the Fixed-Effects General Linear Models (SAS Publishing).

Goodridge, A.G. (1978). Regulation of malic enzyme synthesis by thyroid hormone and glucagon: inhibitor and kinetic experiments. Molecular and cellular endocrinology *11*, 19-29.

Gothe, S., Wang, Z., Ng, L., Kindblom, J.M., Barros, A.C., Ohlsson, C., Vennstrom, B., and Forrest, D. (1999). Mice devoid of all known thyroid hormone receptors are viable but exhibit disorders of the pituitary-thyroid axis, growth, and bone maturation. Genes & development *13*, 1329-1341.

Grillasca, J.P., Gastaldi, M., Khiri, H., Dace, A., Peyrol, N., Reynier, P., Torresani, J., and Planells, R. (1997). Cloning and initial characterization of human and mouse Spot 14 genes. FEBS letters *401*, 38-42.

Grimson, A., Farh, K.K., Johnston, W.K., Garrett-Engele, P., Lim, L.P., and Bartel, D.P. (2007). MicroRNA targeting specificity in mammals: determinants beyond seed pairing. Molecular cell *27*, 91-105.

Grover, G.J., Dunn, C., Nguyen, N.H., Boulet, J., Dong, G., Domogauer, J., Barbounis, P., and Scanlan, T.S. (2007). Pharmacological profile of the thyroid hormone receptor antagonist NH3 in rats. The Journal of pharmacology and experimental therapeutics *322*, 385-390.

Guled, M., Lahti, L., Lindholm, P.M., Salmenkivi, K., Bagwan, I., Nicholson, A.G., and Knuutila, S. (2009). CDKN2A, NF2, and JUN are dysregulated among other genes by miRNAs in malignant mesothelioma -A miRNA microarray analysis. Genes, chromosomes & cancer *48*, 615-623.

Guo, H., Ingolia, N.T., Weissman, J.S., and Bartel, D.P. (2010). Mammalian microRNAs predominantly act to decrease target mRNA levels. Nature *466*, 835-840.

Haddow, J.E., Palomaki, G.E., Allan, W.C., Williams, J.R., Knight, G.J., Gagnon, J., O'Heir, C.E., Mitchell, M.L., Hermos, R.J., Waisbren, S.E.*, et al.* (1999). Maternal thyroid deficiency during pregnancy and subsequent neuropsychological development of the child. The New England journal of medicine *341*, 549-555.

Haitina, T., Lindblom, J., Renstrom, T., and Fredriksson, R. (2006). Fourteen novel human members of mitochondrial solute carrier family 25 (SLC25) widely expressed in the central nervous system. Genomics *88*, 779-790.

Hallgren, S., and Darnerud, P.O. (2002). Polybrominated diphenyl ethers (PBDEs), polychlorinated biphenyls (PCBs) and chlorinated paraffins (CPs) in rats-testing interactions and mechanisms for thyroid hormone effects. Toxicology *177*, 227-243.

Harbers, M., Wahlstrom, G.M., and Vennstrom, B. (1996). Transactivation by the thyroid hormone receptor is dependent on the spacer sequence in hormone response elements containing directly repeated half-sites. Nucleic acids research *24*, 2252-2259.

Harrison, A.P., Tivey, D.R., Clausen, T., Duchamp, C., and Dauncey, M.J. (1996). Role of thyroid hormones in early postnatal development of skeletal muscle and its implications for undernutrition. The British journal of nutrition *76*, 841-855.

Hashimoto, K., Ishida, E., Matsumoto, S., Okada, S., Yamada, M., Satoh, T., Monden, T., and Mori, M. (2009). Carbohydrate response element binding protein gene expression is positively regulated by thyroid hormone. Endocrinology *150*, 3417-3424.

Hashimoto, K., Yamada, M., Matsumoto, S., Monden, T., Satoh, T., and Mori, M. (2006). Mouse sterol response element binding protein-1c gene expression is negatively regulated by thyroid hormone. Endocrinology *147*, 4292-4302.

Hassi, J., Sikkila, K., Ruokonen, A., and Leppaluoto, J. (2001). The pituitary-thyroid axis in healthy men living under subarctic climatological conditions. The Journal of endocrinology *169*, 195-203.

Heyland, A., and Moroz, L.L. (2005). Cross-kingdom hormonal signaling: an insight from thyroid hormone functions in marine larvae. The Journal of experimental biology *208*, 4355-4361.

Higgins, J. (2003). An introduction to modern nonparametric statistics. Brooks/Cole, Pacific Grove, CA.

Hodin, R.A., Lazar, M.A., and Chin, W.W. (1990). Differential and tissue-specific regulation of the multiple rat c-erbA messenger RNA species by thyroid hormone. The Journal of clinical investigation *85*, 101-105.

Hodin, R.A., Lazar, M.A., Wintman, B.I., Darling, D.S., Koenig, R.J., Larsen, P.R., Moore, D.D., and Chin, W.W. (1989). Identification of a thyroid hormone receptor that is pituitary-specific. Science *244*, 76-79.

Horlein, A.J., Naar, A.M., Heinzel, T., Torchia, J., Gloss, B., Kurokawa, R., Ryan, A., Kamei, Y., Soderstrom, M., Glass, C.K.*, et al.* (1995). Ligand-independent repression by the thyroid hormone receptor mediated by a nuclear receptor co-repressor. Nature *377*, 397-404.

Horn, S., and Heuer, H. (2010). Thyroid hormone action during brain development: more questions than answers. Molecular and cellular endocrinology *315*, 19-26.

Hu, X., Schwarz, J.K., Lewis, J.S., Jr., Huettner, P.C., Rader, J.S., Deasy, J.O., Grigsby, P.W., and Wang, X. (2010). A microRNA expression signature for cervical cancer prognosis. Cancer research *70*, 1441-1448.

Huang da, W., Sherman, B.T., and Lempicki, R.A. (2009a). Bioinformatics enrichment tools: paths toward the comprehensive functional analysis of large gene lists. Nucleic acids research *37*, 1-13.

Huang da, W., Sherman, B.T., and Lempicki, R.A. (2009b). Systematic and integrative analysis of large gene lists using DAVID bioinformatics resources. Nature protocols *4*, 44-57.

Iguchi, T., Watanabe, H., and Katsu, Y. (2006). Application of ecotoxicogenomics for studying endocrine disruption in vertebrates and invertebrates. Environmental health perspectives *114 Suppl 1*, 101-105.

Iordanidou, A., Hadzopoulou-Cladaras, M., and Lazou, A. (2010). Non-genomic effects of thyroid hormone in adult cardiac myocytes: relevance to gene expression and cell growth. Molecular and cellular biochemistry *340*, 291-300.

Ishihara, A., Nishiyama, N., Sugiyama, S., and Yamauchi, K. (2003). The effect of endocrine disrupting chemicals on thyroid hormone binding to Japanese quail transthyretin and thyroid hormone receptor. General and comparative endocrinology *134*, 36-43.

Jeyakumar, M., Tanen, M.R., and Bagchi, M.K. (1997). Analysis of the functional role of steroid receptor coactivator-1 in ligand-induced transactivation by thyroid hormone receptor. Molecular endocrinology (Baltimore, Md *11*, 755-767.

Jiang, L., Liu, X., Kolokythas, A., Yu, J., Wang, A., Heidbreder, C.E., Shi, F., and Zhou, X. (2010). Downregulation of the Rho GTPase signaling pathway is involved in the microRNA-138-mediated inhibition of cell migration and invasion in tongue squamous cell carcinoma. International journal of cancer Journal international du cancer *127*, 505-512.

Jugan, M.L., Levi, Y., and Blondeau, J.P. (2010). Endocrine disruptors and thyroid hormone physiology. Biochemical pharmacology *79*, 939-947.

Kaptein, E.M. (1996). Thyroid hormone metabolism and thyroid diseases in chronic renal failure. Endocrine reviews *17*, 45-63.

Kempers, M.J., van der Sluijs Veer, L., Nijhuis-van der Sanden, M.W., Kooistra, L., Wiedijk, B.M., Faber, I., Last, B.F., de Vijlder, J.J., Grootenhuis, M.A., and Vulsma, T. (2006). Intellectual and motor development of young adults with congenital hypothyroidism

diagnosed by neonatal screening. The Journal of clinical endocrinology and metabolism *91*, 418-424.

Kerr, M.K. (2003). Design considerations for efficient and effective microarray studies. Biometrics *59*, 822-828.

Kerr MK, C.G. (2001). Bootstrapping cluster analysis: assessing the reliability of conclusions from microarray experiments. Proc Natl Acad Sci USA *98*, 8961-8965.

Kerr, M.K., and Churchill, G.A. (2001). Statistical design and the analysis of gene expression microarray data. Genetical research *77*, 123-128.

Kohrle, J. (2000). The selenoenzyme family of deiodinase isozymes controls local thyroid hormone availability. Reviews in endocrine & metabolic disorders *1*, 49-58.

Lazar, M.A. (1993). Thyroid hormone receptors: multiple forms, multiple possibilities. Endocrine reviews *14*, 184-193.

Lazar, M.A. (2003). Thyroid hormone action: a binding contract. The Journal of clinical investigation *112*, 497-499.

Lazar, M.A., Berrodin, T.J., and Harding, H.P. (1991). Differential DNA binding by monomeric, homodimeric, and potentially heteromeric forms of the thyroid hormone receptor. Molecular and cellular biology *11*, 5005-5015.

Lazarus, J.H., and Obuobie, K. (2000). Thyroid disorders--an update. Postgraduate medical journal *76*, 529-536.

Lee, C.H., and Wei, L.N. (1999). Characterization of an inverted repeat with a zero spacer (IR0)-type retinoic acid response element from the mouse nuclear orphan receptor TR2-11 gene. Biochemistry *38*, 8820-8825.

Leid, M., Kastner, P., Lyons, R., Nakshatri, H., Saunders, M., Zacharewski, T., Chen, J.Y., Staub, A., Garnier, J.M., Mader, S.*, et al.* (1992). Purification, cloning, and RXR identity of the HeLa cell factor with which RAR or TR heterodimerizes to bind target sequences efficiently. Cell *68*, 377-395.

Leung, J.C., Klein, C., Friedman, J., Vieregge, P., Jacobs, H., Doheny, D., Kamm, C., DeLeon, D., Pramstaller, P.P., Penney, J.B.*, et al.* (2001). Novel mutation in the TOR1A (DYT1) gene in atypical early onset dystonia and polymorphisms in dystonia and early onset parkinsonism. Neurogenetics *3*, 133-143.

Lewis, B.P., Burge, C.B., and Bartel, D.P. (2005). Conserved seed pairing, often flanked by adenosines, indicates that thousands of human genes are microRNA targets. Cell *120*, 15-20.

Li, D., Li, T., Wang, F., Tian, H., and Samuels, H.H. (2002). Functional evidence for retinoid X receptor (RXR) as a nonsilent partner in the thyroid hormone receptor/RXR heterodimer. Molecular and cellular biology *22*, 5782-5792.

Li, D., Yamada, T., Wang, F., Vulin, A.I., and Samuels, H.H. (2004). Novel roles of retinoid X receptor (RXR) and RXR ligand in dynamically modulating the activity of the thyroid hormone receptor/RXR heterodimer. The Journal of biological chemistry *279*, 7427-7437.

Liaw, C.W., and Towle, H.C. (1984). Characterization of a thyroid hormone-responsive gene from rat. The Journal of biological chemistry *259*, 7253-7260.

Ling, C., Ishiai, M., Ali, A.M., Medhurst, A.L., Neveling, K., Kalb, R., Yan, Z., Xue, Y., Oostra, A.B., Auerbach, A.D*., et al.* (2007). FAAP100 is essential for activation of the Fanconi anemia-associated DNA damage response pathway. The EMBO journal *26*, 2104-2114.

Logan, D.W., Marton, T.F., and Stowers, L. (2008). Species specificity in major urinary proteins by parallel evolution. PloS one *3*, e3280.

Lynn, F.C. (2009). Meta-regulation: microRNA regulation of glucose and lipid metabolism. Trends in endocrinology and metabolism: TEM *20*, 452-459.

Mangelsdorf, D.J., Borgmeyer, U., Heyman, R.A., Zhou, J.Y., Ong, E.S., Oro, A.E., Kakizuka, A., and Evans, R.M. (1992). Characterization of three RXR genes that mediate the action of 9-cis retinoic acid. Genes & development *6*, 329-344.

Mangelsdorf, D.J., and Evans, R.M. (1995). The RXR heterodimers and orphan receptors. Cell *83*, 841-850.

Mangelsdorf, D.J., Ong, E.S., Dyck, J.A., and Evans, R.M. (1990). Nuclear receptor that identifies a novel retinoic acid response pathway. Nature *345*, 224-229.

Meeker, J.D. (2012). Exposure to environmental endocrine disruptors and child development. Archives of pediatrics & adolescent medicine *166*, 952-958.

Mees, S.T., Schleicher, C., Mardin, W.A., Senninger, N., Colombo-Benkmann, M., and Haier, J. (2009). Analyzing miRNAs in Ductal Adenocarcinomas of the Pancreas. The Journal of surgical research.

Mendel, C.M., Cavalieri, R.R., and Weisiger, R.A. (1988). Uptake of thyroxine by the perfused rat liver: implications for the free hormone hypothesis. The American journal of physiology *255*, E110-119.

Miller, M.D., Crofton, K.M., Rice, D.C., and Zoeller, R.T. (2009). Thyroid-disrupting chemicals: interpreting upstream biomarkers of adverse outcomes. Environmental health perspectives *117*, 1033-1041.

Morse, D.C., Wehler, E.K., Wesseling, W., Koeman, J.H., and Brouwer, A. (1996). Alterations in rat brain thyroid hormone status following pre- and postnatal exposure to polychlorinated biphenyls (Aroclor 1254). Toxicology and applied pharmacology *136*, 269-279.

Naar, A.M., Boutin, J.M., Lipkin, S.M., Yu, V.C., Holloway, J.M., Glass, C.K., and Rosenfeld, M.G. (1991). The orientation and spacing of core DNA-binding motifs dictate selective transcriptional responses to three nuclear receptors. Cell *65*, 1267-1279.

National Academies of Sciences (2007). Toxicity Testing in the 21st Century: A Vision and a Strategy (Washington, DC).

Ness, G.C., and Lopez, D. (1995). Transcriptional regulation of rat hepatic low-density lipoprotein receptor and cholesterol 7 alpha hydroxylase by thyroid hormone. Archives of biochemistry and biophysics *323*, 404-408.

Ness, G.C., Lopez, D., Chambers, C.M., Newsome, W.P., Cornelius, P., Long, C.A., and Harwood, H.J., Jr. (1998). Effects of L-triiodothyronine and the thyromimetic L-94901 on serum lipoprotein levels and hepatic low-density lipoprotein receptor, 3-hydroxy-3-methylglutaryl coenzyme A reductase, and apo A-I gene expression. Biochemical pharmacology *56*, 121-129.

Nitto, T., Inoue, T., and Node, K. (2008). Alternative spliced variants in the pantetheinase family of genes expressed in human neutrophils. Gene *426*, 57-64.

OECD (2012). Guidance Document on Standardised Test Guidelines for Evaluating Chemicals for Endocrine Disruption. No. 150.

Oerbeck, B., Reinvang, I., Sundet, K., and Heyerdahl, S. (2007). Young adults with severe congenital hypothyroidism: cognitive event related potentials (ERPs) and the significance of an early start of thyroxine treatment. Scandinavian journal of psychology *48*, 61-67.

Oerbeck, B., Sundet, K., Kase, B.F., and Heyerdahl, S. (2003). Congenital hypothyroidism: influence of disease severity and L-thyroxine treatment on intellectual, motor, and school-associated outcomes in young adults. Pediatrics *112*, 923-930.

Paquette, M.A., Dong, H., Gagne, R., Williams, A., Malowany, M., Wade, M.G., and Yauk, C.L. (2011). Thyroid hormone-regulated gene expression in juvenile mouse liver: identification of thyroid response elements using microarray profiling and in silico analyses. BMC genomics *12*, 634.

Perez-Juste, G., Garcia-Silva, S., and Aranda, A. (2000). An element in the region responsible for premature termination of transcription mediates repression of c-myc gene expression by thyroid hormone in neuroblastoma cells. The Journal of biological chemistry *275*, 1307-1314.

Perlmann, T., Rangarajan, P.N., Umesono, K., and Evans, R.M. (1993). Determinants for selective RAR and TR recognition of direct repeat HREs. Genes & development *7*, 1411-1422.

Phan, T.Q., Jow, M.M., and Privalsky, M.L. (2010). DNA recognition by thyroid hormone and retinoic acid receptors: 3,4,5 rule modified. Molecular and cellular endocrinology *319*, 88-98.

Pop, V.J., and Vulsma, T. (2005). Maternal hypothyroxinaemia during (early) gestation. Lancet *365*, 1604-1606.

Rajendran, R.R., Nye, A.C., Frasor, J., Balsara, R.D., Martini, P.G., and Katzenellenbogen, B.S. (2003). Regulation of nuclear receptor transcriptional activity by a novel DEAD box RNA helicase (DP97). The Journal of biological chemistry *278*, 4628-4638.

Rastinejad, F., Perlmann, T., Evans, R.M., and Sigler, P.B. (1995). Structural determinants of nuclear receptor assembly on DNA direct repeats. Nature *375*, 203-211.

Richardson, V.M., Staskal, D.F., Ross, D.G., Diliberto, J.J., DeVito, M.J., and Birnbaum, L.S. (2008). Possible mechanisms of thyroid hormone disruption in mice by BDE 47, a major polybrominated diphenyl ether congener. Toxicology and applied pharmacology *226*, 244-250.

Roman, G.C. (2007). Autism: transient in utero hypothyroxinemia related to maternal flavonoid ingestion during pregnancy and to other environmental antithyroid agents. Journal of the neurological sciences *262*, 15-26.

Rosenbaum, M., Hirsch, J., Murphy, E., and Leibel, R.L. (2000). Effects of changes in body weight on carbohydrate metabolism, catecholamine excretion, and thyroid function. The American journal of clinical nutrition *71*, 1421-1432.

Sadamatsu, M., Kanai, H., Xu, X., Liu, Y., and Kato, N. (2006). Review of animal models for autism: implication of thyroid hormone. Congenital anomalies *46*, 1-9.

Sanders, J.P., Van der Geyten, S., Kaptein, E., Darras, V.M., Kuhn, E.R., Leonard, J.L., and Visser, T.J. (1997). Characterization of a propylthiouracil-insensitive type I iodothyronine deiodinase. Endocrinology *138*, 5153-5160.

Santana-Farre, R., Mirecki-Garrido, M., Bocos, C., Henriquez-Hernandez, L.A., Kahlon, N., Herrera, E., Norstedt, G., Parini, P., Flores-Morales, A., and Fernandez-Perez, L. (2012). Influence of neonatal hypothyroidism on hepatic gene expression and lipid metabolism in adulthood. PloS one *7*, e37386.

Schapira, M., Raaka, B.M., Das, S., Fan, L., Totrov, M., Zhou, Z., Wilson, S.R., Abagyan, R., and Samuels, H.H. (2003). Discovery of diverse thyroid hormone receptor antagonists by high-throughput docking. Proceedings of the National Academy of Sciences of the United States of America *100*, 7354-7359.

Searle, S.R., Speed, F.M., and Milliken, G.A. (1980). The population marginal means in the linear model: An alternative to least squares means. The American Statistician *34*, 216-221.

Seipel, K., Medley, Q.G., Kedersha, N.L., Zhang, X.A., O'Brien, S.P., Serra-Pages, C., Hemler, M.E., and Streuli, M. (1999). Trio amino-terminal guanine nucleotide exchange factor domain expression promotes actin cytoskeleton reorganization, cell migration and anchorage-independent cell growth. Journal of cell science *112 (Pt 12)*, 1825-1834.

Sharlin, D.S., Gilbert, M.E., Taylor, M.A., Ferguson, D.C., and Zoeller, R.T. (2010). The nature of the compensatory response to low thyroid hormone in the developing brain. Journal of neuroendocrinology *22*, 153-165.

Shieh, A.D., and Hung, Y.S. (2009). Detecting outlier samples in microarray data. Stat Appl Genet Mol Biol *8*, Article 13.

Shin, D.J., Plateroti, M., Samarut, J., and Osborne, T.F. (2006). Two uniquely arranged thyroid hormone response elements in the far upstream 5' flanking region confer direct thyroid hormone regulation to the murine cholesterol 7alpha hydroxylase gene. Nucleic acids research *34*, 3853-3861.

Shulha, H., Fu, Y., and Weng, Z. (2007). Oligo-tiling array signal processing by splitter., pp. http://zlab.bu.edu/splitter.

Shupnik, M.A., Ridgway, E.C., and Chin, W.W. (1989). Molecular biology of thyrotropin. Endocrine reviews *10*, 459-475.

Solanes, G., Pedraza, N., Calvo, V., Vidal-Puig, A., Lowell, B.B., and Villarroya, F. (2005). Thyroid hormones directly activate the expression of the human and mouse uncoupling protein-3 genes through a thyroid response element in the proximal promoter region. The Biochemical journal *386*, 505-513.

Spilianakis, C.G., Lalioti, M.D., Town, T., Lee, G.R., and Flavell, R.A. (2005). Interchromosomal associations between alternatively expressed loci. Nature *435*, 637-645.

Stahlberg, N., Merino, R., Hernandez, L.H., Fernandez-Perez, L., Sandelin, A., Engstrom, P., Tollet-Egnell, P., Lenhard, B., and Flores-Morales, A. (2005). Exploring hepatic hormone actions using a compilation of gene expression profiles. BMC physiology *5*, 8.

Sternberger, N.H., Itoyama, Y., Kies, M.W., and Webster, H.D. (1978). Myelin basic protein demonstrated immunocytochemically in oligodendroglia prior to myelin sheath formation. Proceedings of the National Academy of Sciences of the United States of America *75*, 2521-2524.

Sui, L., and Li, B.M. (2010). Effects of perinatal hypothyroidism on regulation of reelin and brain-derived neurotrophic factor gene expression in rat hippocampus: Role of DNA methylation and histone acetylation. Steroids *75*, 988-997.

Taylor, A.H., Stephan, Z.F., Steele, R.E., and Wong, N.C. (1997). Beneficial effects of a novel thyromimetic on lipoprotein metabolism. Molecular pharmacology *52*, 542-547.

Team, R. (2008). R: A language and environment for statistical computing. Vienna, Austria: R Foundation for Statistical Computing.

Tu, H.M., Legradi, G., Bartha, T., Salvatore, D., Lechan, R.M., and Larsen, P.R. (1999). Regional expression of the type 3 iodothyronine deiodinase messenger ribonucleic acid in the rat central nervous system and its regulation by thyroid hormone. Endocrinology *140*, 784-790.

Ueki, T., Tsuruo, Y., Yamamoto, Y., Yoshimura, K., Takanaga, H., Seiwa, C., Motojima, K., Asou, H., and Yamamoto, M. (2012). A new monoclonal antibody, 4F2, specific for the oligodendroglial cell lineage, recognizes ATP-dependent RNA helicase Ddx54: possible association with myelin basic protein. Journal of neuroscience research *90*, 48-59.

Umesono, K., Murakami, K.K., Thompson, C.C., and Evans, R.M. (1991). Direct repeats as selective response elements for the thyroid hormone, retinoic acid, and vitamin D3 receptors. Cell *65*, 1255-1266.

Urbansky, E.T. (2002). Perchlorate as an environmental contaminant. Environmental science and pollution research international *9*, 187-192.

Valencia-Sanchez, M.A., Liu, J., Hannon, G.J., and Parker, R. (2006). Control of translation and mRNA degradation by miRNAs and siRNAs. Genes & development *20*, 515-524.

van der Plas, S.A., Lutkeschipholt, I., Spenkelink, B., and Brouwer, A. (2001). Effects of subchronic exposure to complex mixtures of dioxin-like and non-dioxin-like polyhalogenated aromatic compounds on thyroid hormone and vitamin A levels in female Sprague-Dawley rats. Toxicol Sci *59*, 92-100.

van Rooij, E., Sutherland, L.B., Qi, X., Richardson, J.A., Hill, J., and Olson, E.N. (2007). Control of stress-dependent cardiac growth and gene expression by a microRNA. Science *316*, 575-579.

Velasco, L.F., Togashi, M., Walfish, P.G., Pessanha, R.P., Moura, F.N., Barra, G.B., Nguyen, P., Rebong, R., Yuan, C., Simeoni, L.A.*, et al.* (2007). Thyroid hormone response element organization dictates the composition of active receptor. The Journal of biological chemistry *282*, 12458-12466.

Ventura-Holman, T., Mamoon, A., Maher, J.F., and Subauste, J.S. (2007). Thyroid hormone responsive genes in the murine hepatocyte cell line AML 12. Gene *396*, 332-337.

Verreault, J., Skaare, J.U., Jenssen, B.M., and Gabrielsen, G.W. (2004). Effects of organochlorine contaminants on thyroid hormone levels in Arctic breeding glaucous gulls, Larus hyperboreus. Environmental health perspectives *112*, 532-537.

Visser, W.E., Heemstra, K.A., Swagemakers, S.M., Ozgur, Z., Corssmit, E.P., Burggraaf, J., van Ijcken, W.F., van der Spek, P.J., Smit, J.W., and Visser, T.J. (2009). Physiological thyroid hormone levels regulate numerous skeletal muscle transcripts. The Journal of clinical endocrinology and metabolism *94*, 3487-3496.

Wagner, R.L., Apriletti, J.W., McGrath, M.E., West, B.L., Baxter, J.D., and Fletterick, R.J. (1995). A structural role for hormone in the thyroid hormone receptor. Nature *378*, 690-697.

Weitzel, J.M. (2008). To bind or not to bind - how to down-regulate target genes by liganded thyroid hormone receptor? Thyroid Res *1*, 4.

Weitzel, J.M., Hamann, S., Jauk, M., Lacey, M., Filbry, A., Radtke, C., Iwen, K.A., Kutz, S., Harneit, A., Lizardi, P.M.*, et al.* (2003a). Hepatic gene expression patterns in thyroid hormone-treated hypothyroid rats. Journal of molecular endocrinology *31*, 291-303.

Weitzel, J.M., Iwen, K.A., and Seitz, H.J. (2003b). Regulation of mitochondrial biogenesis by thyroid hormone. Experimental physiology *88*, 121-128.

Williams, G.R., Robson, H., and Shalet, S.M. (1998). Thyroid hormone actions on cartilage and bone: interactions with other hormones at the epiphyseal plate and effects on linear growth. The Journal of endocrinology *157*, 391-403.

Wolff, J. (1998). Perchlorate and the thyroid gland. Pharmacological reviews *50*, 89-105.

World Health Organization, U., ICCIDD (2007). Assessment of iodine deficiency disorders and monitoring their elimination.

Wu H, k., MK, Cui X, Churchill GA (2003). MAANOVA: a software package for the analysis of spotted cDNA microarray experiments.

Wu, H., Kerr, M.K., Cui, X., and Churchill, G.A. (2003). The Analysis of Gene Expression Data; MAANOVA: A Software Package for the Analysis of Spotted cDNA Microarray Experiments (Springer London).

Wu, J., Wang, C., Li, S., Li, S., Wang, W., Li, J., Chi, Y., Yang, H., Kong, X., Zhou, Y.*, et al.* (2013). Thyroid hormone-responsive SPOT 14 homolog promotes hepatic lipogenesis, and its expression is regulated by Liver X receptor alpha through a sterol regulatory element-binding protein 1c-dependent mechanism in mice. Hepatology *58*, 617-628.

Xu, C., Lu, Y., Pan, Z., Chu, W., Luo, X., Lin, H., Xiao, J., Shan, H., Wang, Z., and Yang, B. (2007). The muscle-specific microRNAs miR-1 and miR-133 produce opposing effects on apoptosis by targeting HSP60, HSP70 and caspase-9 in cardiomyocytes. Journal of cell science *120*, 3045-3052.

Yang, Y.H., Dudoit, S., Luu, P., Lin, D.M., Peng, V., Ngai, J., and Speed, T.P. (2002). Normalization for cDNA microarray data: a robust composite method addressing single and multiple slide systematic variation. Nucleic acids research *30*, e15.

Yen, P.M. (2001). Physiological and molecular basis of thyroid hormone action. Physiological reviews *81*, 1097-1142.

Yen, P.M., Feng, X., Flamant, F., Chen, Y., Walker, R.L., Weiss, R.E., Chassande, O., Samarut, J., Refetoff, S., and Meltzer, P.S. (2003). Effects of ligand and thyroid hormone receptor isoforms on hepatic gene expression profiles of thyroid hormone receptor knockout mice. EMBO Rep *4*, 581-587.

Yen, P.M., Sunday, M.E., Darling, D.S., and Chin, W.W. (1992). Isoform-specific thyroid hormone receptor antibodies detect multiple thyroid hormone receptors in rat and human pituitaries. Endocrinology *130*, 1539-1546.

You, S.H., Liao, X., Weiss, R.E., and Lazar, M.A. (2010). The interaction between nuclear receptor corepressor and histone deacetylase 3 regulates both positive and negative thyroid hormone action in vivo. Molecular endocrinology (Baltimore, Md *24*, 1359-1367.

Yu, L., Chen, M., Liu, Y., Gui, W., and Zhu, G. (2013). Thyroid endocrine disruption in zebrafish larvae following exposure to hexaconazole and tebuconazole. Aquatic toxicology *138-139*, 35-42.

Zhang, J., and Lazar, M.A. (2000). The mechanism of action of thyroid hormones. Annual review of physiology *62*, 439-466.

Zhou, Y., Jiang, L., and Rui, L. (2009). Identification of MUP1 as a regulator for glucose and lipid metabolism in mice. The Journal of biological chemistry *284*, 11152-11159.

Zilz, N.D., Murray, M.B., and Towle, H.C. (1990). Identification of multiple thyroid hormone response elements located far upstream from the rat S14 promoter. The Journal of biological chemistry *265*, 8136-8143.

Zimmermann, M.B. (2009). Iodine deficiency. Endocrine reviews *30*, 376-408.

Zoeller, T.R. (2010). Environmental chemicals targeting thyroid. Hormones *9*, 28-40.

SUPPLEMENTARY MATERIAL

Supplementary Table 2.1. Altered genes in male pups, with a FDR-adjusted $p < 0.05$ in at least one of the treatment conditions.

Accession Number	Gene Name	Foldrank	Hyperthyroid		Hypothyroid		Hypothyroid Replacement	
			P-Value	Fold-Change	P-Value	Fold-Change	P-Value	Fold-Change
NM_009042	Reg1	13.83	**0.0336**	**-13.83**	**0.0159**	**-13.53**	0.4415	-4.91
NM_029706	Cpb1	9.09	**0.0000**	**-8.90**	0.0799	-8.22	0.1315	-9.09
NM_033612	Ela1	6.05	**0.0195**	**-5.63**	0.0607	-5.99	0.0811	-6.05
NM_001033875	Ctrc	4.38	0.9999	-1.96	**0.0000**	**-4.38**	0.5434	-2.05
NM_025469	Clps	4.18	**0.0461**	**-4.18**	0.0799	-4.16	0.1552	-4.05
AK158295	E2f8	3.50	0.9999	1.12	**0.0000**	**-3.50**	0.3675	-1.74
AK147478	Auts2	3.07	**0.0000**	**3.07**	0.9999	1.07	**0.0000**	**2.47**
NM_009381	Thrsp	2.82	0.9999	1.64	**0.0361**	**-2.82**	0.9841	-1.10
NM_010358	Gstm1	2.65	0.9999	-1.12	**0.0000**	**2.63**	**0.0000**	**2.65**
AK044145	AK044145	2.59	**0.0000**	**2.59**	0.9999	1.13	**0.0000**	**2.09**
NM_007860	Dio1	2.59	0.9999	1.29	**0.0000**	**-2.59**	0.9812	1.06
NM_001025384	LOC574405	2.57	**0.0000**	**2.17**	0.0679	-1.60	**0.0000**	**2.57**
NM_138313	Bmf	2.42	0.0964	1.82	**0.0000**	**-2.42**	0.2378	1.67
NM_029509	LOC634650	2.31	**0.0000**	**2.31**	0.9999	1.02	0.4519	1.39
XM_981410	9030619P08Rik	2.30	0.9999	1.23	**0.0000**	**-2.30**	0.9170	-1.16
NM_013808	Csrp3	2.29	0.9999	1.03	**0.0000**	**-2.29**	0.4290	-1.38
NM_010359	Gstm3	2.25	0.9999	-1.10	**0.0000**	**2.25**	**0.0000**	**2.21**
NM_144930	AU018778	2.23	0.9999	-1.05	**0.0000**	**2.23**	0.1591	1.80
NM_016854	Ppp1r3c	2.17	0.0851	-1.93	**0.0284**	**2.17**	0.1991	-1.86
D86232	Ly6c	2.12	0.1112	1.43	**0.0000**	**-2.12**	0.9925	1.03
TC1631866	TC1493944	2.09	0.9999	1.17	**0.0000**	**2.09**	0.9261	1.16
NM_009676	Aox1	2.03	0.9999	-1.12	**0.0000**	**2.03**	**0.0258**	**1.64**
AK159732	Slc25a30	2.03	**0.0336**	**2.03**	0.9322	-1.40	0.4892	1.56
NM_008046	Fst	2.02	0.9999	1.38	**0.0455**	**2.02**	0.4388	1.55
NM_001039710	1500041J02Rik	2.02	0.6709	1.45	0.9999	-1.01	**0.0000**	**2.02**
NM_008737	Nrp1	2.00	0.9999	1.19	**0.0000**	**-2.00**	0.2040	-1.39
NM_008706	Nqo1	1.98	0.9999	-1.19	**0.0000**	**1.98**	**0.0445**	**1.45**
NM_025404	Arfl4	1.96	**0.0000**	**1.96**	0.9999	1.18	**0.0000**	**1.95**
AK017206	5033430I15Rik	1.95	**0.0000**	**1.95**	0.2856	-1.47	0.3978	1.41

NM_027153	Pir	1.94	0.9999	-1.12	**0.0000**	**1.94**	**0.0000**	**1.77**
XM_911199	1810008N23Rik	1.93	0.6472	-1.46	**0.0000**	**-1.93**	0.1315	-1.71
AK142275	Stim2	1.92	**0.0000**	**1.92**	0.1018	-1.36	**0.0000**	**1.53**
AK137889	Stat5b	1.89	**0.0000**	**1.89**	0.9999	1.03	0.2090	1.44
NM_001042671	Prei4	1.89	0.1384	1.67	**0.0361**	**-1.89**	0.1315	1.80
NM_009251	Serpina3g	1.85	0.9999	1.18	**0.0000**	**-1.85**	0.5552	-1.27
NM_024437	Nudt7	1.85	**0.0000**	**1.85**	**0.0000**	**-1.76**	0.4027	1.34
NM_009344	Phlda1	1.82	0.9999	1.11	**0.0159**	**-1.82**	0.8588	1.19
NM_033601	Bcl3	1.81	**0.0000**	**1.57**	**0.0000**	**-1.81**	0.2066	1.35
NM_134246	Acot3	1.81	**0.0000**	**-1.63**	**0.0159**	**1.81**	0.3566	-1.39
AK034561	Fzd8	1.81	**0.0000**	**1.81**	0.9999	1.02	**0.0000**	**1.58**
NM_182959	Slc17a8	1.80	0.0657	-1.52	**0.0159**	**-1.64**	**0.0000**	**-1.80**
A_51_P305138	A_51_P305138	1.78	0.9999	1.15	**0.0284**	**1.78**	0.1384	1.65
NM_028133	Egln3	1.78	0.9999	-1.09	**0.0000**	**1.78**	0.9053	1.11
NM_029331	1700019G17Rik	1.78	0.9999	1.16	**0.0361**	**-1.78**	0.8572	-1.21
NM_019972	Sort1	1.77	**0.0195**	**1.77**	0.1586	-1.53	0.5704	1.33
NM_008102	Gch1	1.77	**0.0000**	**1.77**	**0.0000**	**-1.44**	0.0542	1.38
NM_016919	Col5a3	1.75	0.9999	1.01	**0.0000**	**1.75**	0.1991	1.32
BC024137	BC024137	1.74	0.0964	1.56	**0.0284**	**-1.74**	0.8036	1.20
AK046650	BC013529	1.74	**0.0000**	**1.74**	0.9999	-1.05	0.7493	1.24
NM_011488	Stat5a	1.74	**0.0000**	**1.74**	0.1112	-1.44	0.1384	1.44
NM_133898	B230342M21Rik	1.73	0.9999	1.30	**0.0159**	**-1.73**	0.8001	1.22
NM_009469	Ulk1	1.70	0.9999	1.21	**0.0000**	**-1.70**	0.9972	1.01
AK009333	2310014D11Rik	1.67	**0.0000**	**1.67**	0.9280	-1.14	**0.0000**	**1.54**
NM_183249	1100001G20Rik	1.66	0.9999	-1.06	**0.0000**	**-1.63**	**0.0445**	**-1.66**
NM_134154	AW491445	1.66	**0.0000**	**1.65**	**0.0000**	**-1.66**	**0.0000**	**1.46**
AK051378	Map3k13	1.66	**0.0336**	**1.58**	0.9999	-1.10	**0.0000**	**1.66**
NM_018734	Gbp4	1.65	0.1175	1.48	**0.0159**	**-1.65**	0.7851	-1.20
NM_178701	Lrrc8d	1.61	**0.0000**	**1.61**	0.9999	-1.10	**0.0000**	**1.58**
NM_001013785	Akr1c19	1.61	0.9999	-1.05	**0.0000**	**1.61**	0.3068	1.36
NM_178111	Trp53inp2	1.61	0.6801	1.28	**0.0000**	**-1.61**	0.9715	1.06
NM_011243	Rarb	1.60	**0.0000**	**1.60**	0.9999	1.05	0.6877	1.16
AK079336	Gpd2	1.59	**0.0195**	**1.59**	**0.0361**	**-1.58**	0.7638	1.20
NM_029688	Srxn1	1.59	0.9999	-1.04	**0.0000**	**1.59**	**0.0258**	**1.42**
AK014609	4633401B06Rik	1.59	0.4437	1.31	0.3544	-1.33	**0.0000**	**1.59**
NM_153528	Gramd1c	1.58	**0.0000**	**1.58**	0.9999	-1.17	0.4255	1.32

NM_145076	Trim24	1.57	**0.0000**	**1.57**	**0.0284**	**-1.40**	**0.0000**	**1.54**
ENSMUST00000070000	ENSMUST00000070000	1.57	**0.0000**	**1.57**	0.2003	-1.33	0.5370	1.22
NM_026637	A030007L17Rik	1.57	0.9999	1.14	**0.0000**	**-1.57**	0.2507	-1.33
NM_018745	Azin1	1.57	0.9999	1.17	0.9999	-1.03	**0.0258**	**1.57**
U31966	Cbr1	1.56	0.9999	1.07	**0.0361**	**1.56**	0.0636	1.54
NM_172463	Sned1	1.56	**0.0000**	**1.46**	**0.0000**	**-1.56**	**0.0000**	**1.51**
NM_027402	Fndc5	1.55	0.0657	1.51	**0.0361**	**-1.55**	0.8278	1.17
NM_008991	Abcd3	1.55	0.1026	1.25	**0.0000**	**-1.55**	0.9823	1.03
NM_145603	Ces2	1.55	**0.0000**	**1.55**	0.9999	1.04	0.1614	1.38
BC060266	Ddah1	1.55	0.9999	1.08	**0.0000**	**1.55**	**0.0000**	**1.40**
XM_138240	LOC238395	1.54	0.8689	-1.26	0.5564	-1.29	**0.0445**	**-1.54**
NM_026169	1200004M23Rik	1.54	**0.0000**	**1.54**	**0.0000**	**-1.36**	0.8289	1.10
NM_011675	Uck1	1.53	**0.0195**	**1.53**	0.6121	-1.28	0.4809	1.28
XM_161350	1700024P16Rik	1.53	0.9999	-1.04	**0.0000**	**1.53**	0.9801	1.04
NM_010361	Gstt2	1.53	0.9999	1.13	**0.0000**	**1.53**	**0.0000**	**1.51**
NM_177078	Adrbk2	1.52	**0.0195**	**1.52**	0.9999	-1.03	0.1384	1.42
AK085506	4933404O12Rik	1.51	**0.0000**	**1.51**	0.0556	-1.38	0.8757	1.10
NM_054053	Gpr98	1.51	0.9999	-1.05	**0.0000**	**-1.51**	0.1991	-1.27
NM_030069	4432416J03Rik	1.50	0.9999	-1.06	0.7094	-1.23	**0.0000**	**-1.50**
NM_019814	Higd1a	1.50	0.9999	1.13	**0.0000**	**-1.50**	0.8689	-1.10
AK078975	91304300000	1.50	0.7291	-1.23	**0.0000**	**1.50**	0.9962	1.02
AK036010	Vldlr	1.49	0.9999	1.03	**0.0284**	**1.49**	0.1112	1.37
AK007434	1810011H11Rik	1.49	**0.0000**	**1.49**	0.6381	-1.25	0.9944	1.02
NM_010664	Krt18	1.49	0.9999	-1.10	**0.0361**	**1.49**	0.3688	1.31
NM_013541	Gstp1	1.48	0.9999	1.01	**0.0000**	**1.48**	0.0542	1.42
NM_001033335	Serpina3f	1.47	0.9999	1.14	**0.0159**	**-1.47**	0.6863	-1.17
NM_025341	Abhd6	1.47	0.3091	1.22	**0.0000**	**-1.47**	0.9095	-1.07
NM_145482	Setd4	1.47	0.1175	1.34	**0.0361**	**1.42**	**0.0000**	**1.47**
AK133542	Ppm2c	1.47	**0.0461**	**1.47**	0.6067	-1.26	0.7042	1.19
NM_026601	Hyi	1.47	0.9999	1.01	**0.0000**	**1.47**	**0.0445**	**1.32**
NM_025436	Sc4mol	1.46	0.2046	1.35	**0.0284**	**-1.46**	0.8675	-1.12
NM_013490	Chka	1.46	**0.0195**	**-1.46**	0.8540	1.22	0.1705	-1.38
NM_146161	Arhgap24	1.46	**0.0000**	**1.46**	0.7291	-1.24	0.9978	1.00
NM_028894	Lonrf3	1.45	0.9999	-1.15	0.9999	-1.08	**0.0000**	**-1.45**
NM_145933	St6gal1	1.45	0.9999	-1.04	**0.0000**	**1.45**	0.4617	1.19
NM_178890	Abtb2	1.45	**0.0461**	**1.45**	0.9999	-1.03	0.3188	1.32

NM_133942	Plekha1	1.45	**0.0336**	**1.45**	0.9999	-1.14	0.3520	1.31
NM_028089	Cyp2c55	1.44	0.9999	-1.17	**0.0284**	**1.44**	0.9071	1.10
AK078889	BQ952480	1.44	**0.0000**	**1.36**	**0.0000**	**-1.44**	**0.0258**	**1.32**
NM_010828	Cited2	1.43	**0.0000**	**1.43**	0.9999	-1.02	0.1866	1.31
NM_025558	Cyb5b	1.42	0.9999	-1.07	0.9999	-1.03	**0.0000**	**-1.42**
NM_029573	Idh3a	1.42	**0.0000**	**1.42**	0.3434	-1.26	0.7462	1.14
AK050258	AK050258	1.42	**0.0461**	**1.42**	0.2525	-1.35	0.1841	1.37
NM_025958	Cand2	1.41	0.9999	-1.04	**0.0000**	**1.41**	0.8840	1.10
NM_139297	Ugp2	1.41	0.9999	-1.03	**0.0361**	**1.41**	0.9179	1.09
XM_001005594	1700012B18Rik	1.41	**0.0336**	**1.38**	0.4615	-1.27	0.0811	1.41
NM_001077189	Fcgr2b	1.40	0.9999	-1.12	**0.0159**	**-1.39**	0.0542	-1.40
NM_028803	Gbe1	1.40	0.9999	1.07	**0.0000**	**-1.40**	0.2767	-1.20
NM_181399	Usp6nl	1.40	0.9999	-1.06	**0.0000**	**1.40**	0.8924	-1.09
NM_001042719	Ddhd1	1.39	**0.0336**	**1.39**	0.4594	-1.27	0.9720	1.05
BC029185	Ches1	1.38	**0.0000**	**1.38**	0.7936	-1.15	0.1288	1.26
NM_134141	Ciapin1	1.37	**0.0000**	**1.37**	0.9999	-1.05	**0.0445**	**1.33**
BC048176	E430034L04Rik	1.36	**0.0000**	**1.36**	0.9919	-1.12	0.3157	1.21
NM_009466	Ugdh	1.36	0.9999	-1.02	**0.0000**	**1.36**	0.6733	1.13
NM_026574	Inoc1	1.36	0.9999	-1.02	0.9999	-1.04	**0.0000**	**1.36**
NM_023670	Igf2bp3	1.36	0.9999	1.05	**0.0159**	**1.36**	0.7819	1.13
NM_027980	2310003H01Rik	1.36	**0.0000**	**1.36**	0.9999	-1.05	**0.0258**	**1.34**
NM_001026214	Entpd5	1.35	0.9999	-1.03	**0.0000**	**1.35**	0.5127	1.17
NM_175266	Epm2aip1	1.34	**0.0336**	**1.31**	0.9999	-1.07	**0.0445**	**1.34**
NM_029798	2810417J12Rik	1.34	0.9999	1.04	**0.0159**	**-1.34**	0.9855	-1.02
NM_010357	Gsta4	1.34	0.9999	1.08	**0.0000**	**1.34**	**0.0258**	**1.26**
NM_019437	Rfk	1.34	0.5078	1.20	**0.0000**	**-1.34**	0.9115	1.07
BC070459	Qrsl1	1.34	**0.0195**	**1.34**	0.9999	1.09	0.0811	1.31
NM_029431	Them4	1.34	0.9999	1.16	0.9280	-1.13	**0.0258**	**1.34**
NM_027418	Mapk6	1.34	**0.0000**	**1.34**	0.8708	-1.15	0.0811	1.32
NM_173038	Lrrc35	1.34	**0.0000**	**1.28**	0.9999	1.05	**0.0000**	**1.34**
NM_011804	Creg1	1.33	0.9999	-1.04	**0.0000**	**1.33**	0.1526	1.25
NM_153162	Txnrd3	1.33	0.5709	1.18	0.8649	-1.14	**0.0000**	**1.33**
NM_145587	Sbk1	1.32	**0.0000**	**1.32**	**0.0000**	**-1.28**	0.6687	1.09
NM_026310	Mrpl18	1.32	0.9999	1.05	**0.0159**	**1.32**	0.5189	1.16
NM_144884	Tor1a	1.32	0.0657	1.25	0.9999	-1.02	**0.0258**	**1.32**
NM_024221	Pdhb	1.31	0.9999	1.11	**0.0159**	**-1.31**	0.9973	1.00

NM_026310	Mrpl18	1.31	0.9999	-1.00	**0.0159**	**1.31**	0.7819	1.12
NM_177601	Tmem60	1.31	**0.0000**	**1.31**	0.1143	-1.23	0.5724	1.14
AK147592	4930573I19Rik	1.31	0.9999	1.07	0.9999	1.06	**0.0258**	**1.31**
NM_001039386	Nelf	1.30	**0.0336**	**1.30**	0.2991	-1.24	0.9791	1.04
AK031889	AK031889	1.30	**0.0336**	**-1.30**	0.9999	-1.05	0.9801	-1.03
NM_058212	Dpf3	1.30	**0.0336**	**1.30**	0.9999	1.09	0.1661	1.26
AK036317	Raf1	1.30	0.9999	1.01	**0.0159**	**1.30**	0.7254	1.12
NM_018730	Rpl36	1.30	0.9999	1.02	0.8027	1.15	**0.0445**	**1.30**
NM_030153	Mak10	1.29	**0.0461**	**1.29**	0.3147	-1.19	0.7691	1.10
NM_010260	Gbp2	1.29	**0.0000**	**1.29**	0.2723	-1.22	0.9116	-1.07
NM_028404	Top1mt	1.29	0.9999	1.03	**0.0159**	**1.29**	0.2792	1.19
NM_133774	Stard4	1.29	0.9999	-1.01	0.9999	-1.06	**0.0258**	**-1.29**
NM_133655	Cd81	1.28	0.9999	1.05	**0.0000**	**-1.28**	0.3174	-1.14
NM_009013	Rad51ap1	1.28	0.9999	1.01	0.9999	-1.06	**0.0258**	**-1.28**
NM_198300	Cpeb3	1.28	0.9999	1.07	0.4988	1.13	**0.0000**	**1.28**
NM_001042499	Rabl3	1.28	0.9999	1.06	**0.0361**	**1.28**	0.5724	1.14
NM_144862	Lims2	1.27	0.9999	1.12	**0.0159**	**-1.27**	0.8177	1.08
AK133757	Bcl9	1.27	0.9999	-1.12	**0.0455**	**1.27**	0.9496	-1.05
NM_019865	Rpl36a	1.27	0.9999	1.02	0.9999	1.05	**0.0258**	**1.27**
NM_013827	Mtf2	1.27	0.9999	1.04	0.5356	1.14	**0.0000**	**1.27**
NM_017380	Sept9	1.26	**0.0000**	**1.26**	0.9999	1.08	0.4007	1.13
NM_008027	Flot1	1.26	0.9999	-1.03	**0.0159**	**1.26**	0.5447	1.12
NM_011636	Plscr1	1.26	0.9999	1.05	**0.0361**	**1.26**	0.8197	1.08
NM_011930	Clcn7	1.26	**0.0000**	**1.23**	**0.0000**	**-1.26**	0.8924	1.05
NM_001002239	Rpl17	1.25	0.9999	1.01	0.8191	1.10	**0.0258**	**1.25**
AK084512	Plekha6	1.24	**0.0195**	**1.24**	**0.0000**	**-1.24**	0.1361	1.17
NM_023670	Igf2bp3	1.24	0.9999	-1.07	**0.0000**	**1.24**	0.6650	1.10
NM_011424	Ncor2	1.24	**0.0336**	**1.24**	0.9999	-1.01	0.1339	1.21
AK050742	B230217O12Rik	1.24	0.9999	1.01	**0.0361**	**1.24**	0.9881	1.02
NM_031392	Wdr6	1.24	0.9999	1.00	**0.0455**	**1.24**	0.9972	-1.01
XM_990154	Flnb	1.23	0.9999	1.01	**0.0000**	**1.23**	0.9883	1.02
NM_011588	Trim28	1.23	**0.0336**	**1.23**	0.9999	-1.00	0.6143	1.12
NM_177710	Ssh2	1.23	**0.0000**	**1.23**	0.9999	-1.06	0.2751	1.16
NM_025282	Mef2c	1.23	0.9999	1.06	0.9588	1.09	**0.0258**	**1.23**
NM_197945	Prosapip1	1.22	0.9999	-1.03	**0.0455**	**1.22**	0.9892	1.02
NAP026680-1	NAP026680-1	1.22	0.9999	1.03	0.9922	1.08	**0.0258**	**1.22**

NM_134099	Fbxo4	1.22	**0.0195**	**1.22**	0.9999	-1.06	0.9434	1.04
AB011473	Pfdn5	1.21	0.9999	1.03	0.9807	1.08	**0.0000**	**1.21**
NM_177296	Tnpo3	1.21	0.9999	1.01	**0.0455**	**1.21**	0.8854	1.06
NM_173180	Pmpca	1.21	0.9999	1.03	**0.0284**	**1.21**	0.5189	1.10
NM_001039657	Mtl5	1.21	0.9999	1.02	**0.0159**	**1.21**	0.8653	1.06
NM_021422	Dnaja4	1.20	0.9999	1.08	**0.0000**	**-1.20**	0.9908	1.01
NM_019941	Zfp235	1.20	0.9999	-1.04	**0.0159**	**-1.20**	0.7797	-1.08
NM_133756	Xab1	1.19	0.9999	1.04	**0.0284**	**1.19**	0.5189	1.10
NM_198006	6330578E17Rik	1.17	**0.0195**	**1.17**	0.9999	-1.03	0.1361	1.16
ENSMUST00000016770	ENSMUST00000016770	1.16	**0.0195**	**1.16**	0.9999	1.04	0.5724	1.08
BC070412	Diap1	1.16	0.9999	-1.02	**0.0455**	**1.16**	0.9277	1.03
BC030311	Armc8	1.15	**0.0195**	**1.15**	0.0983	1.14	0.8286	1.05
NM_013903	Mmp20	1.12	0.9999	-1.05	**0.0000**	**-1.12**	0.9137	-1.02
NM_010970	Olfr23	1.08	**0.0195**	**-1.08**	0.9999	-1.02	0.3586	-1.06
			Count < 0.05: 74		Count < 0.05: 105		Count < 0.05: 52	

Supplementary Table 2.2. Altered genes in female pups, with a FDR-adjusted p < 0.05 in at least one of the treatment conditions.

Accession Number	Gene Name	Foldrank	Hyperthyroid		Hypothyroid		Hypothyroid Replacement	
			P-Value	Fold-Change	P-Value	Fold-Change	P-Value	Fold-Change
NM_144930	AU018778	3.25	0.9986	1.08	**0.0000**	**3.25**	**0.0000**	**2.72**
NM_007860	Dio1	3.23	0.9834	1.22	**0.0000**	**-3.23**	0.9997	1.20
AK147478	Auts2	2.99	**0.0000**	**2.99**	0.9999	1.05	**0.0000**	**2.47**
AK158295	E2f8	2.82	0.9942	1.17	**0.0000**	**-2.82**	0.9997	-1.45
XM_981410	9030619P08Rik	2.77	0.8310	1.27	**0.0000**	**-2.77**	0.9997	-1.02
AK030395	Agxt2l1	2.69	0.9986	-1.14	**0.0000**	**2.69**	0.9997	-1.26
AK044145	AK044145	2.68	**0.0000**	**2.68**	0.9999	-1.00	**0.0000**	**1.91**
NM_009381	Thrsp	2.66	**0.0185**	**2.39**	**0.0000**	**-2.66**	0.9997	-1.07
NM_010358	Gstm1	2.55	**0.0108**	**-1.37**	**0.0000**	**2.55**	**0.0000**	**2.39**
NM_008630	Mt2	2.46	**0.0000**	**-2.46**	0.9999	1.18	0.9997	-1.52
NM_138313	Bmf	2.44	**0.0413**	**1.73**	**0.0000**	**-2.44**	0.6548	1.51
NM_010145	Ephx1	2.41	0.9960	1.11	**0.0000**	**2.41**	0.2225	1.97
NM_009676	Aox1	2.32	0.9986	-1.07	**0.0112**	**2.32**	0.1446	2.22
D86232	Ly6c	2.28	**0.0000**	**1.55**	**0.0000**	**-2.28**	0.9997	1.13
U96752	H2-Q1	2.28	0.7693	1.34	**0.0000**	**-2.28**	0.9997	-1.25
NM_001025384	LOC574405	2.26	**0.0000**	**1.69**	**0.0000**	**-1.70**	**0.0000**	**2.26**
NM_177380	Cyp3a44	2.22	0.9987	1.06	**0.0491**	**-2.22**	0.9997	-1.59
NM_011172	Prodh	2.21	0.9991	-1.03	**0.0112**	**-2.21**	0.9997	-1.14
NM_008030	Fmo3	2.21	**0.0000**	**-2.21**	0.5922	-1.48	0.3735	-1.78
NM_010359	Gstm3	2.18	0.2604	-1.26	**0.0000**	**2.18**	**0.0000**	**2.09**
NM_144544	2210407C18Rik	2.14	**0.0108**	**1.75**	**0.0000**	**-2.14**	0.3642	-1.70
A_52_P1156957	A_52_P1156957	2.13	**0.0000**	**-1.80**	**0.0000**	**2.13**	0.9997	-1.33
NM_177388	Slc41a2	2.12	**0.0000**	**2.12**	0.9999	1.08	0.9997	1.15
NM_024437	Nudt7	2.10	**0.0000**	**1.68**	**0.0000**	**-2.10**	0.9997	1.28
NM_054088	Pnpla3	2.08	**0.0000**	**2.08**	0.9999	-1.14	0.8965	1.48
NM_021365	Xlr4b	2.08	**0.0000**	**-2.08**	0.9999	1.02	0.9997	-1.41
NM_016854	Ppp1r3c	2.02	**0.0249**	**-1.93**	**0.0112**	**2.02**	0.9564	-1.48
NM_033601	Bcl3	2.02	**0.0000**	**2.02**	0.1837	-1.50	0.7143	1.45
NM_011727	Xlr3b	1.97	**0.0249**	**-1.97**	0.9999	1.07	0.8976	-1.58
AK142275	Stim2	1.95	**0.0000**	**1.95**	0.2061	-1.35	0.2857	1.47
NM_001042671	Prei4	1.95	0.3849	1.44	**0.0491**	**-1.72**	0.0803	1.95
AK042378	Ppargc1b	1.94	0.8878	1.18	**0.0000**	**-1.94**	0.4981	1.43

NM_134154	AW491445	1.94	**0.0000**	**1.94**	**0.0000**	**-1.63**	**0.0000**	**1.60**
NM_197983	0610008F07Rik	1.93	0.9986	1.08	**0.0000**	**1.93**	0.2489	1.66
NM_027153	Pir	1.93	0.9239	-1.19	**0.0000**	**1.93**	0.1205	1.82
AK017206	5033430I15Rik	1.92	**0.0000**	**1.49**	**0.0000**	**-1.92**	0.9997	1.13
NM_029509	LOC634650	1.92	**0.0000**	**1.92**	0.9999	1.09	0.9997	1.16
NM_027997	Serpina9	1.91	**0.0108**	**-1.67**	0.1450	-1.47	**0.0000**	**-1.91**
NM_018881	Fmo2	1.90	**0.0108**	**-1.90**	0.9999	-1.05	0.9997	-1.35
NM_134246	Acot3	1.89	**0.0000**	**-1.70**	**0.0000**	**1.89**	0.9502	-1.28
NM_145564	Fbxo21	1.89	**0.0298**	**-1.89**	0.9999	1.13	0.9997	1.02
NM_009895	Cish	1.87	**0.0185**	**-1.87**	0.9999	-1.05	0.3838	-1.68
NM_008737	Nrp1	1.86	0.7130	1.32	**0.0112**	**-1.86**	0.9997	-1.23
NM_207655	Egfr	1.86	**0.0185**	**-1.86**	0.9999	-1.25	0.9997	-1.45
NM_172119	Dio3	1.86	**0.0298**	**-1.86**	0.7747	1.40	0.9997	-1.28
NM_031188	Mup1	1.85	0.0686	1.69	**0.0192**	**-1.85**	0.9997	-1.02
AY283181	Dio3as	1.85	**0.0000**	**-1.85**	0.9999	1.29	0.9997	-1.06
BC024137	BC024137	1.84	**0.0000**	**1.84**	**0.0000**	**-1.84**	0.8602	1.35
NM_053096	Cml2	1.84	0.4803	1.48	**0.0387**	**-1.84**	0.9997	1.02
NM_019972	Sort1	1.83	**0.0000**	**1.83**	**0.0000**	**-1.50**	0.1009	1.49
NM_009366	Tsc22d1	1.80	**0.0185**	**1.80**	0.9999	1.11	0.9236	1.37
NM_009883	Cebpb	1.79	**0.0354**	**1.79**	0.1073	-1.69	0.8189	1.52
NM_019814	Higd1a	1.75	**0.0000**	**1.75**	0.6875	-1.34	0.9997	1.14
NM_010274	Gpd2	1.75	**0.0249**	**1.49**	**0.0000**	**-1.75**	0.4981	1.39
NM_130455	Grin3b	1.73	0.9986	1.07	**0.0000**	**-1.73**	0.9997	-1.25
NM_009251	Serpina3g	1.72	0.9986	1.05	**0.0000**	**-1.72**	0.9997	1.01
NM_011488	Stat5a	1.71	**0.0000**	**1.71**	**0.0000**	**-1.65**	0.2161	1.57
NM_177251	D830014E11Rik	1.71	**0.0000**	**1.71**	0.9808	-1.18	0.9997	1.12
NM_013703	Vldlr	1.71	0.9810	-1.18	**0.0387**	**1.71**	0.9997	1.26
XM_161350	1700024P16Rik	1.71	0.9991	1.02	**0.0000**	**1.71**	0.9997	1.20
NM_001033453	Ppm2c	1.70	**0.0000**	**1.70**	0.9999	-1.03	0.8801	1.17
NM_026637	A030007L17Rik	1.70	0.9942	1.09	**0.0000**	**-1.70**	0.9997	-1.19
NM_172776	D630002G06Rik	1.69	0.9942	1.14	**0.0445**	**-1.69**	0.9997	-1.09
U31966	Cbr1	1.69	0.9942	1.08	**0.0000**	**1.61**	**0.0000**	**1.69**
NM_027249	2010305C02Rik	1.69	0.9942	1.14	**0.0327**	**-1.69**	0.9997	-1.08
NM_033373	Krt23	1.69	**0.0000**	**-1.69**	0.9999	1.01	0.9997	-1.07
BC024571	Itga6	1.69	**0.0000**	**1.69**	0.1913	-1.38	0.9997	1.06
NM_025436	Sc4mol	1.67	**0.0000**	**1.67**	**0.0112**	**-1.56**	0.9997	-1.19

TC1631866	TC1493944	1.67	0.9991	1.03	**0.0112**	**1.67**	0.9024	1.34
AK014609	4633401B06Rik	1.66	**0.0000**	**1.38**	0.3915	-1.23	**0.0000**	**1.66**
NM_029573	Idh3a	1.66	**0.0000**	**1.66**	0.5708	-1.21	0.3558	1.34
NM_178111	Trp53inp2	1.66	**0.0000**	**1.53**	**0.0000**	**-1.66**	0.9997	1.10
NM_153528	Gramd1c	1.66	**0.0000**	**1.66**	0.0592	-1.31	**0.0000**	**1.43**
AK053456	3021401C12Rik	1.65	**0.0185**	**1.65**	0.9999	-1.16	0.9997	1.29
NM_009124	Atxn1	1.65	0.4334	1.28	**0.0000**	**-1.65**	0.9997	-1.03
AK009333	2310014D11Rik	1.65	**0.0000**	**1.65**	0.9999	-1.12	**0.0000**	**1.52**
NM_133898	B230342M21Rik	1.65	0.6155	1.27	**0.0000**	**-1.65**	0.5287	1.44
NM_008706	Nqo1	1.64	0.9257	-1.19	**0.0257**	**1.64**	0.3838	1.55
NM_172463	Sned1	1.64	**0.0000**	**1.46**	**0.0000**	**-1.64**	**0.0466**	**1.36**
AK036369	Ddhd1	1.63	**0.0000**	**1.63**	0.9999	-1.10	0.9997	1.19
AK137889	Stat5b	1.63	**0.0000**	**1.63**	0.9999	-1.09	0.2489	1.47
NAP124154-1	TC1514546	1.63	**0.0471**	**-1.63**	0.9999	1.07	0.9997	-1.20
NM_027897	Rhpn2	1.63	0.9986	-1.06	**0.0112**	**-1.63**	0.9997	1.16
NM_028133	Egln3	1.63	0.2896	-1.23	**0.0000**	**1.63**	0.9997	-1.05
NM_019414	Selenbp2	1.63	0.9942	-1.08	**0.0000**	**-1.63**	0.9997	-1.22
NM_198649	Ablim3	1.62	**0.0108**	**-1.62**	0.9999	-1.16	0.9997	-1.11
NM_009469	Ulk1	1.62	0.9274	1.15	**0.0000**	**-1.62**	0.9997	1.10
NM_001013785	Akr1c19	1.62	0.9845	-1.10	**0.0000**	**1.62**	0.9456	1.23
AK077979	Fdps	1.61	**0.0000**	**1.61**	0.9999	-1.06	0.9997	-1.15
NM_011675	Uck1	1.61	**0.0000**	**1.61**	**0.0327**	**-1.39**	0.5467	1.32
NM_016919	Col5a3	1.60	0.9926	-1.07	**0.0000**	**1.60**	0.5596	1.24
NM_021462	Mknk2	1.60	**0.0000**	**-1.60**	0.9999	-1.05	0.9997	-1.24
AK080781	AK080781	1.60	**0.0298**	**1.60**	0.5218	-1.32	0.9997	1.13
NM_207269	D330050I23Rik	1.59	**0.0000**	**1.59**	0.9999	-1.15	0.9997	1.10
NM_145076	Trim24	1.59	**0.0108**	**1.41**	**0.0000**	**-1.59**	0.2489	1.38
AK019824	4930581F22Rik	1.59	**0.0185**	**-1.55**	0.9999	-1.04	0.2018	-1.59
NM_010292	Gck	1.57	0.9942	1.12	**0.0387**	**-1.57**	0.9997	1.02
XM_895387	2210408F21Rik	1.57	0.9942	-1.10	**0.0327**	**1.47**	**0.0000**	**1.57**
NM_172710	2310045A20Rik	1.57	**0.0185**	**1.54**	0.9999	-1.17	0.1268	1.57
NM_133232	Pfkfb3	1.56	**0.0000**	**1.56**	0.9999	-1.09	0.3309	1.34
AK077315	Mirg	1.56	0.9783	1.13	**0.0192**	**1.56**	0.9997	-1.00
NM_021352	Crybb3	1.56	**0.0108**	**1.56**	0.9999	-1.19	0.9997	-1.07
NM_201644	Ugt1a9	1.55	0.9991	1.02	**0.0000**	**1.55**	0.9997	1.08
NM_026410	Cdca5	1.55	0.9991	-1.01	0.9999	-1.13	**0.0466**	**-1.55**

NM_172769	Sc5d	1.55	0.7807	1.19	**0.0112**	**-1.55**	0.9997	-1.17
NM_019875	Abcb9	1.54	**0.0000**	**1.54**	0.7701	-1.21	0.8125	1.27
NM_013855	Abca3	1.54	0.9256	1.13	**0.0000**	**-1.54**	0.9997	-1.15
AK007434	1810011H11Rik	1.54	**0.0000**	**1.54**	0.3603	-1.26	0.9997	1.13
NM_029688	Srxn1	1.54	0.9990	-1.01	**0.0000**	**1.54**	**0.0000**	**1.36**
NM_013562	Ifrd1	1.53	**0.0000**	**1.53**	0.9999	-1.17	0.4873	1.35
NM_145942	Hmgcs1	1.53	0.1130	1.44	**0.0192**	**-1.53**	0.9997	1.09
NM_010376	H13	1.53	**0.0000**	**1.53**	0.9999	-1.06	0.2571	1.36
NM_026169	1200004M23Rik	1.53	**0.0000**	**1.53**	**0.0192**	**-1.34**	0.4912	1.26
NM_001039386	Nelf	1.52	0.2681	1.20	**0.0000**	**-1.52**	0.9997	1.02
NM_010139	Epha2	1.52	0.9700	1.15	**0.0192**	**-1.52**	0.9997	-1.05
NM_007956	Esr1	1.52	0.9986	1.03	**0.0112**	**-1.52**	0.9997	1.04
AK050258	AK050258	1.51	0.0930	1.39	**0.0192**	**-1.51**	0.2960	1.47
NM_001039710	1500041J02Rik	1.51	**0.0000**	**1.51**	0.9999	-1.03	0.2711	1.44
NM_008102	Gch1	1.50	**0.0185**	**1.36**	**0.0000**	**-1.50**	0.9997	1.18
NM_153507	Cpne2	1.50	0.9470	1.17	**0.0491**	**-1.50**	0.9997	1.19
NM_011816	E430034L04Rik	1.49	**0.0000**	**1.49**	0.9999	-1.00	0.9997	1.11
NM_011521	Sdc4	1.49	0.9942	1.08	**0.0112**	**-1.49**	0.9997	-1.02
NM_022331	Herpud1	1.48	**0.0471**	**-1.48**	0.0935	-1.45	0.9997	-1.09
NM_007934	Enpep	1.48	0.9942	-1.08	**0.0257**	**1.48**	0.9997	1.19
ENSMUST00000070000	ENSMUST00000070000	1.48	**0.0249**	**1.48**	0.0854	-1.40	0.9997	1.25
AK020546	9530006C21Rik	1.48	0.7821	1.17	**0.0445**	**1.39**	0.1878	1.48
NM_027402	Fndc5	1.47	**0.0000**	**1.47**	0.4994	-1.26	0.9997	1.18
AK085506	4933404O12Rik	1.47	0.3516	1.28	**0.0112**	**-1.47**	0.9997	1.09
NM_011243	Rarb	1.47	**0.0000**	**1.47**	0.9999	-1.01	0.9997	1.16
AK034561	Fzd8	1.47	**0.0249**	**1.47**	0.9999	-1.16	0.9997	1.22
NM_008991	Abcd3	1.46	**0.0108**	**1.30**	**0.0000**	**-1.46**	0.9997	1.06
NM_173375	BC064033	1.46	**0.0000**	**1.46**	0.9762	-1.16	0.9997	-1.07
NM_007678	Cebpa	1.46	**0.0000**	**-1.46**	0.9999	-1.15	0.3683	-1.36
NM_172256	Dync2li1	1.46	0.9437	-1.12	**0.0192**	**1.46**	0.9997	1.07
NM_145603	Ces2	1.46	**0.0000**	**1.42**	0.9999	-1.03	**0.0000**	**1.46**
NM_011804	Creg1	1.45	0.9986	-1.04	**0.0000**	**1.45**	0.3380	1.28
NM_013541	Gstp1	1.45	0.9951	1.04	**0.0000**	**1.45**	**0.0000**	**1.37**
NM_178701	Lrrc8d	1.44	**0.0000**	**1.44**	0.3713	-1.24	0.3036	1.35
NM_138686	Cys1	1.44	**0.0108**	**-1.44**	0.9999	-1.09	0.4213	-1.31
AK046650	BC013529	1.44	**0.0000**	**1.44**	0.9999	-1.03	0.4936	1.20

BC094349	Lrp3	1.44	0.6149	1.15	**0.0000**	**-1.44**	0.9997	1.03
NM_153392	4922503N01Rik	1.44	**0.0108**	**1.44**	0.9999	-1.13	0.9997	-1.04
NM_011397	Slc23a1	1.44	0.2910	1.30	**0.0257**	**-1.44**	0.9997	1.19
AK165240	Slc16a10	1.44	0.9942	1.06	**0.0000**	**-1.44**	0.9997	-1.04
NM_007669	Cdkn1a	1.44	0.9991	1.01	**0.0000**	**-1.44**	0.9997	-1.04
AK033699	Lgr4	1.43	0.9130	1.11	**0.0000**	**-1.43**	0.9997	1.11
NM_026764	Gstm4	1.43	0.9942	-1.08	**0.0192**	**1.43**	0.9992	1.23
NM_001004066	Zfp386	1.43	**0.0000**	**1.43**	0.1288	-1.31	0.9997	1.08
NM_134141	Ciapin1	1.43	**0.0000**	**1.43**	0.9999	-1.11	0.1940	1.29
NM_146161	Arhgap24	1.43	**0.0249**	**1.43**	0.9999	-1.18	0.9997	1.12
NM_175491	Smcr8	1.42	**0.0000**	**1.42**	0.9999	-1.04	0.9997	1.16
NM_178607	Rnf24	1.42	**0.0413**	**1.35**	0.9999	-1.01	0.1205	1.42
NM_026393	Nmral1	1.42	0.9991	-1.02	**0.0257**	**-1.42**	0.9997	1.03
NM_033218	Srebf2	1.42	**0.0354**	**1.42**	0.9999	-1.17	0.9997	-1.03
NM_025341	Abhd6	1.42	**0.0298**	**1.42**	0.1768	-1.33	0.9997	1.09
NM_008255	Hmgcr	1.42	**0.0108**	**1.42**	0.7427	-1.19	0.9997	1.14
NM_026178	Mmd	1.42	**0.0249**	**1.36**	**0.0000**	**-1.42**	0.7975	1.24
NM_153525	Tmem41b	1.42	**0.0000**	**1.42**	0.8475	-1.17	0.9997	1.14
NM_008615	Mod1	1.41	0.0954	1.32	**0.0445**	**-1.36**	0.2225	1.41
NM_007556	Bmp6	1.41	0.9991	-1.01	**0.0000**	**1.41**	0.4936	1.25
NM_008357	Il15	1.40	**0.0000**	**1.40**	0.9999	-1.02	0.9997	1.16
NM_173038	Lrrc35	1.40	**0.0000**	**1.28**	0.9999	1.09	**0.0000**	**1.40**
NM_176998	5730410E15Rik	1.40	0.7988	1.17	**0.0257**	**1.40**	0.9997	-1.01
NM_009466	Ugdh	1.40	0.9972	-1.05	**0.0112**	**1.40**	0.9997	1.10
BC070459	Qrsl1	1.40	**0.0000**	**1.40**	0.9999	1.08	0.5997	1.26
NM_021366	Klf13	1.40	0.4989	1.15	**0.0000**	**-1.40**	0.9000	1.16
NM_009150	Selenbp1	1.40	0.8810	-1.13	**0.0000**	**-1.40**	0.9997	-1.18
NM_054053	Gpr98	1.40	0.9887	1.09	**0.0112**	**-1.40**	0.9997	-1.03
NM_028123	Slc37a3	1.39	**0.0000**	**1.39**	0.2634	-1.23	0.9997	1.11
NM_028651	Tmtc4	1.39	**0.0298**	**1.39**	0.9999	1.04	0.9654	1.21
NM_134255	Elovl5	1.39	0.9942	1.07	**0.0000**	**-1.39**	0.9997	-1.08
NM_010903	Nfe2l3	1.38	**0.0000**	**1.38**	0.7443	-1.14	0.9997	1.06
XM_911199	1810008N23Rik	1.38	0.9942	-1.06	**0.0112**	**-1.38**	0.9997	-1.15
NM_018831	Dclre1a	1.38	0.9942	-1.06	**0.0000**	**1.38**	0.9997	1.03
NM_009171	Shmt1	1.38	**0.0249**	**1.38**	0.9999	-1.11	0.9997	1.17
BC054536	Adam11	1.38	0.6691	-1.19	**0.0257**	**1.38**	0.9997	1.19

NM_009198	Slc17a1	1.38	0.9960	1.06	**0.0192**	**1.38**	0.4981	1.30
NM_008131	Glul	1.38	0.6228	-1.21	**0.0445**	**-1.38**	0.9997	1.05
NM_175244	Hectd3	1.38	**0.0000**	**1.31**	0.9999	-1.06	**0.0000**	**1.38**
NM_030176	2610039E05Rik	1.38	**0.0185**	**-1.37**	**0.0192**	**-1.38**	0.9997	-1.19
NAP053239-1	NAP053239-1	1.38	**0.0108**	**1.38**	0.9999	1.04	0.4981	1.25
AK084512	Plekha6	1.38	0.9887	1.08	**0.0000**	**-1.38**	0.9997	1.15
NM_010664	Krt18	1.38	0.9942	-1.06	**0.0000**	**1.38**	0.9997	1.05
NM_027980	2310003H01Rik	1.37	**0.0000**	**1.37**	0.3208	-1.14	0.0803	1.26
NM_183423	Pla2g12a	1.37	0.8913	-1.14	**0.0387**	**1.37**	0.6674	1.29
NM_030143	Ddit4l	1.37	0.9990	1.02	**0.0327**	**1.37**	0.9997	1.00
NM_030701	Gpr109a	1.37	0.9986	-1.03	**0.0112**	**1.37**	0.9997	-1.05
NM_019437	Rfk	1.37	0.5784	1.18	**0.0000**	**-1.37**	0.9997	1.12
NM_027872	1200006F02Rik	1.37	0.1514	1.30	**0.0112**	**-1.37**	0.9997	1.06
XM_131720	2610002D18Rik	1.37	0.9986	1.04	0.9999	-1.05	**0.0466**	**-1.37**
NM_133942	Plekha1	1.37	**0.0000**	**1.37**	0.5470	-1.18	0.3380	1.28
AK044329	AK044329	1.36	**0.0000**	**-1.36**	0.9999	1.04	0.4131	-1.27
NM_001026214	Entpd5	1.36	0.9986	-1.03	**0.0000**	**1.36**	0.2489	1.26
NM_001024840	Adarb1	1.36	0.9451	1.08	0.9999	-1.08	**0.0466**	**1.36**
NM_001024139	Adamts15	1.36	0.9986	-1.04	**0.0257**	**1.36**	0.9997	-1.01
NM_177601	Tmem60	1.35	**0.0000**	**1.35**	0.1651	-1.16	0.7198	1.14
NM_001033819	9130409I23Rik	1.35	0.9986	-1.03	**0.0000**	**1.35**	0.9778	1.18
NM_011324	Scnn1a	1.35	0.7765	-1.15	**0.0387**	**1.32**	0.1783	1.35
NM_025958	Cand2	1.35	0.9986	-1.02	**0.0000**	**1.35**	0.9997	1.02
NM_027418	Mapk6	1.35	**0.0000**	**1.35**	0.9157	-1.11	**0.0466**	**1.30**
NM_007421	Adssl1	1.35	0.9491	-1.11	**0.0327**	**1.35**	0.9997	1.09
NM_139297	Ugp2	1.35	0.4248	-1.20	**0.0000**	**1.35**	0.9997	1.01
AK021221	C330024D12Rik	1.34	0.9942	-1.06	**0.0000**	**1.34**	0.9997	-1.08
NM_133234	Bbc3	1.34	**0.0298**	**1.28**	**0.0192**	**-1.34**	0.9997	-1.09
NM_145448	9030617O03Rik	1.34	**0.0354**	**1.31**	**0.0112**	**-1.34**	0.9997	1.01
NM_008222	Hccs	1.34	**0.0185**	**1.34**	0.9960	-1.14	0.6182	1.23
NM_020010	Cyp51	1.34	**0.0249**	**1.34**	0.9999	-1.14	0.6674	-1.24
NM_198171	BC015286	1.34	**0.0471**	**1.34**	0.9999	1.00	0.7440	1.26
NM_181399	Usp6nl	1.34	0.9990	-1.02	**0.0491**	**1.34**	0.9997	-1.11
NM_175266	Epm2aip1	1.34	**0.0000**	**1.34**	0.9999	-1.02	0.1205	1.29
AK033655	Sesn3	1.34	**0.0298**	**-1.29**	0.6425	-1.17	0.2018	-1.34
NM_011055	Pde3b	1.33	0.9986	-1.03	**0.0192**	**1.33**	0.9997	1.02

BC080858	Kbtbd11	1.33	**0.0000**	**1.33**	0.9999	-1.09	0.9580	1.16
NM_027496	5730557B15Rik	1.33	**0.0354**	**1.33**	0.9999	-1.05	0.9997	1.14
NM_001037170	Tomm40l	1.33	**0.0185**	**-1.33**	0.9999	1.11	0.9997	-1.01
NM_172765	Btbd15	1.33	**0.0108**	**-1.33**	0.9999	-1.08	0.9997	-1.17
AK012631	2810001G20Rik	1.33	**0.0298**	**1.33**	0.9999	-1.04	0.9819	1.19
BC029185	Ches1	1.33	**0.0354**	**1.31**	0.6786	-1.17	0.2489	1.33
AK153792	D5Ertd135e	1.33	**0.0413**	**1.33**	0.9999	-1.08	0.9580	1.19
NM_011018	Sqstm1	1.33	**0.0108**	**-1.33**	0.9999	-1.07	0.9997	-1.04
NM_010544	Ihh	1.32	**0.0298**	**-1.32**	0.9999	-1.08	0.5320	-1.28
NM_001001144	Scap	1.32	0.9888	1.09	**0.0257**	**-1.32**	0.9997	1.07
NM_026832	Cgrrf1	1.32	**0.0000**	**1.32**	0.9999	-1.11	0.9997	1.14
NM_008999	Rab23	1.32	0.5364	1.18	**0.0257**	**-1.32**	0.9997	1.04
NM_144558	Bivm	1.31	**0.0108**	**1.31**	0.9999	-1.09	0.9216	1.16
NM_028651	Tmtc4	1.31	**0.0000**	**1.31**	0.9999	1.05	0.9997	1.11
NM_029798	2810417J12Rik	1.31	0.9986	1.03	**0.0112**	**-1.31**	0.9997	1.07
NM_153557	BC029214	1.30	**0.0108**	**1.30**	0.5946	-1.16	0.9997	1.04
NM_201362	Ccdc68	1.30	**0.0185**	**1.30**	0.1900	-1.24	0.7902	1.21
NM_008199	H2-Bl	1.30	**0.0000**	**1.30**	0.9999	-1.10	0.9997	1.15
NM_198024	C130037N17Rik	1.30	**0.0000**	**-1.30**	**0.0192**	**1.22**	0.1582	-1.24
NM_025626	3110001A13Rik	1.30	**0.0000**	**1.30**	**0.0192**	**-1.27**	0.2337	1.28
AK050217	C730027H18Rik	1.29	0.9655	-1.09	**0.0445**	**1.29**	0.9997	1.17
NM_008390	Irf1	1.29	**0.0000**	**1.29**	**0.0192**	**-1.26**	0.9997	1.07
NM_170599	Igsf11	1.29	0.4768	1.18	**0.0257**	**-1.29**	0.7837	1.20
NM_175372	Rdh13	1.29	**0.0000**	**1.29**	0.9999	-1.01	0.1940	1.24
NM_001042523	Txnrd1	1.29	0.9451	-1.10	**0.0491**	**1.29**	0.9806	1.18
NM_024221	Pdhb	1.29	**0.0000**	**1.29**	0.9081	-1.12	0.9997	1.09
NM_026062	2900024C23Rik	1.29	0.9942	-1.06	**0.0192**	**-1.29**	0.9997	-1.09
NM_010357	Gsta4	1.28	0.9130	1.10	**0.0000**	**1.28**	0.6590	1.22
NM_146093	D19Ertd721e	1.28	0.8465	1.11	**0.0000**	**-1.28**	0.9997	1.05
NM_134072	Akr1c14	1.28	0.0563	-1.25	**0.0112**	**1.28**	0.9997	1.10
NM_146171	2810406C15Rik	1.28	0.9810	1.06	0.9999	-1.03	**0.0466**	**-1.28**
NM_031170	Krt8	1.28	0.9942	-1.05	**0.0387**	**1.28**	0.9997	1.04
NM_025967	D16Ertd472e	1.28	**0.0000**	**1.28**	0.9999	-1.05	0.9473	1.14
NM_001039089	Sel1h	1.28	**0.0108**	**1.28**	0.9999	-1.07	0.9997	-1.03
NM_011034	Prdx1	1.27	0.9936	1.07	**0.0112**	**1.27**	0.9997	1.11
NM_019769	1500003O03Rik	1.27	**0.0249**	**-1.27**	0.9999	-1.02	0.9997	-1.01

2210408K08	2210408K08	1.27	**0.0298**	**1.27**	0.2847	-1.20	0.9997	1.09
NM_033080	Nudt19	1.27	0.9208	-1.08	**0.0000**	**1.27**	0.9997	1.12
NM_019946	Mgst1	1.27	0.8914	-1.08	**0.0000**	**1.27**	0.3859	1.18
NM_008173	Nr3c1	1.27	0.9991	1.01	**0.0491**	**-1.27**	0.9997	1.01
NM_008252	Hmgb2	1.26	**0.0354**	**1.26**	0.9999	1.02	0.4899	-1.23
NM_172670	Gyltl1b	1.26	0.9810	1.06	**0.0000**	**1.26**	0.9085	1.12
NM_027293	Dopey2	1.26	0.1053	-1.19	**0.0112**	**1.26**	0.9997	-1.08
NM_008358	Il15ra	1.26	**0.0000**	**1.19**	0.9756	-1.06	**0.0000**	**1.26**
AK008281	AK008281	1.25	0.9987	-1.02	**0.0000**	**1.25**	0.9094	1.16
NM_007379	Abca2	1.25	0.9960	1.04	**0.0327**	**-1.25**	0.9997	-1.07
NM_172406	Trak2	1.25	**0.0249**	**1.25**	0.5443	-1.15	0.8876	1.16
NM_023455	Cml4	1.24	**0.0249**	**1.24**	0.3452	-1.16	0.9997	1.03
NM_022883	Lpin3	1.24	0.7127	1.08	0.6875	1.09	**0.0000**	**1.24**
AB025011	Rnf138	1.24	0.2414	1.17	**0.0257**	**-1.24**	0.9997	1.07
AK021412	E130304I02Rik	1.24	**0.0000**	**1.24**	0.9999	-1.03	0.6002	1.16
XM_139295	Card6	1.23	0.9116	-1.08	**0.0257**	**-1.23**	0.9997	1.03
BC059249	Ttbk1	1.23	**0.0185**	**1.23**	0.9999	-1.03	0.9997	1.03
NM_144884	Tor1a	1.23	**0.0185**	**1.22**	0.9999	-1.08	0.1268	1.23
NM_138671	Nadk	1.23	**0.0108**	**1.23**	0.2447	-1.16	0.9997	1.00
NM_009396	Tnfaip2	1.23	**0.0185**	**1.23**	**0.0112**	**-1.21**	0.5061	1.14
NM_138741	Sdpr	1.23	**0.0108**	**1.23**	0.2281	-1.16	0.5287	1.18
NM_009351	Tep1	1.22	**0.0000**	**1.22**	0.8144	-1.11	0.9997	1.03
NM_026425	Nat5	1.22	**0.0000**	**1.22**	0.9999	1.04	0.9997	1.08
NM_024434	Lap3	1.22	0.2164	-1.15	**0.0000**	**1.22**	0.9997	-1.05
NM_013667	Slc22a2	1.22	**0.0000**	**1.22**	0.9999	-1.03	0.9997	1.02
NM_019794	Dnaja2	1.21	**0.0471**	**1.21**	0.9999	-1.10	0.9997	1.10
NM_008879	Lcp1	1.21	0.9987	1.01	**0.0112**	**1.21**	0.9997	1.06
NM_153162	Txnrd3	1.21	**0.0249**	**1.21**	0.2550	-1.16	0.4587	1.19
ENSMUST00000091560	ENSMUST00000091560	1.21	0.3398	1.14	**0.0257**	**-1.21**	0.3309	1.21
NM_025515	2310015N07Rik	1.21	0.9942	1.05	**0.0491**	**1.21**	0.9997	-1.02
NM_007554	Bmp4	1.21	**0.0108**	**-1.21**	0.9999	1.06	0.9997	-1.12
NM_029585	Det1	1.21	**0.0000**	**1.21**	**0.0445**	**-1.17**	0.2489	1.18
NM_199199	AI316787	1.21	**0.0298**	**1.21**	0.9999	1.02	0.9086	1.13
AK029400	Bad	1.21	0.9942	1.05	**0.0257**	**-1.21**	0.9997	-1.09
NM_172116	Pddc1	1.20	0.9960	-1.03	**0.0387**	**1.20**	0.9997	1.02
XM_128781	Lycat	1.20	0.9991	-1.01	**0.0000**	**1.20**	0.9997	1.06

NM_133240	Acot8	1.19	0.9942	1.04	**0.0327**	**-1.19**	0.9997	-1.05
NM_023646	Dnaja3	1.19	0.9997	1.00	**0.0491**	**-1.19**	0.9997	1.06
NM_027946	Wdr68	1.19	0.9986	-1.02	**0.0257**	**1.19**	0.9997	1.01
NM_021464	Ptprt	1.19	**0.0354**	**-1.19**	0.9999	1.02	0.9997	-1.02
NM_028132	Pgm2	1.19	0.9942	1.03	**0.0000**	**1.19**	0.9997	1.03
NM_030153	Mak10	1.18	**0.0298**	**1.18**	0.1014	-1.17	0.8864	1.12
NM_153794	4933403F05Rik	1.18	0.8713	1.05	**0.0000**	**1.18**	0.9997	1.03
AK032144	AK032144	1.18	**0.0298**	**1.17**	0.9999	1.01	0.2519	1.18
NM_021446	0610007P14Rik	1.18	0.9451	1.06	**0.0192**	**-1.18**	0.3629	-1.15
NM_026609	Leprotl1	1.18	**0.0108**	**1.18**	0.9999	-1.03	0.9997	1.05
NM_025295	Btd	1.17	**0.0000**	**-1.17**	0.9999	-1.01	0.9997	-1.00
NM_197945	Prosapip1	1.17	0.2983	-1.13	**0.0491**	**1.17**	0.9997	1.02
NM_183165	BC027061	1.17	0.9142	1.06	**0.0257**	**1.17**	0.9997	1.10
NM_178629	4930579E17Rik	1.14	**0.0108**	**1.14**	0.9999	1.06	0.9997	1.03
BC093515	BC093515	1.14	**0.0413**	**1.14**	0.9999	-1.03	0.9997	1.03
BC055791	2310028O11Rik	1.10	**0.0298**	**1.10**	0.9999	-1.03	0.9997	-1.01
NM_010084	Adam18	1.09	**0.0108**	**-1.09**	0.1936	-1.07	0.2711	-1.09
			Count <0.05: 167		Count <0.05: 162		Count <0.05: 26	

Supplementary Table 2.3. The five most affected pathways, using the list of all significant genes (significant in at least one treatment condition), along with the names of the genes that were affected by TH treatment within the pathway.

Accession	Symbol	Entrez Gene Name
NRF2-Mediated Oxidative Stress Response (p-value = 5.48 E-13)		
NM_009676	AOX1	aldehyde oxidase 1
NM_007620	CBR1	carbonyl reductase 1
NM_019794	DNAJA2	DnaJ (Hsp40) homolog, subfamily A, member 2
NM_023646	DNAJA3	DnaJ (Hsp40) homolog, subfamily A, member 3
NM_021422	DNAJA4	DnaJ (Hsp40) homolog, subfamily A, member 4
NM_008049	FTL	ferritin, light polypeptide
NM_022331	HERPUD1	homocysteine-inducible, endoplasmic reticulum
NM_011034	PRDX1	peroxiredoxin 1
NM_011018	SQSTM1	sequestosome 1
NM_001042523	TXNRD1	thioredoxin reductase 1
Glutathione Metabolism (p-value = 3.75 E-5)		
NM_010357	GSTA4	glutathione S-transferase alpha 4
NM_026764	GSTM4	glutathione S-transferase mu 4
NM_010358	GSTM5	glutathione S-transferase mu 5
NM_010359	GSTM3	glutathione S-transferase, mu 3
NM_013541	GSTP1	glutathione S-transferase pi 1
NM_010361	GSTT2	glutathione S-transferase theta 2
NM_029573	IDH3A	isocitrate dehydrogenase 3 (NAD+) alpha
NM_019946	MGST1	microsomal glutathione S-transferase 1
Xenobiotic Metabolism Signaling (p-value = 9.8 E-7)		
NM_145603	CES2	carboxylesterase 2
NM_010828	CITED2	Cbp/p300-interacting transactivator,
NM_018881	FMO2	flavin containing monooxygenase 2 (non-functional)
NM_008030	FMO3	flavin containing monooxygenase 3
NM_172821	MAP3K13	mitogen-activated protein kinase kinase kinase 13
NM_027418	MAPK6	mitogen-activated protein kinase 6
NM_016700	MAPK8	mitogen-activated protein kinase 8
NM_008706	NQO1	NAD(P)H dehydrogenase, quinone 1
NM_018810	RAF1	v-raf-1 murine leukemia viral oncogene homolog 1
Metabolism of Xenobiotics by Cytochrome P450 (p-value = 3.29 E-6)		
NM_028089	CYP2C18	cytochrome P450, family 2, subfamily C, polypeptide 18
NM_177380	CYP3A4	cytochrome P450, family 3, subfamily A, polypeptide 4
NM_020010	CYP51A1	cytochrome P450, family 51, subfamily A, polypeptide 1
NM_010145	EPHX1	epoxide hydrolase 1, microsomal (xenobiotic)
NM_201644	UGT1A9	UDP glucuronosyltransferase 1 family, polypeptide A9
TR/RXR Activation (p-value = 1.2 E-4)		
NM_033601	BCL3	B-cell CLL/lymphoma 3
NM_007860	DIO1	deiodinase, iodothyronine, type I
NM_172119	DIO3	deiodinase, iodothyronine, type III

NM_008615	ME1	malic enzyme 1, NADP(+)-dependent, cytosolic
NM_011424	NCOR2	nuclear receptor co-repressor 2
NM_011055	PDE3B	phosphodiesterase 3B, cGMP-inhibited
NM_033218	SREBF2	sterol regulatory element binding transcription factor 2
NM_009381	THRSP	thyroid hormone responsive (SPOT14 homolog, rat)

Supplementary Table 4.1. Genes associated with TR-binding site peaks found in at least two samples.

Gene associated to peak	Significant Peaks	Distance from peak to TSS	Width of peak	Chromosome
0610010O12Rik	2	260	550	5
1110054O05Rik	2	17133	401	9
1190002N15Rik	2	40754	1149	7
1200011I18Rik	2	289	545	2
1600020E01Rik	2	4845	364	X
1700011I03Rik	2	2356	467	13
1700012B15Rik	2	1552	211	7
1700022K14Rik	2	627	434	1
1700034E13Rik	2	5554	184	1
1700034E13Rik	2	42762	181	12
1700084C01Rik	2	29651	160	5
1700095J03Rik	2	2796	153	15
1810013D15Rik	2	18712	161	18
1810043H04Rik	2	14651	205	4
2010106G01Rik	2	1203	292	9
2010300C02Rik	2	301	446	14
2310021P13Rik	2	3810	192	6
2310067B10Rik	2	4523	169	18
2310079F23Rik	2	280	197	12
2410006H16Rik	2	1653	175	5
2410018M08Rik	2	6052	204	18
2610018G03Rik	2	1212	591	18
2610029G23Rik	2	5666	439	1
2610528E23Rik	2	15	408	7
2700068H02Rik	2	1708	162	3
2810403A07Rik	2	2896	413	11
2810453I06Rik	2	7065	449	2
2900092E17Rik	2	1311	200	1
4930404H21Rik	2	1113	493	14
4930405A21Rik	2	894	383	11
4930412D23Rik	2	2559	394	5
4930430F08Rik	2	4041	308	11
4930451I11Rik	2	340	257	5
4930461C15Rik	2	1042	548	X
4930562F07Rik	2	906	183	X
4930568K20Rik	2	24177	333	16
4930578I06Rik	2	135	204	4
4930579F01Rik	2	525	361	3
4930593C16Rik	2	1524	278	5
4932438A13Rik	2	158	361	7
4933403G14Rik	2	3089	314	7
4933403G14Rik	2	2657	198	2
4933406I18Rik	2	7022	790	X
4933407I08Rik	2	1725	490	10
4933416C03Rik	2	722	149	7

5430416N02Rik	2	1396	329	16
5730528L13Rik	2	6958	194	1
5730596B20Rik	2	5499	164	5
5730596B20Rik	2	152	561	14
5830432E09Rik	2	1440	416	3
5S_rRNA	2	903	293	9
5S_rRNA	2	576	222	3
6030419C18Rik	2	83167	565	8
6430704M03Rik	2	2860	157	8
7SK	2	856	426	7
7SK	2	34429	305	18
7SK	2	25228	412	10
7SK	2	34715	431	5
8430419L09Rik	2	9821	158	4
9130409I23Rik	2	399	186	6
9130410C08Rik	2	428	379	6
9430021M05Rik	2	2248	330	7
A230083N12Rik	2	17359	223	17
A930007I19Rik	2	113532	164	12
Aanat	2	2399	488	9
Abhd15	2	36048	379	4
AC102525.1	2	682	215	8
AC114668.1	2	42456	572	12
AC122218.1	2	8746	337	19
AC126547.1	2	19285	285	17
AC151577.1	2	6866	171	6
AC163724.1	2	326	439	1
AC166172.1	2	1159	274	4
Acin1	2	1739	361	2
Acly	2	5767	218	4
Acss3	2	931	492	19
Actc1	2	3233	180	11
Actn1	2	5211	369	11
Adam1b	2	28289	221	8
Adam28	2	2706	502	3
Adam3	2	90404	193	16
Adam7	2	23871	433	13
Adck1	2	19691	352	5
Adcy7	2	214842	307	6
Add2	2	753	223	17
Adra1b	2	7834	139	14
Afap1l2	2	4411	273	11
Afap1l2	2	778	470	10
Agpat4	2	2789	199	2
Agpat9	2	1525	313	12
Agxt2l2	2	2826	353	5
AI854517	2	3565	284	14
AL645988.1	2	550	291	8
Aldoc	2	6592	475	14
Alg9	2	1009	157	12

Ankk1	2	6505	280	8
Ankrd34c	2	4801	184	6
Ano1	2	318	384	11
Ano2	2	1588	474	19
Anxa7	2	110846	406	19
Ap1s1	2	183	773	17
Ap3s1	2	5310	448	5
Apobec2	2	5581	319	11
Apol8	2	363	207	7
Arhgap18	2	6120	295	11
Arhgap24	2	2293	168	11
Arhgap4	2	440	205	9
Arsb	2	25984	153	9
Asah2	2	528	292	9
Asb12	2	69839	155	7
Asb2	2	19487	455	6
Ascc3	2	1333	200	14
Aspscr1	2	4917	504	5
Atcay	2	720	290	18
Atf7	2	1842	451	17
Atg5	2	5095	454	15
Atoh8	2	19537	265	10
Atp4b	2	175049	791	5
Atxn7l3	2	10986	263	X
Axin1	2	1619	303	13
Axin1	2	42111	204	19
Axin2	2	244	326	X
B020004J07Rik	2	6301	163	12
B230217C12Rik	2	5960	446	10
B3galt2	2	898	305	11
B3gntl1	2	1280	378	10
B430010I23Rik	2	1954	337	15
B430010I23Rik	2	17596	420	10
B430319F04Rik	2	212	367	6
Bach1	2	523	177	8
BC024479	2	6293	355	11
BC027582	2	712	224	17
Bcl2l13	2	7016	176	17
Bpgm	2	953	169	11
Bpifb2	2	7211	573	4
Bpifb3	2	14837	421	11
Bpnt1	2	403	468	1
Brd9	2	2177	350	11
Btd	2	4106	298	8
C130050O18Rik	2	3068	163	8
C1qtnf3	2	6679	283	7
C1qtnf6	2	1585	182	16
C230036H16Rik	2	3784	224	9
C430049B03Rik	2	767	201	3
Cacna1h	2	385	166	6

Cacng3	2	6599	431	6
Calcrl	2	1832	166	2
Calr4	2	6573	326	2
Cblc	2	4385	232	1
Cbln4	2	1758	158	13
Ccdc14	2	6225	431	14
Ccdc23	2	2063	223	5
Ccdc88c	2	3759	312	15
Ccdc9	2	948	210	15
Ccdc90a	2	3665	463	8
Ccnb1ip1	2	12412	542	X
Ccng1	2	1478	192	17
Cct2	2	2017	326	7
Cd69	2	46341	274	2
Cdc7	2	841	166	4
Cdh11	2	6245	188	7
Cdkn3	2	2046	351	2
Cdx1	2	5143	603	16
Cdx2	2	2073	444	4
Cdx4	2	1746	315	12
Cep164	2	848	151	7
Cftr	2	758	172	13
Cgnl1	2	266	180	14
Chd9	2	2075	201	11
Chst8	2	2582	381	10
Chst9	2	3351	199	6
Clgn	2	4732	159	5
Cmtm2b	2	812	166	8
Cnot6l	2	404	166	14
Col12a1	2	2399	166	18
Col18a1	2	1645	338	5
Col24a1	2	938	436	X
Col2a1	2	3990	385	9
Cops4	2	611	329	6
Cpa5	2	7659	172	9
Cpne4	**3**	935	328	8
Cpne8	2	1536	163	7
Crtac1	2	35162	283	18
Csnk1g3	2	6159	402	8
Cspp1	2	418	159	8
Cstad	2	25504	596	5
Ctbp2	**3**	1359	440	9
Ctbp2	2	4502	351	10
Cux1	2	149	490	3
Cux2	2	1570	310	15
Cux2	2	1147	478	5
D030018L15Rik	2	556	406	6
D230025D16Rik	2	5954	189	15
D2hgdh	2	1543	206	19
D930030I03Rik	2	35253	274	18

Dapk1	2	8141	294	1
Dck	2	4610	165	2
Dctn1	2	1619	284	7
Dcun1d4	2	3430	389	5
Ddr1	2	3180	212	5
Ddx28	2	69840	171	5
Ddx54	**3**	6516	301	15
Defb45	2	4193	439	8
Defb8	2	641	387	1
Dennd2a	2	60	173	16
Dhx36	2	1222	169	13
Dicer1	2	6381	354	5
Diras1	2	1233	368	6
Dnajb6	2	2191	359	5
Dsg4	2	313	296	17
Duoxa2	**3**	293	296	8
Dusp6	2	2754	182	2
Dusp7	2	2488	536	8
Dym	2	690	337	6
Dynlt1b	2	1828	258	3
E230019M04Rik	2	1698	588	12
Ech1	2	57	459	10
Eef1a2	2	2520	165	5
Efcab8	2	2043	312	18
Eftud1	2	5759	363	10
Ehf	2	1790	218	9
Eif4g3	2	21636	299	18
Elf3	2	19014	184	17
Elf4	2	3244	255	X
Elmo2	2	2371	158	7
Eml5	2	1138	224	2
Emx2os	2	948	547	2
Enthd1	2	352	436	7
Epb4.1l3	2	10059	194	2
Epb4.1l4a	2	1952	271	4
Erc2	2	560	370	1
Erc2	2	2324	324	X
Erf	2	1908	166	2
Ern1	2	2746	374	12
Esrrb	2	947	184	19
Exosc4	2	8099	155	15
Ezr	2	1105	381	17
Ezr	2	2070	484	18
Ezr	2	31410	156	14
F830001A07Rik	2	254093	362	14
Fam117b	2	2403	618	7
Fam131a	2	1270	228	11
Fam159b	2	57530	147	12
Fam168b	2	1548	327	15
Fam183b	2	21513	250	17

Fam196b	2	1388	252	17
Far1	2	3382	326	17
Fat1	2	68170	164	9
Fermt1	2	1118	186	1
Fezf2	2	691	212	16
Fgfr2	2	879	240	13
Fgg	2	12472	166	1
Fhl1	2	2901	191	11
Fip1l1	2	4886	208	11
Flnc	2	5492	198	7
Flrt1	2	6791	421	8
Fmo1	2	1594	273	2
Folr4	2	1828	215	14
Foxa2	2	33599	223	7
Foxb1	2	4413	219	3
Frmd5	2	987	214	X
Frs3	2	2229	382	5
Fxyd6	2	488	161	6
Fzd10	2	278	415	19
G2e3	2	8454	174	1
G3bp2	2	105	217	9
Gab1	2	3278	259	2
Gabra1	2	719	754	9
Gabra2	2	43279	191	2
Gbp5	2	1267	190	17
Gjb2	2	2617	209	9
Gjb3	2	1695	341	5
Gjc1	2	1707	291	12
Gm10138	2	12276	176	5
Gm10602	2	1638	355	8
Gm10638	2	937	419	11
Gm10657	2	1045	417	5
Gm11157	2	1827	218	3
Gm11465	2	609	325	14
Gm12577	2	2269	197	4
Gm12785	2	162	504	11
Gm12899	2	4075	151	1
Gm12979	2	56	170	7
Gm13012	2	1021	445	8
Gm13059	2	10008	252	9
Gm13091	2	4588	276	6
Gm13091	2	955	426	2
Gm13389	2	26122	308	4
Gm13389	2	9009	220	4
Gm13480	2	1541	298	4
Gm13541	2	1460	166	4
Gm14222	2	29108	153	4
Gm14335	2	40760	591	4
Gm14376	2	83920	421	4
Gm14454	2	79160	161	4

Gm14526	2	7997	244	2
Gm14567	2	61	457	2
Gm14703	2	44478	388	2
Gm14927	2	8573	399	2
Gm14978	2	732	344	2
Gm15050	2	8863	219	6
Gm15536	2	56	150	7
Gm15589	2	5796	193	2
Gm15589	2	1391	451	11
Gm15718	2	14543	586	X
Gm15771	2	1014	214	X
Gm15820	2	4754	276	X
Gm15984	2	161	462	2
Gm15991	2	36	450	6
Gm16010	2	50252	492	10
Gm16096	2	292	818	5
Gm16118	2	1303	203	5
Gm16131	2	49764	434	7
Gm16132	2	78497	227	15
Gm16140	2	8533	325	5
Gm16225	2	10808	340	5
Gm16518	2	2172	313	8
Gm16578	2	11835	287	9
Gm16638	2	6177	401	9
Gm16723	2	20454	346	8
Gm16796	2	13287	409	9
Gm16882	2	10128	514	13
Gm17216	2	232	507	11
Gm17261	2	1005	333	4
Gm17547	2	22551	185	11
Gm17551	2	3668	374	13
Gm17585	2	6065	227	7
Gm1977	2	1673	175	6
Gm20476	2	4352	244	2
Gm3054	2	31039	587	18
Gm364	**3**	131	319	6
Gm4117	2	5642	549	X
Gm4775	2	2971	1002	13
Gm4945	2	64	224	7
Gm5417	2	1186	471	4
Gm5560	2	1756	382	5
Gm5607	2	3206	430	7
Gm5903	2	180	1068	5
Gm5965	2	11204	237	13
Gm608	2	76	451	14
Gm6665	2	1668	170	17
Gm6899	2	25923	161	15
Gm6939	2	7027	566	5
Gm7123	2	1125	279	8
Gm8213	2	83677	319	7

Gm9104	2	3190	220	16
Gnb2l1	2	11768	535	16
Golga1	2	2521	235	18
Golga4	2	4740	555	11
Gpc6	2	696	169	7
Gpr165	2	5085	254	X
Gpr174	2	3029	216	6
Gprc5d	2	334	328	17
Gpx1	2	3077	469	11
Grik4	2	3082	218	2
Grin1	2	4204	342	9
Guk1	2	2394	313	14
Has1	2	5465	317	X
Hcrtr1	2	4444	194	X
Hes6	2	3508	227	6
Hnrnpl	2	966	402	9
Hoxa9	2	4519	384	9
Htatip2	2	859	162	2
Htr5a	2	57	164	11
Htr7	2	739	362	17
Icosl	2	1120	592	4
Id1	2	4279	246	1
Idh2	2	1147	551	7
Igkj1	2	3825	220	6
Ikbke	2	4824	631	7
Ikzf2	2	1243	475	5
Il20rb	2	12372	189	19
Insrr	2	5377	412	10
Ints9	2	1579	212	2
Iqca	2	596	249	7
Iqca	2	3869	354	6
Isl1	2	327	183	1
Isoc1	2	728	543	1
Itfg1	2	6338	172	9
Itgb4	2	2452	343	3
Itpr2	2	6715	371	14
Kank2	2	4417	529	1
Kap	2	3638	172	1
Kbtbd10	2	5007	376	13
Kcnj14	2	781	234	18
Kctd10	2	1630	403	8
Kctd13	2	7031	217	11
Kctd14	2	609	281	6
Kctd15	2	2948	180	9
Khsrp	2	2007	160	6
Kif6	2	1322	162	2
Kitl	2	2069	247	7
Klf3	2	2108	359	5
Kpna3	2	2681	209	7
Krt42	2	3223	169	7

Krt5	2	1571	183	7
Krt75	2	3765	285	17
Krt80	2	747	468	17
Krtap5-5	2	7464	208	10
Krtap7-1	2	5408	252	5
l7Rn6	2	3754	267	14
Lactbl1	2	2180	160	11
Lalba	2	1494	379	15
Lancl3	2	4743	305	15
Lcn13	2	1709	196	15
Lcorl	2	648	190	7
Ldhc	2	3169	210	16
Lect2	2	464	194	7
Lepre1	2	849	339	4
Lgr4	2	136	413	15
Lhfpl2	2	574	256	X
Lin7b	2	6403	430	2
Lins	2	78727	180	5
Lipg	2	5137	448	7
Lmx1b	2	3567	196	13
Loxl1	2	1746	362	4
Lpl	2	109	581	2
Lpo	2	2619	368	13
Lpo	2	6481	439	7
Lrfn1	2	9476	472	7
Lrrc3	2	6636	367	18
Lrrc57	2	10115	336	2
Lypd6	2	5264	190	9
Lyrm1	2	2774	382	8
Madd	2	3024	282	11
Mageb16	2	5352	348	11
Mboat2	2	4664	169	7
Mc4r	2	8978	161	10
Mccc2	2	4228	406	2
Mdk	2	2844	186	2
Meis1	2	3719	456	7
Meis1	2	726	260	2
Melk	2	3161	288	X
Mettl10	2	1210	285	12
Mettl17	2	5792	434	18
Mettl22	2	5861	320	13
Mgst2	2	283	216	2
Mir10b	2	1239	431	11
Mir183	2	5887	604	11
Mir1936	2	5124	380	4
Mir1955	2	1655	176	7
Mir1964	2	3640	280	14
Mir1967	2	2971	158	16
Mir2861	2	6913	161	3
Mir449c	**3**	3616	274	2

Mir539	2	1317	322	6
Mir568	2	6877	460	12
Mir574	2	5471	205	2
Mir719	2	4855	339	7
Mir7-2	2	2436	213	8
Mir9-3	2	1910	194	2
Mirlet7a-1	2	188	294	12
Mis18bp1	2	512	304	16
Mkks	2	4477	225	5
Mlf1ip	2	820	163	14
Mms22l	2	2346	235	7
mmu-mir-689-2	2	1583	149	7
Morn4	2	4894	260	13
Mpdu1	2	1702	156	12
Mpped1	2	12980	162	2
Mpped1	2	4390	271	8
Mrpl24	2	935	322	4
Mrpl49	2	580	450	16
Msh3	2	75	277	19
Mtap7	2	336	162	11
Mtmr4	2	2285	161	15
Muc3	2	4461	298	15
Mxd3	2	229	219	3
Mxi1	2	292	394	19
Mycbpap	2	6076	180	13
Myd88	2	58985	439	10
Myf5	2	5842	338	11
Myf6	2	672	533	5
Myl12b	2	1792	174	13
Myo16	2	19964	172	19
Myoz3	2	6576	198	11
N4bp2	2	6465	181	9
Nat3	2	1176	455	10
Ncoa4	2	740	352	10
Ndel1	2	2466	574	17
Ndp	2	119130	507	8
Ndufc2	2	30953	195	18
Neurog1	2	6002	211	5
Nfix	2	509	174	8
Nhp2	2	8179	259	14
Nkx2-5	2	443	356	11
Nlrp14	2	1030	370	X
Nmnat2	2	1252	154	7
Nol6	2	5233	175	13
Nphp4	2	29044	289	8
Nphs1as	2	1683	387	11
Nr5a2	2	6205	171	17
n-R5s173	2	6115	232	7
n-R5s24	2	6723	169	1
n-R5s77	2	307	355	4

Nrg1	2	24188	398	4
Nsun6	2	2409	556	7
Ntn1	2	5908	459	1
Nudt7	2	2301	227	5
Numa1	2	1782	163	18
Nxf1	2	25413	820	10
Olfr401	2	942	1051	8
Olfr504	2	1460	362	2
Olfr520	2	6503	347	11
Olfr702	2	830	349	8
Olfr758-ps1	2	7464	163	7
Olfr76	2	1051	180	19
Olfr904	2	184	256	11
Olfr94	2	6332	356	7
Olfr97	2	240	409	7
Onecut1	2	1099	244	7
Ooep	2	2250	522	17
Opalin	2	7250	344	19
Opn1sw	2	823	203	9
Orc1	2	4471	191	17
Ormdl1	2	2534	417	17
Otud3	2	5647	529	9
Otud7a	2	2619	185	9
Otud7b	2	4321	716	19
Ovgp1	2	1392	190	6
P2ry6	2	1660	331	4
Pacsin1	2	858	274	1
Panx2	2	8991	619	4
Pcgf3	2	1380	375	7
Pde2a	2	1620	417	3
Pde8a	**3**	2634	398	3
Pds5b	2	283	182	7
Pdss1	2	1741	355	17
Pdzk1ip1	2	564	263	15
Pelp1	2	13940	400	5
Per1	2	2299	504	7
Pex19	2	870	156	5
Pfn4	2	1637	178	2
Pgap2	2	4169	169	4
Pglyrp2	2	4718	194	11
Pgr15l	2	1009	466	11
Phf17	2	1205	214	1
Phox2a	2	3707	160	12
Phxr2	2	13348	183	7
Pipox	2	3404	247	17
Pkd2l1	2	1703	393	X
Pkia	2	2487	230	3
Plagl1	2	4537	178	7
Plcg2	2	5327	350	10
Plcg2	2	1688	303	11

Plekha2	2	1346	310	19
Plekhb2	**3**	14143	181	3
Plekhf1	2	701	693	10
Plekhg1	2	4442	309	8
Pln	2	591	259	8
Plod2	2	14873	224	8
Plxna3	2	2399	164	7
Ppcdc	2	445	207	10
Ppp1r3b	2	4279	167	10
Ppp1r3c	2	1684	202	9
Ppp3r1	2	673	222	X
Prcp	2	7699	296	9
Prdm2	2	6850	222	8
Prdx6b	2	7397	261	19
Prkcq	2	3951	202	11
Prkx	2	1337	380	7
Pten	2	1511	191	4
Ptgir	2	4276	532	2
Ptprb	2	55806	454	2
Ptprn	**3**	136	156	X
Rab5b	2	7108	163	19
Rab6b	2	1649	236	7
Rag1	2	2737	299	10
Rag2	2	627	205	10
Ran	2	1796	165	9
Ranbp3	2	4419	199	2
Raph1	2	831	349	2
Rcvrn	2	1806	229	5
Rdh12	2	1588	177	17
Retsat	2	1934	223	1
Rfxap	2	6478	234	11
Rgl2	2	2611	265	12
Rgnef	2	4557	276	6
Rhoj	2	18812	368	3
Ripply1	2	1416	152	17
Rit2	2	52724	373	13
RNaseP_nuc	2	1501	213	12
Rnf112	2	684	153	X
Rnf113a2	2	3773	182	18
Rnf180	2	72475	234	3
Rnf43	2	3230	281	11
Ror2	2	1970	295	12
RP23-118L1.1	2	29848	286	13
RP23-181K4.1	2	4065	452	11
RP23-397G23.1	2	1559	363	13
RP23-398K14.3	2	3313	244	5
Rph3al	2	58477	269	7
Rpl13	2	188	315	19
Rpl24	2	1582	278	3
Rpp14	2	6431	191	11

Rptor	2	4396	223	8
Rrp1b	2	5381	350	16
Rrp7a	2	1825	246	14
Rtdr1	2	2229	324	11
Rtn4ip1	2	9445	353	17
Rtp2	2	597	185	15
Rttn	2	437	450	10
Rufy3	2	18142	447	10
Rufy3	2	640	273	16
Rwdd2a	2	499	780	18
S100a10	2	285	426	5
Safb	2	19166	235	5
Sall1	2	720	226	9
Samd15	2	2781	226	3
Sap30	2	5224	247	17
Scgb1c1	2	3242	257	8
Sdcbp2	2	182	525	12
Sdr42e1	2	9045	179	8
Sec16b	2	1411	278	7
Sema4a	2	6994	240	2
Serpina3c	2	4173	171	8
Serpinb6c	2	6260	179	1
Setd3	2	493	151	3
Setx	2	554	184	12
Sfmbt1	2	2185	210	13
Sfswap	2	13834	321	12
Sftpd	2	3664	353	2
Sgsm3	2	2748	319	14
Shc3	2	7149	197	5
Shisa5	2	5959	157	14
Shkbp1	2	138	280	15
Shroom4	2	568	318	13
Slc12a8	2	2997	422	9
Slc13a5	2	1153	153	7
Slc16a1	2	1772	227	X
Slc1a6	2	66438	164	16
Slc25a27	2	2970	162	11
Slc25a30	2	6734	273	3
Slc29a3	2	924	306	10
Slc39a4	2	1015	364	17
Slc40a1	2	4213	183	14
Slc5a8	2	6873	161	10
Slc7a6	2	1653	392	15
Slmo2	2	5918	584	1
Slu7	2	205	213	10
Smad5	2	3529	501	8
Smg1	2	2930	436	2
Smoc2	2	356	162	11
Smtnl2	2	18314	168	13
SNORA17	2	2001	400	7

SNORA26	2	3773	156	17
Snora47	2	762	157	11
SNORA71	2	890	408	5
SNORA79	2	2027	215	12
SNORD18	2	657	353	13
SNORD41	2	667	367	6
SNORD88	2	2528	188	16
Snord91a	2	645	237	9
snosnR60_Z15	2	3943	159	8
Snrpd2	2	61252	967	10
Soat1	2	87	332	11
Sostdc1	2	26585	340	11
Spaca1	2	3745	284	7
Spats2	2	2108	337	1
Spcs1	2	6011	168	12
Spert	2	9312	450	4
Spon2	2	1225	196	15
Sprr2j-ps	2	4660	405	14
Spsb2	2	828	182	14
Sptlc3	2	1499	465	5
Srd5a3	2	297	583	3
Ssh2	2	3457	749	6
St5	2	540	985	2
Stard4	2	1220	444	5
Steap3	2	543	339	11
Ston2	**3**	1362	384	7
Stxbp6	2	3696	397	18
Styx	2	4212	181	1
Sult2b1	2	923	185	12
Sumo2	2	831	196	14
Supt4h1	2	958	187	7
Susd1	2	1729	450	11
Svil	2	15520	439	11
Synpo	2	4379	488	4
Syt1	2	76367	650	18
Syt10	2	29410	172	18
Taf1	2	578	205	10
Taf7	2	1436	254	15
Tagap	2	809	290	X
Tank	2	3705	184	18
Tbc1d24	2	2543	312	17
Tcea2	2	7221	550	2
Tcp11	2	9053	343	17
Tcte2	2	923	159	2
Tdg	2	2317	170	17
Tdrkh	2	508	173	17
Tecpr2	2	8744	758	10
Tfap2d	2	1008	559	3
Tfe3	2	5156	165	12
Tfpi	2	7797	169	1

Tgfbr1	2	2427	262	X
Tgfbr3	2	12006	184	2
Tgif2	2	69908	721	4
Tiam1	2	292	443	5
Timm50	2	4738	186	2
Tlr1	2	3396	362	16
Tmed7	2	4812	201	7
Tmem119	2	201	175	5
Tmem161a	2	747	327	18
Tmem213	2	362	401	5
Tmem229a	2	1589	168	8
Tmem33	2	3808	267	6
Tmem37	2	6632	298	6
Tmem59	2	5535	291	5
Tmod2	2	4939	171	1
Tmod3	2	7114	162	4
Tnc	2	9546	444	9
Tnfrsf13c	2	6166	170	9
Tnni1	2	27047	392	4
Tnr	2	1046	448	15
Tns3	2	13036	310	1
Tor1aip1	2	1453	519	1
Tpst1	**3**	1207	266	11
Trav1	2	12799	358	1
Trbv12-2	2	4067	188	14
Treh	2	657	192	6
Trerf1	2	1693	346	9
Trim32	2	1811	737	17
Trim52	2	3465	280	4
Trio	2	812	432	14
Tspan11	2	101270	594	15
Ttc21a	2	3513	374	6
Ttc9b	2	3389	305	9
Ttk	2	2761	627	7
Tub	2	1174	453	9
Tuba1b	**3**	1151	280	7
U1	2	16031	290	5
U2	2	19397	218	3
U6	2	9032	258	11
U6	2	85857	339	3
U6	2	2620	230	7
U6	2	34061	374	1
U6	2	11573	257	4
U6	2	5263	165	11
U6atac	2	4414	247	3
U7	2	1027	161	1
Ube2j2	2	2733	741	4
Ube2r2	2	995	184	4
Ube2u	2	8086	431	4
Upk1b	2	1214	165	16

Usp1	2	3750	207	4
Usp12	2	1666	151	5
Usp18	2	3227	405	6
Usp2	2	2621	173	9
Usp25	2	7232	281	16
Usp47	2	25687	156	7
Utp18	2	1537	200	11
Uvrag	2	5671	305	7
Vasn	2	224	570	16
Vax1	2	753	316	19
Vdac1	2	8958	161	11
Veph1	2	1317	230	3
Vim	2	4804	354	2
Vrk2	2	5168	167	11
Wdr4	2	7220	187	17
Wdr61	2	15721	257	9
Wdr78	2	21150	166	4
Wnt16	2	4548	178	6
Xpo6	2	1214	192	7
Xpo7	2	9537	282	14
Y_RNA	2	24269	176	2
Yrdc	2	4469	148	4
Ywhab	2	10900	164	2
Zadh2	2	2529	210	18
Zbtb41	2	1157	271	1
Zcchc16	2	1536	258	X
Zfhx3	2	3630	169	8
Zfhx3	2	1109	493	8
Zfp189	2	803	571	4
Zfp27	2	2348	161	7
Zfp382	2	359	342	7
Zfp41	2	860	227	15
Zfp568	2	3890	160	7
Zfp609	2	806	186	9
Zfp628	2	3002	367	7
Zfp704	2	1424	347	3
Zfp773	2	6109	324	7
Zfp819	2	6770	230	7
Zfp831	2	520	326	2
Zfp90	2	3368	165	8
Zfp93	2	713	191	7
Zfp957	2	1759	162	14
Zfx	2	19798	151	X
Zfyve27	2	12512	272	19
Zic4	2	358	303	9
Zmat3	2	6441	386	3